E. WOLF, PROGRESS IN OPTICS XXXV

V

COHERENT POPULATION TRAPPING IN LASER SPECTROSCOPY

BY

E. ARIMONDO*

JILA,
University of Colorado at Boulder,
Boulder, CO 80309-0440, USA

CONTENTS

This article is dedicated to the memory of A. Gozzini and G.W. Series, great teachers in atomic spectroscopy.

§ 1. Introduction

Spectroscopic investigations of atoms and molecules are based on the interaction of near-resonant radiation with the species under investigation. The use of monochromatic, intense, and continuously tunable radiation sources, permits very high sensitivity and accuracy to be attained in the determination of the atomic or molecular levels. Although the attention of spectroscopists was restricted to two-level systems for a long time, the possibility of irradiating samples by several electromagnetic fields simultaneously has produced multiphoton transitions and other nonlinear phenomena, whose application has been explored in the continuously expanding field of nonlinear spectroscopy. In comparison to the two-level system, the three-level system, interacting with two monochromatic radiation fields, represents a configuration in which the nonlinear phenomena are greatly enhanced both in the number of possible laser configurations and in the magnitude of the nonlinearities. The development of monochromatic and tunable laser sources has produced a large variety of high-resolution spectroscopic investigations on three-level systems.

Among the different nonlinear processes associated with the three-level atomic systems, the application of two continuous wave radiation fields leads to the preparation of the atom in a coherent superposition of states, which is stable against absorption from the radiation field. This phenomenon has been designated as coherent population trapping, to indicate the presence of a coherent superposition of the atomic states and the stability of the population. Coherent population trapping may be also described as the pumping of the atomic system in a particular state, the coherent superposition of the atomic states, which is a nonabsorbing state. The exciting radiation creates an atomic coherence such that the atom's evolution is prepared exactly out of phase with the incoming radiation and no absorption takes place. This phenomenon was observed for the first time by Alzetta, Gozzini, Moi and Orriols [1976], as a decrease in the fluorescent emission in a laser optical pumping experiment on sodium atoms, involving a three-level system with two ground levels and one excited level. In that experiment, because an inhomogeneous magnetic field was applied along the sodium cell axis, the nonabsorption was produced in only a small region inside the cell, and the phenomenon appeared as a dark line inside

the bright fluorescent cell. As a consequence, names such as dark resonance or nonabsorption resonance have been used in the literature to describe coherent population trapping. At the same time, and independently, the pumping and trapping originated by two laser fields resonant with two coupled transitions was investigated theoretically for three levels in cascade by Whitley and Stroud [1976], and experimentally in sodium atoms with two ground levels and one excited level by Gray, Whitley and Stroud [1978]. The theoretical analyses by Arimondo and Orriols [1976] and Gray, Whitley and Stroud [1978], pointed out that the sodium atoms were pumped in a nonabsorbing state because of the presence of interfering processes. Population trapping during laser-induced molecular excitation and dissociation was examined theoretically by Stettler, Bowden, Witriol and Eberly [1979]. The title of a paper by Gray, Whitley and Stroud [1978] contains, for the first time, the term *coherent trapping*, and in the conclusion of the paper, the phenomenon is defined as a coherent trapping of a population. The complete designation of coherent population trapping appeared for the first time in the abstract of a paper by Agrawal [1981] on the possibilities of using three-level systems for optical bistability. Then the title of a work by Dalton and Knight [1982a] contained the full designation of coherent population trapping with evidence on the main characteristic of the phenomenon.

The process remained a sort of amusing scientific curiosity for some time. If one resonant laser beam is switched on inside a sodium cell, some very bright fluorescence is emitted by the cell. If a second laser beam is sent into the cell, this second laser being slightly detuned from the first one but also in near resonance with the sodium atoms, it produces its own bright fluorescence. The simultaneous application of the two lasers produces coherent population trapping and eliminates the sodium bright fluorescence. This interference effect, produced by the presence of atomic coherence, appears at the macroscopic level. Coherences between states of a quantum-mechanical system are generated whenever an interaction or measurement leaves the system in a linear superposition of the energy eigenstates defined in the absence of the field. Interferences produced by the presence of coherences have been known since the development of quantum mechanics, and their creation has been largely exploited in spectroscopy and quantum optics. However, a macroscopic effect such as the total suppression of fluorescence emission by coherent population trapping is quite unusual.

In the early 1980s some theoretical attention was given to the process of coherent population trapping, with extensions to the case in which the upper state of the three-level system lies in the continuum, e.g., Knight [1984]. However, the

real rise in interest waited for the extensions or applications on the experimental side. The first application, to metrology, is linked to the work by Tench, Peuse, Hemmer, Thomas, Ezekiel, Leiby Jr, Picard and Willis [1981], and Thomas, Hemmer, Ezekiel, Leiby Jr, Picard and Willis [1982] (see also discussion in Knight [1982]), who demonstrated how very high-frequency accuracy in the measurement of the sodium ground-state hyperfine splitting could be obtained by using what they called Ramsey fringes in Raman three-level transitions. That now should be defined as a Ramsey fringe investigation of coherent population trapping. The next application was to optical bistability; Walls and Zoller [1980] investigated theoretically the optical bistability from three-level atoms contained in an optical cavity and driven into the coherent-trapping superposition. That optical bistability was observed for the first time by Mlynek, Mitschke, Deserno and Lange [1982]. After those early observations, the phenomenon of coherent population trapping has been exploited in very different applications: in high-resolution spectroscopy, laser multiphoton ionization, four-wave mixing, and laser-induced structures in the continuum. Increased attention is due to the work of Aspect, Arimondo, Kaiser, Vansteenkiste and Cohen-Tannoudji [1988] on the application of velocity-selective coherent population trapping to laser cooling. Very soon other interesting phenomena such as adiabatic transfer, lasing without inversion, matched pulse propagation, and photon statistics, strictly connected to the trapping properties of the three-level system, were discovered. It should be noted here that even if some theoretical work has considered the extension to molecular systems, the evidence of coherent population trapping in molecules is still very limited and has been associated with the adiabatic transfer experiments of Gaubatz, Rudecki, Schiemann and Bergmann [1990] and of Dam, Oudejans and Reuss [1990].

For the most important steps in the theoretical understanding of coherent population trapping, Hioe and Eberly [1981], and later Hioe [1983, 1984a, 1984b], have shown a relation with the invariants in the density matrix equations: coherent population trapping is related to the SU(3) group symmetries of the Hamiltonian and to some conservation laws satisfied by the density matrix elements of a three-level system during the time evolution. Smirnov, Tumaikin and Yudin [1989] and Tumaikin and Yudin [1990] have presented generalizations in the construction of the coherent population-trapping atomic superposition. Radmore and Knight [1982] and Dalibard, Reynaud and Cohen-Tannoudji [1987] have derived the dressed atom description.

Coherent trapping as an interference phenomenon is closely related to other interference processes well exploited in spectroscopy, such as the Fano windows in the autoionization profile, the level crossing, or the Hanle effect. A strict

connection also exists between coherent population trapping and the weak interaction decay of the K_0 and $\bar{K}_0$ mesons. In coherent population trapping, the two linear superpositions of ground atomic or molecular states present very different lifetimes for the interaction of these superpositions with the radiation field. Owing to weak interaction mixing between the K_0 and $\bar{K}_0$ mesons, their linear superpositions, K_S and K_L, should be considered. Those superpositions have different lifetimes, short and long, with respect to the weak interaction decay. However, it should be noted that the reduction of coherent population trapping to an interference feature is a reductive description: the experimental observations are strongly based on the role played by optical pumping in the atomic preparation into that quantum superposition that presents interference in the absorption or radiative decay.

Coherent population trapping has been examined in several review papers. An early review was presented by Dalton and Knight [1983]. Yoo and Eberly [1985] presented an analysis of the most important theoretical features of the phenomenon, although their attention was devoted to three-level atoms inside an optical cavity. A review by Arimondo [1987] summarized the experimental observations at that time. A more recent review, with more attention toward the theoretical features and the extensions to laser cooling, has been written by Agap'ev, Gornyi and Matisov [1993].

The organization of this chapter is as follows. In § 2 a theoretical introduction presents the basic properties of an atomic system prepared with the coherent population-trapping superposition of states. § 3 deals with several experimental observations concerned with the establishment of coherent trapping in different discrete systems. § 4 very briefly treats the theoretical and experimental aspects of trapping which involves states of the continuum, because a recent review on that subject has been written by Knight, Lauder and Dalton [1990]. The remaining sections are devoted to a review of both the theoretical and experimental features associated with coherent population trapping in laser cooling, adiabatic transfer, lasing without inversion, pulse matching, and photon statistics. The large amount of theoretical work that has been published with respect to the phenomenon and to the constants of motion with relation to the SU(3) symmetry will not be reported here; the book by Shore [1990] and the recent review by Agap'ev, Gornyi and Matisov [1993] deal with most of those features. Nevertheless, § 8 is devoted to the theoretical aspect of coherent population trapping created by spontaneous emission, which is a possibility considered in some theoretical papers. Even if there is little chance of observing the phenomenon, it is presented because of its fundamental connection with coherent population trapping and lasing without inversion.

§ 2. Analysis for Discrete States

2.1. DENSITY MATRIX

The atomic (or molecular) three-level systems considered here are shown in fig. 1. The levels, defined in the absence of any radiation field, are labeled as $|1\rangle$, $|2\rangle$, and $|0\rangle$, with their energies E_j $(j=0, 1, 2)$, and the energy separation between levels $|i\rangle$ and $|j\rangle$ denoted as $\hbar\omega_{ij}=E_i-E_j$. The three cases of fig. 1 will be denoted as Λ, cascade, and V configurations. The Hamiltonian $\mathcal{H}_0$ that describes the internal energy of the three levels is written as:

$$\mathcal{H}_0=\sum_{ij} E_j\,|i\rangle\,\langle i|. \tag{2.1}$$

The common level $|0\rangle$ is coupled to both levels $|1\rangle$ and $|2\rangle$ through electric dipole transitions induced by two applied classical laser fields,

$$\mathcal{E}_{L1}(z)\boldsymbol{u}_1\cos(\omega_{L1}t+\phi_1), \qquad \mathcal{E}_{L2}(z)\boldsymbol{u}_2\cos(\omega_{L2}t+\phi_2),$$

where $\boldsymbol{u}_i$, ω_{Li}, and ϕ_i $(i=1, 2)$ are the unit vector, the angular frequency, and the phase of each field, respectively. The three-level configurations of fig. 1 may be treated by a single formalism if proper definitions of the atomic energies and laser frequencies are introduced. The convention to be used here is slightly different from that introduced by most authors (e.g., Feld and Javan [1969] or Kelley, Harshman, Blum and Gustafson [1994]), because attention is concentrated on the Λ scheme. In the Λ scheme of fig. 1a, the energies are in the order $E_1 \leqslant E_2 \leqslant E_0$ and the laser frequencies are all positive. In the cascade

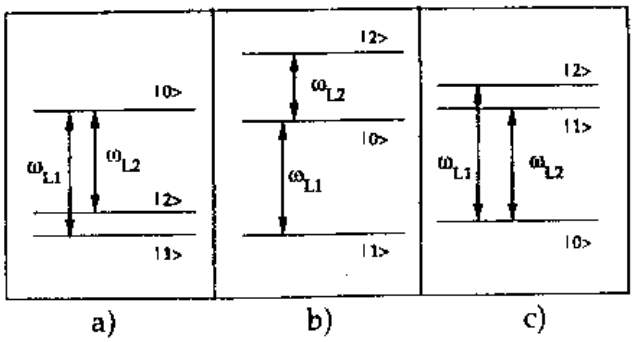

Fig. 1. Three-level systems in (a) Λ, (b) cascade, and (c) V configurations. Levels $|1\rangle$ and $|2\rangle$ are connected by dipole transitions only to level $|0\rangle$. See text for signs of the energy splittings and laser frequencies in each configuration.

scheme of fig. 1b, with $E_1 \leqslant E_0 \leqslant E_2$, ω_{01} and ω_{L1} are positive, whereas ω_{02} and ω_{L2} are negative. Finally, in the V scheme of fig. 1c, with $E_0 \leqslant E_1 \leqslant E_2$, all the angular frequencies are negative.

In the preliminary analysis the atoms will be supposed to be at rest along the propagation direction of the laser fields and located at the z position of the coordinate. It will be supposed in all of our analyses that, either due to selection rules produced by a proper choice of the polarizations of the two laser fields or because of the properly chosen frequency detunings, each laser field acts only on one dipole transition, and specifically, that laser 1 acts on the $|1\rangle \rightarrow |0\rangle$ transition, and laser 2 on the second one. It is convenient to define the detuning, δ_{L1} and δ_{L2}, of each laser from its resonance:

$$\delta_{L1} = \omega_{L1} - \omega_{01}, \qquad \delta_{L2} = \omega_{L2} - \omega_{02}, \tag{2.2a,b}$$

and also the Raman detuning δ_R from the Raman two photon-resonance:

$$\delta_R = \omega_{L1} - \omega_{L2} - (\omega_{01} - \omega_{02}). \tag{2.2c}$$

Introducing the electric dipole moments μ_{01} and μ_{02} between the three states, the Rabi frequencies characterize the atom laser interaction:

$$\Omega_{R1} = -\frac{\mu_{01}\mathcal{E}_{L1}}{\hbar}, \qquad \Omega_{R2} = -\frac{\mu_{02}\mathcal{E}_{L2}}{\hbar}, \tag{2.3}$$

where, for simplicity, very often the Rabi frequencies are supposed to be real but should be considered complex in the general case. The atom–laser interaction Hamiltonian V_{AL} may be written as:

$$\begin{aligned} V_{AL} = {} & \hbar\frac{\Omega_{R1}}{2}\exp[-i(\omega_{L1}t + \phi_1)]\,|0\rangle\langle 1| \\ & + \hbar\frac{\Omega_{R2}}{2}\exp[-i(\omega_{L2}t + \phi_2)]\,|0\rangle\langle 1| + \text{h.c.} \end{aligned} \tag{2.4}$$

The standard rotating wave approximation (RWA) has been used to eliminate the nonresonant terms within the interaction Hamiltonian. The two levels $|1\rangle$ and $|2\rangle$, due to the electric dipole selection rules, have the same parity so that electric dipole transitions cannot be induced between them, but magnetic dipole transitions are possible.

In order to complete the description of the three-level system, the relaxation terms produced by spontaneous emission, collisions, and any other damping mechanism, have to be considered. All those relaxation terms of the ρ density

matrix will be introduced through an operator $\mathfrak{R}$ in the optical Bloch evolution equation:

$$i\frac{d\rho(t)}{dt} = \frac{1}{\hbar}[\mathcal{H}_0 + V_{AL}, \rho(t)] + \mathfrak{R}\rho(t). \tag{2.5}$$

The relaxation operator $\mathfrak{R}$ contains Γ_{ij} terms describing the dephasing rates of the ρ_{ij} off-diagonal element; $\Gamma_{i'\to i}$ terms describing the rates of population transfer from state i' to state i; and finally Γ_i, the total rate of ρ_{ii} population decay from state i. The general formulation introduced by Kelley, Harshman, Blum and Gustafson [1994] allows the relaxation terms and steady-state solution of the density matrix to be written in the most general case. However, in most cases of coherent population trapping, very simple relaxation processes, such as those produced by the spontaneous emission rates Γ_i^{sp} ($i = 0, 1, 2$), must be considered. For instance, for the Λ configuration only the following rates are different from zero: $\Gamma_0 = \Gamma_0^{sp}$, $\Gamma_{0\to 1} = \Gamma_{0\to 2} = \Gamma_0^{sp}/2$, and $\Gamma_{01} = \Gamma_{10} = \Gamma_{02} = \Gamma_{20} = \Gamma_0^{sp}/2$. When experiments in the presence of collisions are to be analyzed, the decay rate $\Gamma_{12} = \Gamma_{21}$ for the coherences ρ_{12} and ρ_{21} between the two lower levels, the population transfers $\Gamma_{1\to 2}$ and $\Gamma_{2\to 1}$, and the population losses Γ_1 and Γ_2, have to be introduced, in addition to spontaneous emission.

For the Λ system, the following density matrix elements in the interaction picture may be introduced to eliminate the fast dependencies in the time evolution equations:

$$\begin{aligned}
&\tilde{\rho}_{0i} = \rho_{0i}\exp[i(\omega_{Li}t + \phi_i)] \quad (i = 1, 2),\\
&\tilde{\rho}_{12} = \rho_{12}\exp\{-i[(\omega_{L1} - \omega_{L2})t + (\phi_1 - \phi_2)]\}.
\end{aligned} \tag{2.6}$$

Then the evolution equations are:

$$\begin{aligned}
\frac{d\rho_{00}}{dt} &= -\Gamma_0\rho_{00} + i\frac{\Omega_{R1}^*}{2}\tilde{\rho}_{01} + i\frac{\Omega_{R2}^*}{2}\tilde{\rho}_{02} + \text{c.c.},\\
\frac{d\rho_{11}}{dt} &= \frac{\Gamma_0}{2}\rho_{00} - (\Gamma_1\rho_{11} - \Gamma_{2\to 1}\rho_{22}) - i\frac{\Omega_{R1}^*}{2}\tilde{\rho}_{01} + \text{c.c.},\\
\frac{d\rho_{22}}{dt} &= \frac{\Gamma_0}{2}\rho_{00} - (\Gamma_2\rho_{22} - \Gamma_{1\to 2}\rho_{11}) - i\frac{\Omega_{R2}^*}{2}\tilde{\rho}_{02} + \text{c.c.},\\
\frac{d\tilde{\rho}_{01}}{dt} &= -\left[\frac{\Gamma_0}{2} + i\delta_{L1}\right]\tilde{\rho}_{01} + i\frac{\Omega_{R1}}{2}(\rho_{00} - \rho_{11}) - i\frac{\Omega_{R2}}{2}\tilde{\rho}_{21},\\
\frac{d\tilde{\rho}_{02}}{dt} &= -\left[\frac{\Gamma_0}{2} + i\delta_{L2}\right]\tilde{\rho}_{02} + i\frac{\Omega_{R2}}{2}(\rho_{00} - \rho_{22}) - i\frac{\Omega_{R1}}{2}\tilde{\rho}_{21}^*,\\
\frac{d\tilde{\rho}_{12}}{dt} &= -[\Gamma_{12} + i\delta_R]\tilde{\rho}_{12} - i\frac{\Omega_{R2}^*}{2}\rho_{02} + i\frac{\Omega_{R1}}{2}\tilde{\rho}_{01}^*,
\end{aligned} \tag{2.7}$$

with $\rho_{i0} = \tilde{\rho}_{0i}^*$. The steady-state solutions of these equations have been reported by Kelley, Harshman, Blum and Gustafson [1994]. Here it is relevant only to

report that the two-photon Raman resonance between the $|1\rangle$ and $|2\rangle$ levels is described by the two-photon operator $\hat{T}$:

$$\hat{T} = -\frac{|\Omega_{R1}|^2 |\Omega_{R2}|^2}{D_{12} + \hat{S}_{light}}, \tag{2.8}$$

with the resonant two-photon denominator given by

$$D_{12} = -i\delta_R + \Gamma_{12}, \tag{2.9}$$

the light shift $\hat{S}_{light}$ given by

$$\hat{S}_{light} = \frac{|\Omega_{R2}|^2}{D_2} + \frac{|\Omega_{R1}|^2}{D_1}, \tag{2.10a}$$

and the resonant one-photon denominators given by

$$D_i = -i\delta_{Li} + \Gamma_{0i} \quad (i = 1, 2). \tag{2.10b}$$

All of the above expressions may also be used for the cascade and V schemes (fig. 1) when the appropriate sign changes, as defined above, are applied to the angular frequencies. It will be helpful for later analysis to report the dependence of the coherence term ρ_{12} on the laser frequencies in the case of the cascade configuration:

$$\rho_{12} = \tilde{\rho}_{12} \exp\{-i[(\omega_{L1} + \omega_{L2})t + \phi_1 + \phi_2)]\}. \tag{2.11}$$

2.2. NUMERICAL RESULTS

As shown by Arimondo and Orriols [1976], Gray, Whitley and Stroud [1978], and Orriols [1979], the simplest way to illustrate the phenomenon of coherent population trapping is to present the numerical solution for the steady-state values of the density equations. In this respect it may be stated that nothing really new was discovered by the numerical analyses referred to above because everything was already contained in the general density matrix general solution, for instance, by Wilcox and Lamb Jr [1960], Schlossberg and Javan [1966], Hänsch and Toschek [1970], and Feldman and Feld [1972]. However, the clear appearance of coherent population trapping requires a proper choice of the density matrix relaxation rates, and that represents an original contribution by Arimondo and Orriols [1976], Gray, Whitley and Stroud [1978], and Orriols [1979].

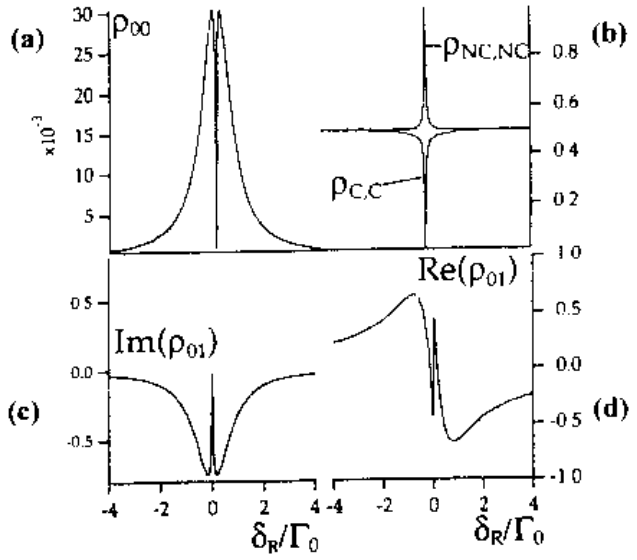

Fig. 2. (a) Steady-state excited-state population ρ_{00}^{st} for Λ system as a function of the Raman detuning δ_R, with the typical central dip associated with the coherent population-trapping phenomenon; (b) occupation of the noncoupled and coupled states (see § 2.3), $\rho_{NC,NC}^{st}$ and $\rho_{C,C}^{st}$, respectively, versus δ_R; (c) imaginary and (d) real parts of the optical coherence on the $|1\rangle \rightarrow |0\rangle$ transition, $\mathrm{Im}(\rho_{01})$ and $\mathrm{Re}(\rho_{01})$, respectively, versus δ_R. The lineshapes of the absorption coefficient, and the index of refraction versus the laser frequency are given by these plots. Parameters: $\delta_{L2} = 0$, $\Omega_{R1} = \Omega_{R2} = 0.2\,\Gamma_0$ and $\Gamma_{12} = 0.001\,\Gamma_0$.

Very peculiar narrow features appear for the occupation of the $|0\rangle$ upper level in the Λ system when the two-photon condition is satisfied; i.e., around the two-photon Raman resonance condition $\delta_R = \delta_{L1} - \delta_{L2} \simeq 0$. Figure 2a shows numerical results for the steady-state solution of the density matrix ρ_{00}^{st} in the closed Λ system, with values for the Rabi frequencies and relaxation rates as in typical experimental investigations. In fig. 2a, laser 2 is fixed at its resonance value $\delta_{L2} = 0$, whereas laser 1 is swept around its optical resonance. When the two laser field frequencies are scanned around the Raman resonance value, the population of the upper $|0\rangle$ level increases following the Lorentzian profile of the absorption line, and a maximum value of ρ_{00}^{st} is expected with both lasers in resonance. However, a strong decrease occurs in a narrow region around the Raman resonance (whose width is given in § 2.3), where the atoms remain distributed over the lower $|1\rangle$ and $|2\rangle$ levels, without occupation of the upper level; the population of the Λ system is trapped in the lower states. The coherent nature of the trapping cannot be derived from this numerical analysis and requires further physical investigation of the nature of the process. The fluorescent emission from the upper level, which is proportional to the excited-

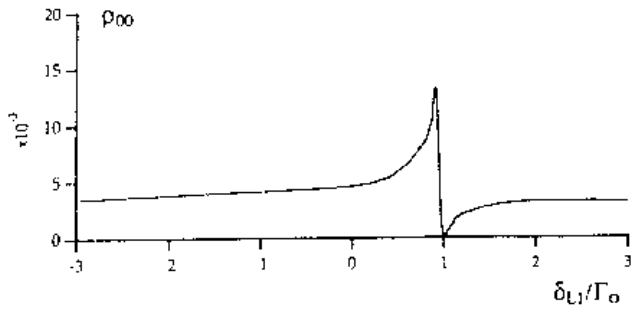

Fig. 3. ρ_{00}^{st} for Λ system as a function of the laser 1 detuning δ_{L1} at $\delta_{L2} = \Gamma_0$; parameters: $\Omega_{R1} = 0.6\,\Gamma_0$, $\Omega_{R2} = 0.1\,\Gamma_0$, and $\Gamma_{12} = 0.001\,\Gamma_0$.

state population, presents a strong resonant decrease at the Raman resonance value, which has been denoted as a dark line by Alzetta, Gozzini, Moi and Orriols [1976]. Away from the Raman resonance, the occupation of the three states is determined by the process of optical pumping (Cohen-Tannoudji and Kastler [1966]). Even if laser 2 is on resonance, when laser 1 is not on resonance, i.e., at large values of $|\delta_R|$, the excited-state population remains small. The optical pumping process by laser 2 transfers all the population to the $|1\rangle$ level. Furthermore, because of the optical pumping redistribution among the three levels, the results of fig. 2a do not depend on the initial level populations.

Figure 3 reports a similar numerical analysis for the excited-state population in the Λ system with laser 2 fixed at a value not corresponding to the optical resonance ($\delta_{L2} \neq 0$), and scanning the frequency of laser 1 around the resonance Raman condition $\delta_R = 0$, i.e., $\delta_{L1} = \delta_{L2}$. Because of the detuning of laser 2 from the optical resonance, at the optical resonance for laser 1, $\delta_{L1} = 0$, i.e., $\delta_R = -\delta_{L2}$, some population is transferred to the upper state, with a limit imposed by the optical pumping. However, at the Raman resonance, coherent population trapping is again produced and a drastic decrease in the excited-state occupation takes place. It can be barely noticed from the data of fig. 3, that the minimum of the excited-state occupation does not take place precisely at $\delta_R = 0$ but presents a shift from that value. That shift, the ac Stark shift or light shift, appears when the lasers are not in resonance with the optical transitions, and originates from a modification in the energies of the atomic levels through nonresonant transitions (see Cohen-Tannoudji, Dupont-Roc and Grynberg [1992]). That light shift is exactly equal to the term $\widehat{S}_{light}$ that appears in the denominator of the two-photon operator $\widehat{T}$, so that the Raman resonance occurs at:

$$\delta_R = \widehat{S}_{light}. \tag{2.12}$$

In fig. 3, the occupation of the excited-state population versus the Raman

detuning presents a large increase on one side of the coherent population-trapping dip. That anomalous increase of upper state population was detected by Alzetta, Moi and Orriols [1979] as an increase in the emitted fluorescence in their first experimental observation of coherent population trapping, and was described as a bright line, in contrast to the dark line in the fluorescence emission corresponding to the trapping process. Radmore and Knight [1982] also pointed out the presence of that dispersive feature and investigated its dependence on the laser parameters. A physical explanation for the appearance of that peak in the excited-state population has been derived by Lounis and Cohen-Tannoudji [1992] through the quantum interference described in § 2.5, and the peak characteristics have been examined in the theoretical and experimental analyses of Janik, Nagourney and Dehmelt [1985], Hemmer, Ontai and Ezekiel [1986], and Siemers, Schubert, Blatt, Neuhauser and Toschek [1992]. Hemmer, Ontai and Ezekiel [1986] compared, with good agreement, experimental and theoretical lineshapes. Siemers, Schubert, Blatt, Neuhauser and Toschek [1992] investigated the dependence of the bright line peak resonance on the intensities of the lasers. That bright line peak appears also in the cascade scheme, as in experimental and theoretical observations by Kaivola, Bjerre, Poulsen and Javanainen [1984] and Gea-Banacloche, Li, Jin and Xiao [1995].

The narrow resonance produced by the coherent population-trapping phenomenon may also be observed on the absorption coefficient α or on the index of refraction n for each of the two laser fields acting on the three-level system. α and n are derived from the imaginary and real parts of the susceptibility, χ'' and χ', respectively, that connect the optical polarization P to the applied electric field (Sargent, Scully and Lamb Jr [1974]). The complex polarization of N atoms or molecules associated with the atomic transitions $|1\rangle \rightarrow |0\rangle$ and $|2\rangle \rightarrow |0\rangle$ is given by:

$$P = N(\mu_{01}\rho_{01} + \mu_{02}\rho_{02}) + \text{c.c.} \tag{2.13}$$

The Fourier components at frequencies ω_{Li} $(i = 1, 2)$ are given by:

$$P(z, \omega_{Li}) = \varepsilon_0 \left(\chi'(\omega_{Li}) + i\chi''(\omega_{Li})\right) \mathcal{E}_{Li}(z). \tag{2.14}$$

The above equation leads to:

$$\chi'(\omega_{Li}) = \frac{N}{2\varepsilon_0 \hbar \mathcal{E}_{Li}} (\mu_{0i}\rho_{0i} + \text{c.c.}), \qquad \chi''(\omega_{Li}) = \frac{N}{2i\varepsilon_0 \hbar \mathcal{E}_{Li}} (\mu_{0i}\rho_{0i} - \text{c.c.}), \tag{2.15}$$

The dependence of the real and imaginary parts of the optical coherences ρ_{0i} on the laser frequencies determines the lineshapes of the index of refraction

and of the absorption coefficient of the medium under coherent population-trapping resonance. Figures 2c and 2d show the steady-state values of the imaginary and real parts of ρ_{01}, respectively. The imaginary part in fig. 2c, which determines the absorption coefficient α, has the same lineshape as the excited-state population ρ_{00} of fig. 2a, with an increase around the optical resonance whose linewidth is given by spontaneous emission and saturation broadening, and a narrow decrease in absorption in the central region near the Raman resonance condition. The real part of ρ_{01}, which determines the index of refraction n, presents two dispersion lineshapes, the broad one with linewidth given by spontaneous emission and saturation broadening, and a narrow inverted one, produced by the coherent population trapping, around the Raman resonance, whose width is discussed in § 2.3.

2.3. COUPLED AND NONCOUPLED STATES

A unitary transformation is very useful for understanding the process of coherent population trapping. Let us analyze first the simple case in which the two lower levels, $|1\rangle$ and $|2\rangle$, are degenerate and the two laser fields have the same frequency ω_L and phase ϕ_L. Let us consider the following two orthogonal linear combinations of the lower states in the Λ configuration:

$$|\mathrm{NC}\rangle = \frac{\Omega_{R2}}{G}|1\rangle - \frac{\Omega_{R1}}{G}|2\rangle, \qquad |\mathrm{C}\rangle = \frac{\Omega_{R1}^*}{G}|1\rangle + \frac{\Omega_{R2}^*}{G}|2\rangle, \tag{2.16a}$$

where G is given by

$$G = \sqrt{|\Omega_{R1}|^2 + |\Omega_{R2}|^2}. \tag{2.16b}$$

This defines the noncoupled and coupled states which have the property that, according to the atom–laser interaction Hamiltonian of eq. (2.4), the transition matrix element between $|\mathrm{NC}\rangle$ and $|0\rangle$ vanishes:

$$\langle 0|V_{AL}|\mathrm{NC}\rangle = 0, \tag{2.17a}$$

whereas

$$\langle 0|V_{AL}|\mathrm{C}\rangle = \frac{\hbar}{2}\sqrt{|\Omega_{R1}|^2 + |\Omega_{R2}|^2}\exp[-\mathrm{i}(\omega_L t + \phi_L)]. \tag{2.17b}$$

Consequently, an atom in the noncoupled state $|\mathrm{NC}\rangle$ cannot absorb photons and cannot be excited to $|0\rangle$. For an atom prepared in the $|\mathrm{NC}\rangle$ state, the Schrödinger equation under the Hamiltonian $\mathcal{H}_0 + V_{AL}$ results in:

$$\frac{\mathrm{d}}{\mathrm{d}t}|\mathrm{NC}\rangle = \frac{1}{i\hbar}(\mathcal{H}_0 + V_{AL})|\mathrm{NC}\rangle = 0. \tag{2.18}$$

Thus an atom prepared in $|\mathrm{NC}\rangle$ remains in that state and cannot leave it either by the free evolution (effect of the free Hamiltonian $\mathcal{H}_0$), or by absorption of

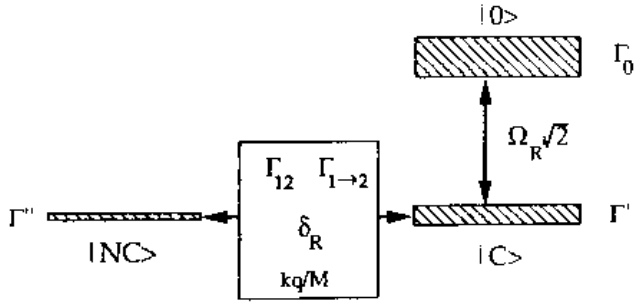

Fig. 4. Couplings and effective loss rates for the states $|0\rangle$, $|C\rangle$, and $|NC\rangle$. $|C\rangle$ is coupled to $|0\rangle$ by the laser interaction, with matrix element $\Omega_R\sqrt{2}$; as a result of this coupling $|C\rangle$ acquires a loss rate Γ'. $|NC\rangle$ and $|C\rangle$ are coupled through ground-state relaxation rates, Raman detuning δ_R, and, for laser cooling, the kinetic energy operator.

a laser photon (effect of the atom–laser interaction V_{AL}). Moreover, because $|NC\rangle$ is a linear combination of the two ground states, and is radiatively stable, the atom cannot leave $|NC\rangle$ by spontaneous emission. The various couplings between $|NC\rangle$, $|C\rangle$, and $|0\rangle$, due to $\mathcal{H}_0$ and V_{AL}, are represented in fig. 4. The $|C\rangle$ and $|0\rangle$ states are coupled by the atom–laser interaction with Rabi frequency G. The excited state $|0\rangle$ has an effective loss rate Γ_0 determined by spontaneous emission. For resonant excitation ($\delta_{L1} = \delta_{L2} = \phi$) and weak-intensity limit ($G \ll \Gamma$), the Rabi coupling between $|C\rangle$ and $|0\rangle$ gives to the state $|C\rangle$ an effective loss rate of

$$\frac{\mathrm{d}}{\mathrm{d}t}\rho_{C,C} = -2\Gamma'\rho_{C,C} = -\frac{G^2}{\Gamma_0}\rho_{C,C}. \tag{2.19}$$

The preparation of the three-level system in the coupled/noncoupled states implies the production of a coherence between the $|1\rangle$ and $|2\rangle$ states, as follows from the relations for the density matrix elements in the two bases:

$$\begin{aligned}
\rho_{C,C} &= \frac{1}{G^2}\left(|\Omega_{R1}|^2\rho_{11} + |\Omega_{R2}|^2\rho_{22} + \Omega_{R1}\Omega_{R2}^*\tilde{\rho}_{12} + \Omega_{R1}^*\Omega_{R2}\tilde{\rho}_{21}\right), \\
\rho_{NC,NC} &= \frac{1}{G^2}\left(|\Omega_{R2}|^2\rho_{11} + |\Omega_{R1}|^2\rho_{22} - \Omega_{R1}\Omega_{R2}^*\tilde{\rho}_{12} - \Omega_{R1}^*\Omega_{R2}\tilde{\rho}_{21}\right).
\end{aligned} \tag{2.20}$$

The time evolution of the coupled/noncoupled states should be completed by the evolution associated with the relaxation processes. The relaxation terms for the time evolution for the density matrix elements in the coupled/noncoupled basis are derived from the density matrix eqs. (2.7). The spontaneous emission decay leads to the following terms:

$$\left.\frac{\mathrm{d}}{\mathrm{d}t}\rho_{C,C}\right|_{sp} = \left.\frac{\mathrm{d}}{\mathrm{d}t}\rho_{NC,NC}\right|_{sp} = \frac{\Gamma_0}{2}\rho_{00}. \tag{2.21}$$

This equation shows that through spontaneous emission the population occupations of the coupled and noncoupled states increase with a rate $\Gamma_0/2$. However, the coupled state $|C\rangle$ experiences the loss rate Γ' because of absorption to the excited state, whereas the noncoupled state is stable against absorption. Then through the process of depopulation pumping of the $|C\rangle$ state and spontaneous emission into the $|NC\rangle$ state, all atoms could be accumulated in the noncoupled state of the coherent population trapping: a pure $|NC\rangle$ state is formed through the irreversible process of spontaneous emission.

It may be surprising to find that the rate of filling the two states $|C\rangle$ and $|NC\rangle$ does not depend on the values of the laser Rabi frequencies that determine the two coherent superpositions of eq. (2.16a). The noncoupled state is made up of two particular laser modes, laser 1 and laser 2, so that it is decoupled from those two modes. On the contrary, in spontaneous emission the decay takes place through emission into all the possible modes of the radiation field, so that no modification of the spontaneous emission process is produced by the coherent population trapping, and in an average over all the emission directions the coupled and noncoupled states are equivalent.

To be precise, the pumping process of the noncoupled state takes place through a more subtle mechanism: the preparation in that state occurs through a filtering process in the selective light absorption (Aspect and Kaiser [1990]). Inverting eq. (2.16), the ground states are written:

$$|1\rangle = \frac{1}{G}\left(\Omega_{R1}|C\rangle + \Omega_{R2}^{*}|NC\rangle\right), \qquad |2\rangle = \frac{1}{G}\left(\Omega_{R2}|C\rangle - \Omega_{R1}^{*}|NC\rangle\right). \tag{2.22}$$

Within those superpositions $|NC\rangle$ is perfectly stable, whereas $|C\rangle$ is not because of the excitation by the lasers at a rate Γ'. After a long time, compared to $(\Gamma')^{-1}$, the atom will be either in $|NC\rangle$ where it will remain trapped, or it will be involved in some absorption and fluorescence cycle. Thus, this selective light absorption process acts as a filter and leaves a fraction of the atoms (determined by the Rabi frequencies) in the noncoupled state, bringing the remaining ones into absorption/fluorescence cycles. The optical pumping into the noncoupled state arises from the filtering process in laser absorption. The physical mechanism involved in the filtering process is the laser interaction that builds up a coherence between the $|1\rangle$ and $|2\rangle$ states. From the solution of the Schrödinger equation for the three-level system under the Hamiltonian $\mathcal{H}_0 + V_{AL}$ and the relaxation processes, as shown by Agap'ev, Gornyi and Matisov [1993] and Scully [1994], it is possible to examine the filtering process starting from each atomic state.

When the decay rate Γ_{12} of the ground state coherence and the $\Gamma_1 = \Gamma_2 = \Gamma_p$ population losses, with $\Gamma_{1\to 2} = \Gamma_{2\to 1} = 0$, are included into the density matrix

equations, one arrives at the equations reported here for the simple case of $\Omega_{R1} = \Omega_{R2}$:

$$\begin{aligned}
\frac{d}{dt}\rho_{C,C}|_{rel} &= -\frac{\Gamma_{12}}{2}\left(\rho_{C,C} - \rho_{NC,NC}\right), \\
\frac{d}{dt}\rho_{NC,NC}|_{rel} &= -\frac{\Gamma_{12}}{2}\left(\rho_{NC,NC} - \rho_{C,C}\right), \\
\frac{d}{dt}\rho_{C,NC}|_{rel} &= -\frac{\Gamma_{p}}{2}\left(\rho_{C,NC} + \rho_{NC,C}\right) - \frac{\Gamma_{12}}{2}\left(\rho_{C,NC} - \rho_{NC,C}\right).
\end{aligned} \tag{2.23}$$

From these equations it appears that the states $|NC\rangle$ and $|C\rangle$ are coupled through the ground-state relaxation processes, so that the coherent population trapping in the $|NC\rangle$ state is limited by those relaxation processes.

The last limiting factor in the preparation of the coupled/noncoupled states is the laser detuning from the Raman condition. This part of coupled/noncoupled evolution is derived by applying an adiabatic elimination of the optical coherence and of the excited-state occupation under the assumption that the Rabi frequencies are small compared to spontaneous emission decay. If the laser frequencies are not in resonance with the optical transitions, but their detunings δ_{L1} and δ_{L2} are small compared to Γ_0, the evolution of ground state populations and coherence results in:

$$\begin{aligned}
\frac{d}{dt}\rho_{C,C} &= -\frac{d}{dt}\rho_{NC,NC} = \frac{i}{2}\delta_R\left(\rho_{NC,C} - \rho_{C,NC}\right), \\
\frac{d}{dt}\rho_{C,NC} &= -\frac{i}{2}\delta_R\left(\rho_{NC,C} - \rho_{C,NC}\right).
\end{aligned} \tag{2.24}$$

Figure 4 shows the ground-state relaxation and the Raman detuning δ_R as the loss mechanisms between the coupled and noncoupled states. Figure 2b shows the occupation $\rho_{C,C}$ and $\rho_{NC,NC}$ of the coupled and noncoupled states for the same conditions as fig. 2a. It may be noticed that at the Raman resonance condition the entire population is concentrated in the noncoupled state, and that the occupation of the coupled state, given by the ratio between the ground-state relaxation rates and the spontaneous emission rate, is very small. From eqs. (2.18)–(2.24) the occupations of the following coupled/noncoupled states are derived:

$$\rho_{NC,NC} - \rho_{C,C} = \frac{\Gamma'}{\Gamma' + \Gamma_{12}} \frac{1}{1 + \left(\frac{\delta_R}{\delta_{1/2}}\right)^2}, \tag{2.25a}$$

i.e., for $\delta_{L1}, \delta_{L2} \ll \Gamma_0$, they are described through a Lorentzian lineshape whose halfwidth is

$$\delta_{1/2} = \Gamma' + \Gamma_{12}. \tag{2.25b}$$

These expressions show that the coherent population-trapping resonance is modified at $\Gamma' \approx \Gamma_{12}$, i.e., when the laser intensity reaches the value I_c where:

$$I_c = \frac{c\hbar^2}{4\pi} \frac{\Gamma_0 \Gamma_{12}}{\mu_{01}\mu_{02}}. \tag{2.26}$$

The coherence saturation intensity I_c, being determined by the ground-state coherence relaxation rate, is much smaller than the saturation intensity I_s of the optical transition (see Agrawal [1983a], Kocharovskaya and Khanin [1986], Gornyi, Matisov and Rozhdestvensky [1989a]). I_s is given by an expression similar to eq. (2.26), replacing Γ_{12} by Γ_{02}.

2.4. DRESSED STATES

The dressed states are obtained whenever a time-independent matrix is obtained for the Hamiltonian $\mathcal{H}_0 + V_{AL}$. Even if the dressed state description does not include the influence of dissipative processes, it still provides a good understanding of the physical phenomena. In semiclassical theory, a unitary transformation derives a time-independent Hamiltonian for a three-level system (see Series [1978]), and more recently Narducci, Scully, Oppo, Ru and Tredicce [1990], Manka, Doss, Narducci, Ru and Oppo [1991], Glushko and Kryzhanovsky [1992]). Quantization of the laser field is another powerful approach, which has been applied to three-level systems by Cohen-Tannoudji and Reynaud [1977], Radmore and Knight [1982], Swain [1982], and by Dalibard, Reynaud and Cohen-Tannoudji [1987].

In the case of an asymmetric Λ system with an energy separation between the ground states and with different laser frequencies, the wavefunctions of the three-level system may be written as:

$$\begin{aligned} |\psi_i\rangle = &\exp(-i\Lambda_i t)\exp(-iE_1 t/\hbar) \\ &\times \Big\{ C_{i1}|1\rangle + C_{i0}\exp[i(\omega_{L1}t + \phi_{L1})]|0\rangle \\ &+ C_{i2}\exp\{i[(\omega_{L2} - \omega_{L1})t + \phi_{L1} - \phi_{L2}]\}|2\rangle \Big\}, \end{aligned} \tag{2.27}$$

where Λ_i and C_{ij} are determined by imposing the condition that $|\psi_i\rangle$ are the eigenstates of the Hamiltonian $\mathcal{H}_0 + V_{AL}$ (Glushko and Kryzhanovsky [1992]). The phases of the laser fields have been explicitly included into the atomic wavefunctions because of their important role in the noncoupled-state evolution.

The set of states $|\psi_i\rangle$ has an energy $\hbar\Lambda_i$ with respect to that of the $|1\rangle$ state. At the Raman resonance, $\delta_R = 0$, the following eigenvalues are obtained:

$$\Lambda_1 = 0, \qquad \Lambda_{2,3} = \frac{\delta_{L1}}{2}\left[1 \pm \left(1 + \frac{G^2}{\delta_{L1}^2}\right)^{1/2}\right]. \tag{2.28a}$$

with wavefunction $|\psi_1\rangle = |\mathrm{NC}\rangle$):

$$\begin{aligned} |\psi_1(t)\rangle &= |\mathrm{NC}(t)\rangle \\ &= \frac{\exp(-iE_1 t/\hbar)}{G}\left(\Omega_{R2}|1\rangle - \Omega_{R1}\exp\{-i[(\omega_{L2} - \omega_{L1})t + \phi_{L2} - \phi_{L1}]\}|2\rangle\right). \end{aligned} \tag{2.28b}$$

State $|\psi_1\rangle$ represents the noncoupled superposition of lower levels which satisfies eq. (2.17a) when the lower states do not have the same energy. In contrast to the symmetrical Λ system, for which the time dependence of the noncoupled state is trivial, here, owing to the time dependence of eq. (2.28b), $|\mathrm{NC}\rangle$ at different times is a different combination of ground states. The dependence of the noncoupled state on the relative phase of the two lasers evidences the requirement on their stability in any experimental situation.

In the quantized field approach, the states are denoted through the atomic quantum number ($i = 0, 1, 2$) and the number of laser photons, n_1 for laser 1, and n_2 for laser 2. The Hamiltonian is written:

$$\begin{aligned} \mathcal{H} = {} & E_1|1\rangle\langle 1| + E_2|2\rangle\langle 2| + E_3|3\rangle\langle 3| \\ & + (\hbar g_{R1} a_{R1}|1\rangle\langle 0| + \hbar g_{R2} a_{R2}|2\rangle\langle 0| + \mathrm{h.c.}), \end{aligned} \tag{2.29a}$$

with the modes at frequencies ω_{R1} (ω_{R2}) characterized by the annihilation and creation operators a_{R1} and $a_{R1}^\dagger$ (a_{R2} and $a_{R2}^\dagger$). For radiation fields with large n_1 and n_2 photon numbers, the constants g_{R1} and g_{R2} of the interaction Hamiltonian give matrix elements equivalent to those of eq. (2.4):

$$g_{R1}\langle n_1|a_{R1}|n_1 + 1\rangle = \frac{\Omega_{R1}}{2}, \qquad g_{R2}\langle n_2|a_{R1}|n_2 + 1\rangle = \frac{\Omega_{R2}}{2}. \tag{2.29b}$$

These matrix elements define a closed family $\mathcal{F}(n_1, n_2)$ whose states are coupled through the absorption and stimulated emission processes:

$$|1, n_1 + 1, n_2\rangle, \quad |0, n_1, n_2\rangle, \quad |2, n_1, n_2 + 1\rangle. \tag{2.30}$$

Eigenstates of the dressed-state quantized Hamiltonian of eq. (2.29a) are linear combinations of these states. Simple expressions may be derived in

relevant cases. At the Raman resonance and laser resonance $\delta_{L1} = \delta_{L2} = \delta_R = 0$ with $\Omega_{R1} = \Omega_{R2} = \Omega_R$, the eigenstates within the family $\mathcal{F}(n_1, n_2)$ are (Cohen-Tannoudji and Reynaud [1977]):

$$
\begin{aligned}
|\mathrm{NC}\rangle &= \frac{1}{\sqrt{2}}\left(|1, n_1 + 1, n_2\rangle - |2, n_1, n_2 + 1\rangle\right), \\
|s\rangle &= \frac{1}{2}\left(|1, n_1 + 1, n_2\rangle + |2, n_1, n_2 + 1\rangle\right) + \frac{1}{\sqrt{2}}|0, n_1, n_2\rangle, \\
|t\rangle &= -\frac{1}{2}\left(|1, n_1 + 1, n_2\rangle + |2, n_1, n_2 + 1\rangle\right) + \frac{1}{\sqrt{2}}|0, n_1, n_2\rangle,
\end{aligned}
\tag{2.31a}
$$

with eigenenergies

$$
E_t = -\frac{\hbar\Omega_R}{\sqrt{2}}, \qquad E_{\mathrm{NC}} = 0, \qquad E_s = \frac{\hbar\Omega_R}{\sqrt{2}}. \tag{2.31b}
$$

The dressed state $|\mathrm{NC}\rangle$ of eq. (2.31a), corresponding to the semiclassical $|\mathrm{NC}\rangle$ state defined in § 2.3, presents a similar interference in the absorption process. The $|\mathrm{C}\rangle$ state does not have a correspondence with the $|t\rangle$ and $|s\rangle$ dressed states, because it has been derived under the assumption of weak laser fields. Equation (2.31b) shows that the noncoupled state is not perturbed in its energy, whereas the other states experience an energy shift. The equidistance of the $|t\rangle$ and $|s\rangle$ from $|\mathrm{NC}\rangle$ is a consequence of the simplifying assumption of one- and two-photon resonance conditions. The spontaneous emission process produces a jump from the states $|s\rangle$ and $|t\rangle$ of the $\mathcal{F}(n_1, n_2)$ family to one with a lower energy, $\mathcal{F}(n_1 - 1, n_2)$ or $\mathcal{F}(n_1, n_2 - 1)$ (Cohen-Tannoudji, Zambon and Arimondo [1993]). If the $|\mathrm{NC}\rangle$ state is reached after a spontaneous emission, the time evolution stops because $|\mathrm{NC}\rangle$ is stable against laser absorption and spontaneous emission. Cohen-Tannoudji and Reynaud [1977] have shown how the relaxation processes may be included into the dressed-state evolution to determine the occupations of the atomic states.

In the analysis by Narducci, Doss, Ru, Scully, Zhu and Keitel [1991] for lasing without inversion in an asymmetric Λ system, the two lasers acting on the two arms of the Λ system had the same frequency, nearly halfway between the two optical transitions, i.e., $\delta_{L1} = -\delta_{L2} \approx \omega_{21}/2$, as in fig. 5a. The coherent population trapping in this configuration may be explored either by changing the laser frequency, as in lasing without inversion experiments, or by modifying the frequency separation ω_{21} between the lower levels, for instance by applying a magnetic field to the three-level system. Numerical results of that coherent population trapping are shown in fig. 5b for the occupation ρ_{00}^{st} versus the laser

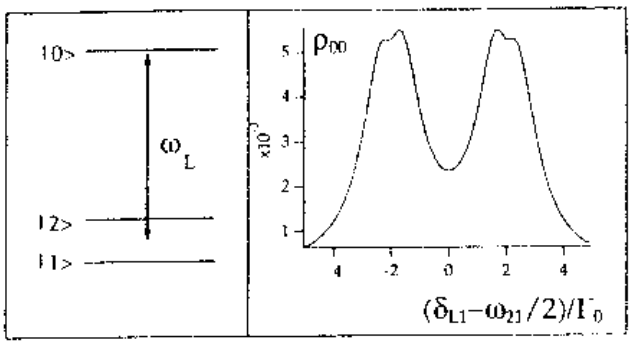

Fig. 5. (a) Schematic level diagram for coherent population trapping with a single laser of frequency ω_L acting on the three-level system; (b) ρ_{00}^{st} as a function of laser detuning $\delta_{L1} = -\delta_{L2}$; parameters: $\omega_{21} = 4\,\Gamma_0$, $\Omega_{R1} = \Omega_{R2} = 0.2\,\Gamma_0$, and $\Gamma_{12} = 0.1\,\Gamma_0$.

frequency, at fixed ω_{21} separation. The decrease at the center is evidence for the presence of coherent population trapping.

2.5. QUANTUM INTERFERENCES

The dispersion lineshape presented in fig. 3 of the excited-state population versus the laser frequency is very similar to the Fano lineshape produced when a discrete state is coupled to a continuum, as in the autoionizing resonances (Fano [1961]). In that case the quantum interference between discrete and continuum excitations produces an asymmetric characteristic lineshape. The connection between coherent population trapping and Fano lineshape has been worked out by Lounis and Cohen-Tannoudji [1992]. Their analysis treated a Λ system, in the case of $\Omega_{R1} \ll \Omega_{R2}$, and determined the absorption of the weak Ω_{R1} probe at frequency ω_{L1}, as perturbed by a strong Ω_{R2} field. They examined the different contributions to the ω_{L1} absorption cross section produced by the scattering of one ω_{L1} photon from the initial state $|1\rangle$, with decay back to that state emitting a spontaneous emission photon of frequency ω_L. Because the excited-state population is proportional to that scattering cross section, the determination of the physical processes contributing to the cross section provided a physical interpretation for the frequency dependence of the excited-state population.

The simplest process for ω_{L1} absorption, with transfer of an atom to the excited state $|0\rangle$ and decay back to the $|1\rangle$ state by spontaneous emission of photon ω_L, is represented by fig. 6a. A similar atomic evolution may take place through a stimulated Raman process, bringing the atom from $|1\rangle$ to $|2\rangle$ with absorption of ω_{L1} and stimulated emission of ω_{L2}, followed by

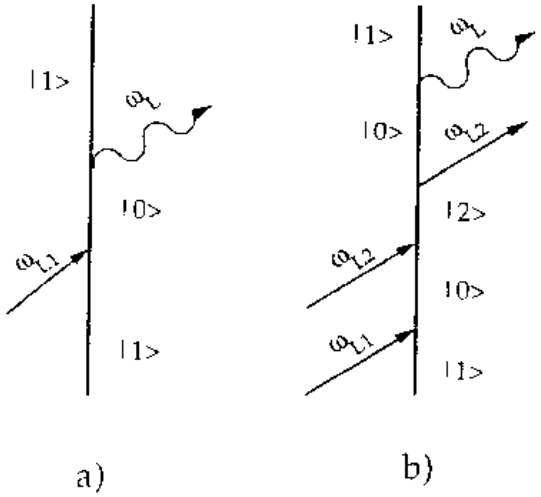

Fig. 6. Diagrammatic representation of the scattering processes of an ω_L photon for an atom in initial state $|1\rangle$ and absorbing one ω_{L1} photon, in the presence of a strong ω_{L2} field. The interference between the two diagrams produces a dispersion-like Fano profile in the excited-state population.

another spontaneous Raman process from $|2\rangle$ to $|1\rangle$ with ω_{L2} absorption and ω_L spontaneous emission, as in fig. 6b. When the contribution of the ω_{L2} photons is considered nonperturbatively to all orders, this second process leads to a scattering amplitude comparable to or even larger than the amplitude of the first path. However, the second path interferes with the first one, and that destructive interference between the two diagrams of fig. 6 produces at $\delta_R = 0$ a zero value for the scattering cross section and also for the excited-state population, neglecting ground-state relaxation processes. Moreover, that interference creates the asymmetric lineshape for the case $\delta_{L1}, \delta_{L2} \neq 0$.

A similar destructive interference between diagrams occurs for $\Omega_{R2} \ll \Omega_{R1}$, in the case of initial occupation of the $|2\rangle$ state: thus, in the general case of comparable Rabi frequencies, both interferences play an important role in determining the lineshape associated with coherent population trapping. Another key feature of the phenomenon is the atomic preparation in a coherent superposition of the two ground states, the coupled/noncoupled states; additional interferences, constructive or destructive for the two superpositions, respectively, occur between symmetric scattering processes starting from each of the ground states. The difference between the Fano lineshape interference of fig. 6 and the interference of the noncoupled state is that the first one is present for any atomic preparation in the ground state, whereas the noncoupled-state interference requires an atomic preparation in a ground superposition state, and hence

requires a preliminary efficient depopulation pumping or the light filtering process of § 2.3.

2.6. LEVEL CONFIGURATIONS

The simplest atomic level configuration for the realization of coherent population trapping is the $J_g = 1 \rightarrow J_e = 1$ configuration shown in fig. 7a, under the application of σ^+, σ^- laser beams: with those excitations the

$$\left(|J_g = 1, m_J = -1\rangle, |J_e = 1, m_J = 0\rangle, |J_g = 1, m_J = 1\rangle\right)$$

form a closed Λ system (Aspect, Arimondo, Kaiser, Vansteenkiste and Cohen-Tannoudji [1988]). Furthermore, through optical pumping the entire population of the $|J_g = 1, m_J = 0\rangle$ level is transferred into the other states, so that finally the complete population can be trapped in the noncoupled state. Also, the $J_g = 1 \rightarrow J_e = 0$ configuration has a simple Λ structure for the σ^+, σ^- excitation; however, because it is not a closed one, incoherent pumping on the $|J_g = 1, m_J = 0\rangle \rightarrow |J_e = 0\rangle$ transition is required to avoid population loss. The σ^+, σ^- excitation for coherent population trapping can be extended to other level schemes (Hioe and Carroll [1988], Smirnov, Tumaikin and Yudin [1989], Tumaikin and Yudin [1990], Papoff, Mauri and Arimondo [1992]). The basic requirement is an odd number of levels ($N \geqslant 3$) between ground and excited states, with the ground-level number being larger by one than the excited one, so that all excitation channels from the ground levels interfere destructively. For σ^+, σ^- excitation on the $J_g = 2 \rightarrow J_e = 2$ transition, as shown in fig. 7c, the Zeeman-level structure produces two chains of Zeeman levels. The chain marked in the figure, called inverted W or M, contains three ground levels interfering in all transitions to the excited state. In the other chain, not marked in the figure, the ground extreme elements of the chain do not have another channel with which to interfere, so no coherent population trapping can be constructed on that chain. Coherent population-trapping superpositions with σ^+, σ^- are possible on the $J \rightarrow J$ and $J \rightarrow J - 1$ transitions, but not on the $J \rightarrow J + 1$ ones. Additional laser configurations, for instance with elliptical polarized light and Zeeman levels separated by an applied magnetic field, were considered by Tumaikin and Yudin [1990], confirming the above requirements on the angular momenta. The linear superpositions of ground-state wavefunctions corresponding to the different configurations have been reported by Smirnov, Tumaikin and Yudin [1989].

Use of σ and π light produces additional trapping superpositions; this scheme applied to the $J_g = \frac{1}{2} \rightarrow J_e = \frac{1}{2}$ transition allows the preparation of a

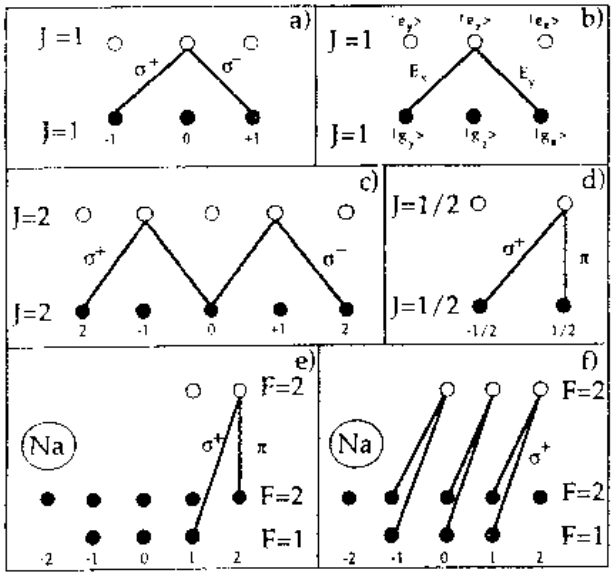

Fig. 7. Optical transitions for coherent population-trapping investigations. (a) and (b) Three-level Λ schemes in the $J_g = 1 \rightarrow J_e = 1$ transition induced by σ^+,σ^- circular polarized, and lin ⊥ lin linearly polarized light, respectively; (c) σ^+,σ^- excitation of the $J_g = 2 \rightarrow J_e = 2$ transition; (d) σ^+,π excitation of $J_g = 1/2 \rightarrow J_e = 1/2$ transition; (e) and (f) different schemes for coherent population trapping between the hyperfine levels of Na using D_1 excitation (by Alzetta, Gozzini, Moi and Orriols [1976] and Fry, Li, Nikonov, Padmabandu, Scully, Smith, Tittel, Wang, Wilkinson and Zhu [1993], respectively).

trapping superposition involving Zeeman levels with $\Delta m_J = 1$, as in fig. 7d. A combination of σ and π light is obtained when in the presence of a magnetic field defining the quantization axis, a circularly polarized laser beam makes an angle α different from 0 or $\frac{1}{2}\pi$ with the magnetic field direction. That configuration of laser propagation in the presence of an applied magnetic field was used by Alzetta, Gozzini, Moi and Orriols [1976], Alzetta, Moi and Orriols [1979], and Xu [1994] in sodium investigations. Their level scheme is shown in fig. 7e: the ground Zeeman levels of the trapping superposition were $(|3^2S_{1/2}, F = 1, m_F = 1\rangle, |3^2S_{1/2}, F = 2, m_F = 2\rangle)$ making a closed Λ scheme with the excited $|3^2P_{1/2}, F = 2, m_F = 2\rangle$ level under σ^+,π excitation. Another sodium-level configuration for coherent population trapping between ground hyperfine states has been used by Fry, Li, Nikonov, Padmabandu, Scully, Smith, Tittel, Wang, Wilkinson and Zhu [1993] in the context of lasing without inversion. The scheme, shown in fig. 7f, is based on two σ^+ lasers generating a trapping superposition for each couple of levels $(|3^2S_{1/2}, F = 1, m_F\rangle, |3^2S_{1/2}, F = 2, m_F\rangle)$ with $(m_F = -1, 0, 1)$. Several coherent trapping superpositions are created simultaneously in the ground state, and

all of them contribute independently to the nonabsorption from ground state. The Λ schemes of this configuration are open, i.e., with spontaneous emission from the excited state of one Λ scheme to ground levels not belonging to that scheme. Thus, the ground state coherence created within a given interaction time is reduced. Using the D_2 resonance line in alkalis, $F \to F + 1$ transitions are excited, so that a completely destructive interference does not take place, and the preparation of coherent population-trapping superposition is not so efficient as for the D_1 resonance (Alzetta, Moi and Orriols [1979], de Lignie and Eliel [1989], Eliel and de Lignie [1989,1990], Eliel [1993]).

For an angular momentum of $J = 1$, the wavefunction describing the Zeeman levels has three components and can be treated as a vector. This leads to interesting symmetry properties for transitions involving a $J = 1$ state. For those states a linear atomic basis can be defined with respect to the eigenvectors $|J = 1, i\rangle$ $(i = x, y, z)$ with zero eigenvalue of the operators $\hat{J}_i$ $(i = x, y, z)$ (Mauri and Arimondo [1991, 1992], Arimondo [1992]). The $|J = 1, x\rangle$ and $|J = 1, y\rangle$ states are the symmetric and antisymmetric combinations of the $|J = 1, m_J = -1\rangle$ and $|J = 1, m_J = 1\rangle$ states, respectively. The convenience of the linear atomic basis results when we consider the selection rules for transitions induced by a laser field E_j linearly polarized along the j axis, as for $J_g = 1 \to J_e = 1$:

$$\langle J_e = 1, i | E_j | J_g = 1, k \rangle = C\varepsilon_{ijk} \qquad (i = x, y, z), \tag{2.32a}$$

where C is a constant depending on the oscillator strength and ε_{ijk} is the third-rank unit antisymmetric tensor. The transitions induced by linearly polarized electric fields, for the $J_g = 1 \to J_e = 1$ case, are marked in fig. 7b. It turns out that coherent population-trapping superpositions with Λ schemes may be formed using orthogonally linearly polarized lasers. For the $J_g = 1 \to J_e = 0$ transition the linear atomic basis leads to the selection rules:

$$\langle J_e = 0 | E_j | J_g = 1, k \rangle = C\delta_{jk} \qquad (i = x, y, z), \tag{2.32b}$$

where δ_{jk} is the Kronecker delta.

The Hanle effect for the ground state (Hanle [1923], Corney [1977]) is closely related to the preparation of the coherent population-trapping superposition, and its lineshape is that of fig. 2a (McLean, Ballagh and Warrington [1985]). The Hanle effect occurs when an optical transition, excited by a single optical frequency radiation, is split into its Zeeman components by an applied magnetic field B. At zero magnetic field the Zeeman levels are degenerate, and the interaction with the radiation is described through a two-level system. For an applied

magnetic field different from zero, the Zeeman structure becomes relevant, and coherent superpositions of the Zeeman levels can be created. A resonance is observed when scanning the magnetic field around the zero value and monitoring the fluorescence emitted under irradiation by light linearly polarized along a direction perpendicular to the magnetic field. The simplest process to analyze is the transition $J_g = 1 \rightarrow J_e = 0$ in the linear basis $(|e_0\rangle, |g_i\rangle \ (i = x,y,z))$, with selection rules given by eq. (2.32b). For light linearly polarized along the x axis, the $|J_g = 1,x\rangle \rightarrow |J_e = 0\rangle$ transition is excited, and optical pumping out of the $|g_x\rangle$ state takes place, bringing atoms to ground states $|g_y\rangle$ and $|g_z\rangle$; as a consequence absorption and fluorescence do not take place. Applying the magnetic field, the states $|g_y\rangle$ and $|g_z\rangle$ become nonstationary because they are not eigenstates of the magnetic field interaction Hamiltonian. Thus, even in the presence of optical pumping, the state $|g_x\rangle$ becomes occupied, and fluorescent emission is observed. The width of the resonance observed around the zero field depends on the ground-state coherence relaxation. For cases where the excited state has an angular momentum larger than zero, the interpretation of the signal becomes more involved because of the coupling by the ground state coherence to the excited-state evolution (Gorlicki and Dumont [1974], Decomps, Dumont and Ducloy [1976]). The coherent superposition of states created in the Hanle effect for magnetic fields different from zero is closely related to the coherent superposition created in the scheme of fig. 5a. A combination of the Hanle effect and excitation by σ, π light, i.e., with the creation of Zeeman coherences and their destruction through a longitudinal pumping, was studied by Ballagh and Parigger [1986] for experiments on the magnetic control of polarization switching by Parigger, Hannaford, Sandle and Ballagh [1985], Parigger, Hannaford and Sandle [1986], and Sandle, Parigger and Ballagh [1986], as discussed in § 3.5. The Hanle effect in the excited state has a similar coherent origin, with a similar resonant lineshape, except that the width of the central dip in the resonance fluorescence is determined by the optical linewidth. The nonlinear Hanle effect, introduced by Feld, Sanchez, Javan and Feldman [1974], again produces a resonance centered at zero magnetic field. Because this process has been described through saturation population only, and the creation of coherence between lower levels apparently does not play a role, it will be not analyzed here.

Smirnov, Tumaikin and Yudin [1989] have also considered in their general treatment the case of atomic preparation in a state not interacting with the radiation, but for which the atomic wavefunction is not written as a linear superposition of atomic states. For instance, optical pumping with σ^+ light on a $J \rightarrow J$ transition pumps atoms in the ground $|J, m_J = J\rangle$ state. This state is nonabsorbing, or dark, and is described by a single eigenstate in the atomic

basis with the z quantization axis. However, if considered in the atomic basis with the quantization axis along the x or y axes, that state is represented through a coherent superposition of atomic states. This transformation through different bases, reducing the wavefunction from a coherent superposition of states to a single one or vice versa, has been used in the above treatment of the $J_g = 1 \rightarrow J_e = 0$ Hanle effect. The question arises whether it is always possible to find an appropriate basis where, instead of coherent superposition of states presenting destructively interfering transitions to the excited state, a dark state not excited by the light is obtained. That basis transformation can be found when the atomic states forming the coherent superposition have the same energy and same total angular momentum. When these conditions do not apply, the coherent population-trapping superposition corresponds to the creation of coherences that cannot be eliminated in any basis. The close connection between coherent population-trapping superpositions and dark states also results from the limiting case of eqs. (2.16) when one Rabi frequency is very small compared to the other one (Cohen-Tannoudji, Zambon and Arimondo [1993]). For $\Omega_{R1} \ll \Omega_{R2}$, the coupled and noncoupled states become:

$$|\mathrm{NC}\rangle \approx |1\rangle\,, \qquad |\mathrm{C}\rangle \approx |2\rangle\,. \tag{2.33}$$

Thus, the dark state $|1\rangle$ coincides with the noncoupled state. However, for Ω_{R1} which are very small, but different from zero, the small value of the absorption on the $|1\rangle \rightarrow |0\rangle$ transition arises from the quantum interference of § 2.5.

2.7. DOPPLER BROADENING

Doppler broadening for a three-level laser interaction is treated by means of the ensemble-averaged density matrix $\rho(v, z, t)$, which describes an ensemble of three-level systems at coordinates $\{z, t\}$ moving with velocity v along the z axis of propagation of the laser radiation. For a given z position, the three-level system is described through the velocity-averaged density matrix. The simplest case is for Λ systems moving at constant velocity v, with $z = z_0 + vt$, interacting with two traveling-wave lasers described by $\mathcal{E}_{L1}\boldsymbol{u}_1 \{\exp[\mathrm{i}(\omega_{L1}t - k_1 z + \phi_1)] + \mathrm{c.c.}\}/2$ and $\mathcal{E}_{L2}\boldsymbol{u}_2 \{\exp[\mathrm{i}(\omega_2 t - k_2 z + \phi_2)] + \mathrm{c.c.}\}/2$, with wavenumbers k_1 and k_2. The atom-laser interaction Hamiltonian V_{AL} of eq. (2.4) is slightly modified and the unitary transformation of eq. (2.6) to eliminate the fast time dependence of the out diagonal density matrix elements becomes:

$$\begin{aligned} &\tilde{\rho}_{0i} = \rho_{0i}\exp[-\mathrm{i}(k_i z_0 + k_i v t - \omega_{Li} t - \phi_i)] \quad (i = 1, 2), \\ &\tilde{\rho}_{12} = \rho_{12}\exp\{\mathrm{i}\,[(k_1 - k_2)z_0 + (k_1 - k_2)vt - (\omega_{L1} - \omega_{L2})t - (\phi_1 - \phi_2)]\}\,. \end{aligned} \tag{2.34}$$

Thus, for each class with velocity v, the laser detunings are modified in order to include the Doppler shift:

$$\delta_{L1}(v) = \omega_{L1} - \omega_{01} - k_1 v, \tag{2.35a}$$

$$\delta_{L2}(v) = \omega_{L2} - \omega_{02} - k_2 v, \tag{2.35b}$$

$$\delta_R(v) = \omega_{L1} - \omega_{L2} - (\omega_{01} - \omega_{02}) - (k_1 - k_2) v. \tag{2.35c}$$

where the Doppler shifts on the two transitions have the same sign for copropagating lasers and opposite signs for counterpropagating lasers. By using those velocity-dependent detunings, the steady-state solutions of § 2.1 may be used to describe the density matrix elements of each velocity class. If the copropagating lasers acting on the Λ system have $k_1 = k_2$, the velocity dependence in the Raman detuning δ_R disappears and all the velocity classes present the Raman resonance at the same values of the laser frequencies. Thus, the configuration with copropagating lasers is the most convenient for investigating experimentally the coherent population trapping in the Λ configuration of a Doppler broadened medium. The copropagating configuration for the Λ system is related to the laser configuration requirement for realizing two transitions without Doppler effect; a compensation of the Doppler shifts occurs for the copropagating configuration in the Λ system and for counterpropagating lasers in the cascade system.

The influence of Doppler broadening on coherent population trapping has been investigated by several authors through numerical calculations for different sets of parameters (Orriols [1979], Kaivola, Thorsen and Poulsen [1985], Manka, Doss, Narducci, Ru and Oppo [1991], Meyer, Rathe, Graf, Zhu, Fry, Scully, Herling and Narducci [1994], Gea-Banacloche, Li, Jin and Xiao [1995]). These results confirm that with Doppler broadening coherent population trapping is preserved, although it is somewhat reduced.

The case of two optical transitions driven by a standing wave laser field requires a much more involved theoretical analysis, as presented by Feldman and Feld [1972]. However, from the experimental point of view, there is no particular advantage to using that configuration except for applications in laser cooling, as discussed in § 5.

2.8. RELAXATION PROCESSES

The relaxation rates Γ_{12}, Γ_i and Γ_{i-j} $(i,j = 1, 2)$ effecting the coherent population trapping have been investigated by McLean, Ballagh and Warrington [1985], Parigger, Hannaford and Sandle [1986], Eliel [1993], Nottelman, Peters

and Lange [1993], and Graf, Arimondo, Fry, Nikonov, Padmabandu, Scully and Zhu [1995]. A detailed analysis of the relaxation processes has never been performed, even though a large amount of results in different experimental conditions has been obtained by Nicolini [1980] and Xu [1994]. For isotropic relaxation, the rates should be expressed through their components in the basis of the irreducible tensorial components of the density matrix (Omont [1977]). Thus, for coherent population trapping in the $J_g = 1$ ground state as illustrated in fig. 7a, the coherence relaxation rate is equal to the alignment decay rate, whereas the population transfer rates depend on the decay rates of both the orientation and the alignment components. For the case of superposition between hyperfine levels, e.g., figs. 7e and 7f, the tensorial component approach is more elaborate. The relaxation rates of the orientation and alignment tensorial components have been measured quite accurately in samarium by Parigger, Hannaford and Sandle [1986].

Because the depopulation pumping between the ground-state coupled and non-coupled states is affected by the relaxation processes, the treatment of relaxation in optical pumping (Cohen-Tannoudji and Kastler [1966], Happer [1972]) should also apply to coherent population trapping. In coherent population-trapping experiments on a Doppler-broadened atomic vapor in a cell, the presence of a buffer gas modifies the creation of the ground-state coherences because (i) the diffusion through the buffer gas increases the interaction time between atoms and radiation, and (ii) the collisions with the buffer gas may destroy the coherence. By using the optical pumping theory, these relaxation processes can be described through the escape rate Γ_t from the laser beam with radius R and collision decay Γ_{coll} produced by the buffer gas:

$$\Gamma_{12} = \Gamma_1 = \Gamma_2 = \Gamma_t + \Gamma_{coll} = 2.405^2 \frac{D_g}{R^2 \left(1 + c\frac{\lambda}{R}\right)} + \Gamma_{coll}, \tag{2.36}$$

where for simplicity the loss rates of populations and coherences are supposed to be equal. In the second equality the escape rate Γ_t depends on the atomic diffusion coefficient D_g in the buffer gas, the mean free path λ, with 2.405 the lowest zero of the zeroth-order Bessel function and c, a numerical constant depending on the kind of collisional process (Happer [1972]). This theory is most appropriate for steady state conditions in experiments in a cell, which should be matched approximately to the zeroth order diffusion mode. In the presence of Doppler broadening of the optical transitions, the effective laser detunings depend on the atomic velocity, as evident from eqs. (2.35). Moreover, through velocity-changing collisions with the buffer gas, the atoms travel back and forth through the velocity space, experiencing different resonance conditions with

the lasers. It is reasonable to suppose that for coherent trapping superpositions between Zeeman or hyperfine levels, the velocity-changing collisions preserve the ground state coherence, because the interatomic potential is insensitive to the nuclear spin orientation involved in the superposition, as pointed out by de Lignie and Eliel [1989]. However, this hypothesis has not been verified. Velocity-changing collisions produce an atomic transfer to velocity classes on the wing of the Doppler profile where an atom is in resonance with only one of the two lasers producing the coherent superposition. Under those conditions the coherent trapping superposition is destroyed by the absorption process (Eliel [1993], Graf, Arimondo, Fry, Nikonov, Padmabandu, Scully and Zhu [1995]), and this process represents an additional loss for ground-state coherence. The dependence of the coherent population-trapping coherences on the buffer gas collisions has been tested experimentally by Xu [1994] and by Nikonov, Rathe, Scully, Zhu, Fry, Li, Padmabandu and Fleischhauer [1994]. Figure 8 presents experimental results obtained by Xu for the strength of sodium coherent population-trapping resonance versus helium buffer gas pressures, as observed on the fluorescent emission, using the level configuration of fig. 7e. Figure 8 evidences a slow decrease of the coherent population-trapping efficiency for helium pressures up to several hundred torr. The experimental results of Nikonov, Rathe, Scully, Zhu, Fry, Li, Padmabandu and Fleischhauer [1994] were obtained in the context of lasing without inversion using the level configuration of fig. 7f; in that case, the dependence of the ground-state coherence on the helium buffer gas pressure was more drastic, and a helium pressure of 10 torr destroyed completely the coherent population trapping. The main difference between the two investigations is the different hyperfine levels involved in the two coherent superpositions. The buffer gas presence enhances optical pumping which with σ^+ light brings atoms into the Zeeman level with the highest m_F number. In the investigations by Alzetta, Gozzini, Moi and Orriols [1976] and Xu [1994], the optical pumping brings atoms into one of the levels involved in the coherent trapping superposition, thereby favoring coherent population trapping. In the investigation by Nikonov, Rathe, Scully, Zhu, Fry, Li, Padmabandu and Fleischhauer [1994], optical pumping brings atoms into a Zeeman level inaccessible for the coherent population-trapping preparation, and thereby inhibits the phenomenon. A fit of the results of fig. 8 with eqs. (2.25) and (2.36) should determine the effective collisional relaxation rate of the ground-state coherence, which would include the role of velocity-changing collisions.

The preceding analysis has been based on two monochromatic radiation fields acting on the three-level scheme: the creation of an atomic coherence in the system arises from the spatial and temporal coherence in the radiation

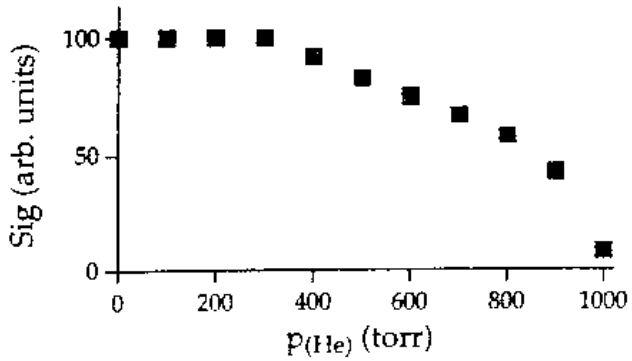

Fig. 8. Experimental results for the signal, in arbitrary units, of the coherent population-trapping resonance in sodium versus the helium buffer gas pressure (from Xu [1994]), with a laser intensity of a few Watts/cm^2 and a laser beam radius $R = 0.17$ cm.

fields, as noted explicitly in eqs. (2.11) and (2.28b). Very relevant to the experimental detection of coherent population trapping is the role played by the laser bandwidth (Dalton and Knight [1982a,b, 1983], Kennedy and Swain [1984], Dalton, McDuff and Knight [1985], Pegg [1986], Mazets and Matisov [1992], Taichenachev, Tumaikin and Yudin [1994]). Dalton and Knight [1982a] examined the effects of laser fluctuations on coherent population trapping using a phase-diffusion model for the laser fields. The laser spectra were considered to be Lorentzian, and a cross-correlation was introduced to describe the relative phase diffusions of the two lasers. The laser bandwidths dephase the atomic coherence, leading to a destruction of the coherent population-trapping superposition. The laser bandwidth may be taken into account in the previous analysis by introducing an effective relaxation rate Γ_{12}^{eff} for the ground state coherence:

$$\Gamma_{12}^{\text{eff}} = \Gamma_{12} + \Delta_{L1} + \Delta_{L2} - 2\Delta_{L1,L2}, \tag{2.37}$$

where Δ_{L1} and Δ_{L2} are the bandwidths of the two lasers, and $\Delta_{L1,L2}$ is the cross-correlated bandwidth. For completely cross-correlated laser beams, as for those generated through frequency modulation from a single source, the cross-correlated bandwidth is equal to the bandwidth of each beam, and the laser bandwidth terms cancel out in eq. (2.37).

2.9. THREE-LEVEL SPECTROSCOPY

In the late 1960s a great effort was devoted to high-resolution spectroscopy in three-level systems owing to their interesting features for saturation Doppler-free spectroscopy. In these systems, besides the resonances associated with

the saturation of the population distribution, additional Raman resonances are produced (Letokhov and Chebotayev [1977]). In the Λ scheme those Raman resonances are obtained when a weak laser field $\mathcal{E}_{L1}$ is applied to one arm of the Λ-scheme and a strong laser field $\mathcal{E}_{L2}$ is applied to the second arm. These Raman resonances have been investigated theoretically (Notkin, Rautian and Feoktistov [1967], Feld and Javan [1969], Hänsch and Toschek [1970], Feldman and Feld [1972]) and have produced very precise experimental determinations (Beterov and Chebotayev [1969], Hänsch, Keil, Schabert and Toschek [1969]). They have the same features as coherent population trapping: they are connected to the creation of a ρ_{12} coherence in the ground state and their characteristics are determined by the relaxation rate Γ_{12} of that coherence. A density-matrix calculation for the absorption coefficient α_{L1} of a weak probe was performed by Feld, Burns, Kühl, Pappas and Murnick [1980] including the excited state decay into the ground states (see also Murnick, Feld, Burns, Kühl and Pappas [1979]). That calculation, in the limit of weak saturation (intensity I_{L1} of laser 1 smaller than coherence intensity I_c), gave:

$$\alpha_{L1} = \alpha_{01}\left[1 + \frac{I_{L1}}{2I_c}\left(\frac{\frac{1}{2}\Gamma_0^2}{\Gamma_0^2 + (\omega_{L1} - \omega_{01})^2} - \frac{\Gamma_{12}^2}{\Gamma_{12}^2 + (\omega_{L1} - \omega_{01})^2}\right)\right], \tag{2.38}$$

with α_{01} the small-signal absorption coefficient of the $|1\rangle \rightarrow |0\rangle$ transition. The lineshape of eq. (2.38) reproduces the coherent population-trapping resonance with a narrow resonant decrease in absorption having linewidth Γ_{12} (the Raman-type contribution produced by the ρ_{12} coherence), superimposed on a broader resonance structure with width Γ_0, representing the population saturation contribution.

§ 3. Spectroscopy for Discrete States

3.1. EARLY EXPERIMENTAL WORK

In the investigation by Bell and Bloom [1961] on sodium optical pumping in a transverse magnetic field, broadband pumping light from a circularly polarized resonance lamp was modulated at a frequency equal to the Zeeman splitting frequency in the ground state of sodium atoms in the MHz range. On the light transmitted through the cell, an optical pumping signal was observed at the modulation frequency. Those observations are evidence of coherent population trapping. The three-level system was composed of two

Zeeman levels in the ground state and one excited level. The modulation of the light source generated sidebands of the pumping light at the modulation frequency. Two neighboring sidebands produced an optical pumping into the noncoupled state, when the sideband separation matched the Zeeman splitting. The transmitted light monitored the noncoupled state preparation as an increase of the transmission at the modulation frequency.

In an experiment by Takagi, Curl and Su [1975], sodium atoms were irradiated by D_1 resonant laser light, containing a central mode and optical sidebands, and an increase in the transparency of the sodium vapor was observed when the frequency separation of the optical sidebands from the central mode matched the Zeeman splitting in the sodium ground state. The signal was analyzed on the basis of populations only, and the creation of a coherence was not considered. This mode-crossing technique, i.e., the simultaneous saturation of two transitions in a three level system, has been used routinely for the determination of molecular structures. However, no evidence related to the creation of ground-state coherence trapping has been reported in those molecular observations. It should be pointed out that in most molecular systems, owing to the high-level degeneracy, the coherences are expected to have a short lifetime, and thus the coherent trapping efficiency is expected to be quite low.

3.2. EXPERIMENTAL EVIDENCE

The first experimental observation by Alzetta, Gozzini, Moi and Orriols [1976] took place in an optical pumping experiment performed on sodium atoms with radiation from a multimode dye laser tuned to the resonant transition between the $3^2S_{1/2}$ ground state and the $3^2P_{1/2}$ excited state. The frequency separation between the laser modes was around 350 MHz, so that the separation between six adjacent modes matched the hyperfine separation of the sodium ground state. The experiment was performed in the presence of a magnetic field B, whose variation allowed matching the laser frequencies to the level separation (see fig. 9). The experimental set-up presented a nice way to make the optical pumping phenomena clearly visible: a magnetic field gradient was introduced along the laser beam to change the splitting of the Zeeman sublevels in the hyperfine states. In this way the coherent population trapping; i.e., the decrease in the excited-state population, appeared as a black line along the fluorescent path of the laser beam across the sodium cell.

Figure 10, from a more recent investigation (Xu [1994]), shows an experimental record of the decrease in fluorescent light at the magnetic field position corresponding to the matching between the laser separation and the sodium level

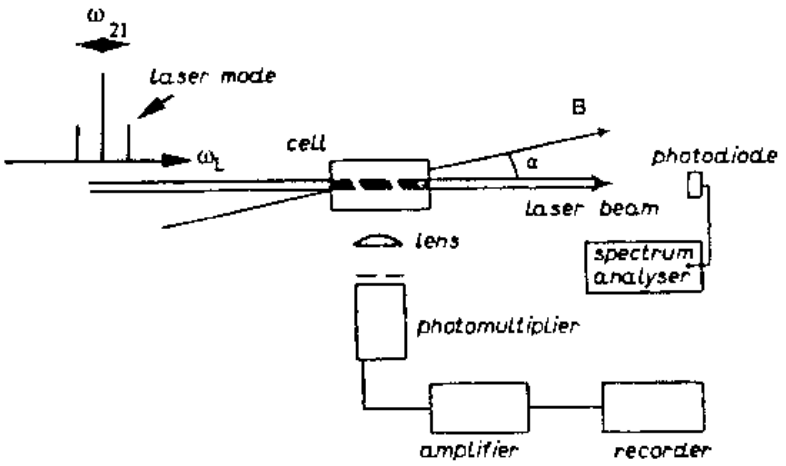

Fig. 9. Sketch of the experimental apparatus used for the observation of coherent population trapping in sodium atoms in the presence of an inhomogeneous magnetic field (adapted from Alzetta, Moi and Orriols [1979]).

splitting. Alzetta, Gozzini, Moi and Orriols [1976] reported atomic preparation in coherent trapping superposition for different values of the magnetic field and different Zeeman sublevels of the sodium hyperfine states. Alzetta [1978], and Alzetta, Moi and Orriols [1979] completed that investigation by reporting a deformation of the fluorescent emission lineshape, similar to that shown in fig. 3, when the laser was tuned within the Doppler profile. In the Xu [1994] investigation, a dye laser with only three modes was used, and the separation between the two external modes matched the sodium hyperfine splitting. The jitter in the frequency separation between the two laser modes producing coherent population trapping was in the 10 kHz range. In order to realize a three-level scheme and optical pumping at the same time, circularly polarized laser light was used. Let us imagine σ^+ with the laser propagation direction at an angle between 0° and 50° with the magnetic field direction. With respect to the magnetic field, the laser light contained σ^+ and π components, and also a σ^- component. The σ^+ and π components produced the atomic superposition of the three levels reported in fig. 7e; the σ^- component did not produce coherent trapping, and, for the angles investigated in the experiment, did not significantly perturb the coherent superposition. Nicolini [1980] and Xu [1994] investigated the width of the coherent population-trapping resonance as a function of the buffer gas and of the sodium relaxation rates. Very narrow features were obtained when the interaction time of the sodium atoms with the radiation fields was increased by expanding the laser beam diameter or adding a buffer gas. Xu [1994] used a special cell whose walls were coated by a polydimethylsiloxane (as

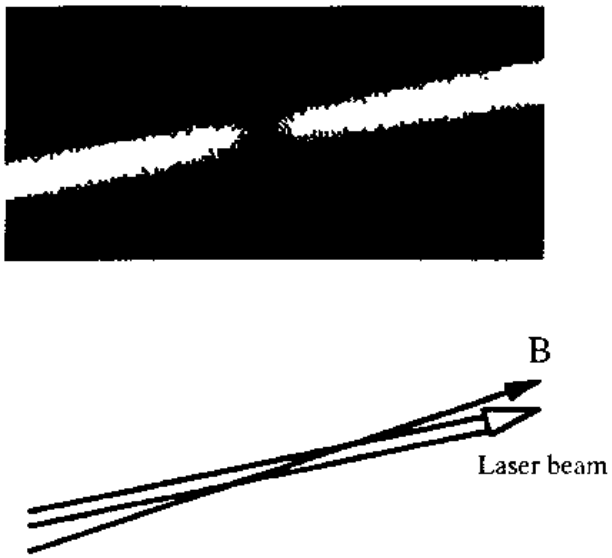

Fig. 10. CCD image of the fluorescence of sodium vapor irradiated by a D_1 resonant multimode laser. A black line in the fluorescence occurs at the magnetic field resonance condition for coherent population trapping (from Xu [1994]). Laser intensity 180 mW on three modes and beam radius $R = 0.075$ cm.

described in Gozzini, Mango, Xu, Alzetta, Maccarrone and Bernheim [1993]), so that even at room temperature the sodium density was large enough for detection of the fluorescence.

Accurate experiments on sodium atoms were performed by Gray, Whitley and Stroud [1978] who used two independent single-mode dye lasers. The decrease in population of the upper level in the coherent trapping conditions was observed as a function of one laser tuning. The experimental observations by that group are reproduced in fig. 11, together with their theoretical analysis, to evidence the very good agreement with the experiment results. The resonant decrease in the excited-state population associated with the coherent population trapping in sodium was examined by Murnick, Feld, Burns, Kühl and Pappas [1979] and by Feld, Burns, Kühl, Pappas and Murnick [1980] using two independent lasers, with resonance linewidth around 6 MHz, determined by the relative frequency fluctuations of the two lasers, as in all experiments with independent sources.

The decrease of the upper-state fluorescence in the three-level system was investigated, both experimentally and theoretically within the context of laser cooling experiments on barium ions in a radiofrequency trap, by Toschek and Neuhauser [1981], Janik, Nagourney and Dehmelt [1985], and Siemers, Schubert, Blatt, Neuhauser and Toschek [1992]. The coherent population-trapping features appeared when, besides the cooling laser at 493 nm from the

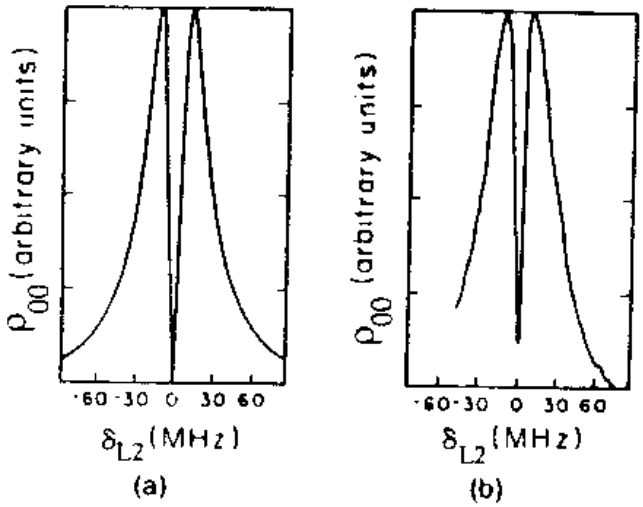

Fig. 11. (a) Theoretical predictions and (b) experimental results for the steady-state excited population ρ_{00} monitored in fluorescence by Gray, Whitley and Stroud [1978] on a sodium atomic beam. One fixed frequency laser was at exact resonance, $\delta_{L1} = 0$, with Rabi frequency $\Omega_{R1} \approx 1.8\,\Gamma_0$. The second laser, with Rabi frequency $\Omega_{R2} \approx 2.9\,\Gamma_0$, was tuned around the resonance value.

$6^2S_{1/2}$ to $6^2P_{1/2}$ states, a second laser at 650 nm was simultaneously applied to the ions in order to avoid the loss of the ions into the metastable $5^2D_{3/2}$ state. The second laser exciting from the $5^2D_{3/2}$ state was required to repump the ions and keep them in interaction with the cooling laser. Janik, Nagourney and Dehmelt [1985] performed an analysis of the coherent trapping lineshape and noticed the reduction in coherent population trapping arising with detuned lasers and different Rabi frequencies. They reported coherent population-trapping resonances associated with the different Zeeman levels split by an applied magnetic field. Schubert, Siemers and Blatt [1989] performed a detailed analysis for the fluorescence lineshapes produced by the ions in the trap illuminated by the two lasers, taking into account the ion motion, and they evidenced lineshape distortions similar to those shown in fig. 3.

The three-level Λ scheme pumped by two copropagating lasers, with the deformation in the resonant lineshape, was carefully investigated by Kaivola, Thorsen and Poulsen [1985]. A fast beam of calcium atoms excited by two red dye lasers was the medium. Very good agreement was realized between the experimental spectra and the Voigt profile obtained from a numerical integration over the velocity distribution of the steady-state ρ_{00} density matrix. A similar careful analysis for fluorescence lineshape in the presence of inhomogeneous broadening, with a comparison to the density equation model, was performed by McLean, Ballagh and Warrington [1985] on the neon

$1s_4(J=1) \rightarrow 2p_3(J=0)$ transition. Their experimental set-up was similar to that used for the Hanle effect in the ground state, as discussed in § 2.6.

Cesium ground-state coherences with excitation based on the different components of the D_2 line in a Hanle-type configuration were created by Théobald, Dimarcq, Giordano and Cérez [1989]. A laser diode source with a 30 MHz linewidth was employed. The linewidth of the coherent population-trapping resonance around zero magnetic field was investigated as a function of several parameters, such as the laser intensity and the interaction time. The authors verified that for the measured linewidth good agreement was obtained with the results of a density matrix numerical calculation including all the cesium levels.

The decay to a metastable level and the use of a second laser to repump atoms from that metastable level also occurred in the study of laser isotope separation of gadolinium by Adachi, Niki, Izawa, Nakai and Yamanaka [1991]. The three-level system was formed by the ground state $6s^2\ ^9D_2$, the excited $6s6p\ ^9F_2$, and the metastable $6s^2\ ^9D_3$. The laser sources employed for the excitation, two narrow-band pulsed dye lasers (with Rhodamine 6G) injected from two continuous wave (c.w.) lasers, presented excellent spectral qualities. Detection was based on ionization of the upper level through a third broad-band laser at the rate Γ_{ion}. The authors noticed that the maximum ionized fraction of gadolinium atoms was around 50%, with this upper limit imposed by the gadolinium pumping into the coherent population-trapping state. In order to avoid trapping and produce the maximum ionization, very different Rabi frequencies Ω_{R1} and Ω_{R2} were used, the two lasers were detuned far from resonance, and finally the Rabi frequencies were equal to the Γ_{ion} rate from the upper level, controlled by the third laser. Those experimental observations evidenced that coherent population-trapping preparation could also be realized on the nanosecond scale, but with Rabi frequencies and excited-state loss rate on an even faster timescale of $\sim 2 \times 10^{-10}$ s.

The decrease in fluorescence from the excited-state population was examined by Young, Dinneen and Mansour [1988] on a Sc^+ beam, with a three-level Λ scheme based on different hyperfine levels of the ground state and generating a sideband through an electro-optic modulation around 140 MHz off the main laser beam.

Continuing with the Λ configuration, coherent population trapping has been examined in rubidium atoms by Akul'shin, Celikov and Velichansky [1991] using two independent laser diodes tuned to the D_1 line. They reported a minimum linewidth of the coherent population-trapping resonance (FWHM) of 70 kHz, which led them to estimate the sum of the two laser linewidths to 50 kHz, with additional broadening contributions from the transit time of the atoms

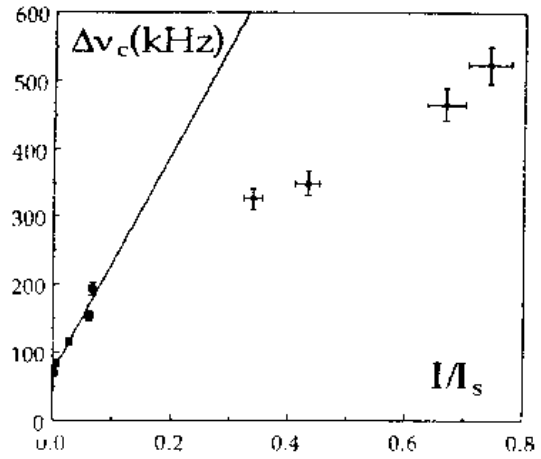

Fig. 12. Data, from Akul'shin, Celikov and Velichansky [1991], for the linewidth $\Delta\nu_c$ of the ^{87}Rb coherent population trapping versus the laser intensity I, in units of the optical transition saturation intensity I_s, and linear fit with the saturation broadening law of eq. (2.25) (from Arimondo [1994]). A coherence saturation intensity $I_c = 70\,\mu W/cm^2$ was obtained from the fit.

through the laser beam and from magnetic field inhomogeneity. That result, the narrowest resonance measured in experiments with cells, represents quite an achievement for an observation with two independent laser sources, and evidences the advances in the stability of laser diodes. In fig. 12 the dependence of the resonance linewidth on the applied laser intensity has been adapted from the original data in order to derive the coherence saturation intensity I_c via eq. (2.26) (Arimondo [1994]). From the fit, I_c is $70\,\mu W\,cm^2$, compared with $I_s = 1.6\,mW\,cm^2$, the saturation intensity of the rubidium D_1 optical transition. Akul'shin, Celikov and Velichansky [1991] reported a maximum contrast C of 60%, the contrast being defined as the ratio of the maximum and minimum in the fluorescence emission, or equivalently in the excited-state occupation. More recently, Akul'shin and Ohtsu [1994] demonstrated frequency pulling by the coherent population-trapping resonance of a rubidium cell within a laser diode cavity, pulling that could be used for the stabilization of the laser frequency. A Λ scheme based on the ground hyperfine $F = 1$ and $F = 2$ $5^2S_{1/2}$ states and excited $5^2P_{1/2}$ $F = 2$ state of ^{87}Rb has been investigated experimentally and compared to theory by Li and Xiao [1995].

A quite different nonoptical method of studying the coherent population trapping of sodium in an atomic beam under D_1 light pumping has been developed by Gieler, Aumayr and Windholz [1992]. Their detection scheme was based on the electron capture of $Na^*(^3P_{1/2})$ atoms by 10 keV He^{2+} projectile ions, with production of He^+ ($n = 5$). The charge-exchanged He^+ ions were

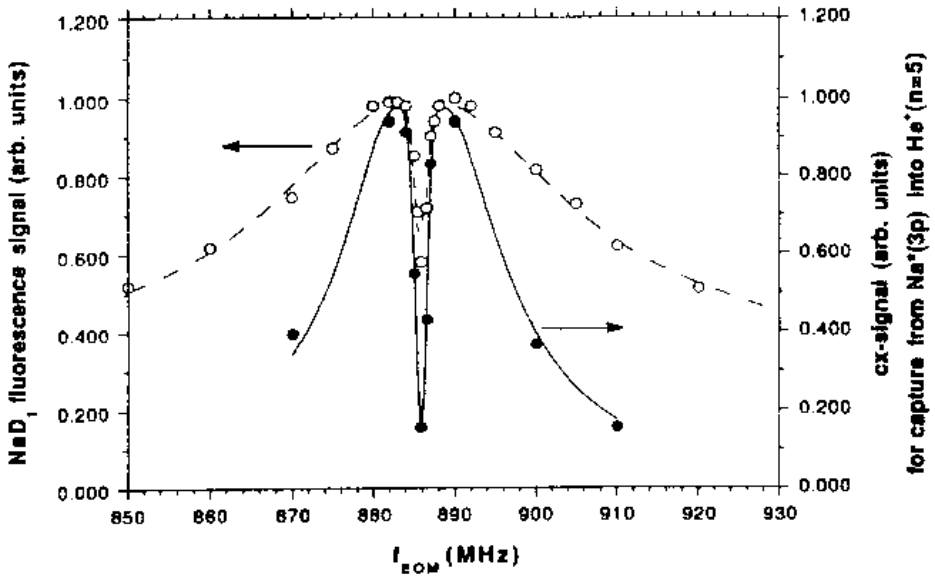

Fig. 13. Sodium coherent population-trapping signals obtained by Gieler, Aumayr and Windholz [1992] on the intensities of the Na D_1 fluorescence (right scale) and of the He^+ ($n=5$) charge exchange from excited $Na^*(^3P_{1/2})$ (left scale), as functions of the microwave frequency applied to the laser electro-optical modulator.

separated from the primary ions by a deceleration lens and measured in their translational energy through an energy analyzer. The three-level excitation of sodium atoms was based on laser light tuned at the center of the hyperfine ground structure, with production of the first sidebands through an electro-optic modulator around 886 MHz (one half the hyperfine splitting). While keeping the dye laser frequency fixed, the microwave frequency was slowly scanned until the separation between the sidebands matched the ground-state hyperfine splitting. The experimental results are shown in fig. 13: both the Na D_1 fluorescence and the charge-exchange signal were monitored. The lineshapes observed on both signals presented a decrease at the center, which is evidence of coherent population trapping. The lineshapes produced by the coherent population trapping were quite different in the two detections. The authors claimed that the difference arose because the charge exchange probed only the central part of the divergent Na beam, whereas the fluorescence detector collected light emitted from sodium atoms present in the Doppler-shifted outer beam regions.

The cascade configuration of fig. 1b has been investigated in an experiment by Kaivola, Bjerre, Poulsen and Javanainen [1984], again on a fast beam of ^{20}Ne atoms in the metastable $3s[3/2]_2$ state. Laser excitation at 592.5 nm to

the $2p'[3/2]_2$ state, and from there at 248.0 nm to the $4d'[5/2]_3$ state, was used. The cascade configuration requires counterpropagating beams in order to realize Doppler-free resonances. Using only one laser, reflected back on itself along the direction of the fast moving ^{20}Ne atoms, the laser frequency ω_L of the copropagating or counterpropagating photons appeared blue- or red-shifted in the rest frame of the atom. Thus the two-photon resonance condition was realized by modifying the velocity of the fast atoms. The fluorescence from the intermediate $|0\rangle$ level was monitored as a function of the laser frequency, and at Rabi frequencies comparable to the spontaneous emission decay rates from the intermediate and upper levels, a narrow dispersion-like structure, similar to the bright line feature of the Λ scheme of fig. 3, was observed on the Doppler-broadened profile of the emitted fluorescence. That dispersion-like structure was not reproduced precisely by the numerical analysis taking into account Doppler line broadening. However, that dip on the fluorescent spectrum from the intermediate level is related to the population trapped into the two terminal states while the intermediate level acquires an anomalously small population. The dispersion lineshape distortion on the cascade configuration has been confirmed by Gea-Banacloche, Li, Jin and Xiao [1995] in experiments on rubidium atoms in a cell using two laser diodes to excite the $5^2S_{1/2}$ $F=3$ to $5^2P_{3/2}$ $F=4$ hyperfine component of the D_2 line at 780 nm and from there the $5^2D_{5/2}$ $F=5$ state with 776 nm radiation, using orthogonal polarizations for the two lasers. The Rabi frequency Ω_{R2} for the laser acting on the upper transition was quite large, with the laser intensity around ten times the optical saturation intensity, so that the linewidth of the coherent population-trapping resonance was determined from that Rabi frequency. The experimental results were fitted through the numerical solution of the density matrix equations, taking the Doppler broadening properly into account. A very good agreement was obtained when the diode laser bandwidth was included in the density matrix equation as an effective relaxation rate Γ_{12}^{eff} [see eq. (2.37)].

3.3. MODULATED AND PULSED LIGHT

The periodic modulation of the laser source for the creation of ground state coherences has been reinvestigated by some authors in a laser version of the Bell and Bloom [1961] work. Mlynek, Drake, Kersten, Frölich and Lange [1981] used an electro-optic modulator to generate low-frequency sidebands on laser light resonant with the sodium D_1 line. The modulation created by the sodium Zeeman coherences was detected on the transmission of a probe laser beam. The periodic modulation of light from a diode laser through an acousto-optic modulator for the

creation of cesium ground-state coherences in the presence of a magnetic field was investigated by Mishina, Fukuda and Hashi [1988]. Their geometry, with light propagating along the z axis of the magnetic field and polarized along the x axis, was similar to a Hanle effect geometry with modulated light. Thus, they detected the production of ground-state coherences either at zero magnetic field or when the modulation frequency matched a Zeeman splitting. The detection scheme was based on the detection by a probe beam of the anisotropy produced by the coherence precession in the magnetic field.

A different set of experiments has been performed using mode-locked lasers with pulses in the nanosecond or picosecond range, whose repetition rate could be precisely controlled. The main idea was to generate and monitor coherences ρ_{21} in Λ- or V-three-level systems. The generation was based on the excitation of atoms by a short pulse of radiation: if the pulse duration τ_p is short compared to the precession time $1/\omega_{21}$, or the Fourier spectral width $1/\tau_p$ of the pulse is large compared to the energy splitting ω_{21}, the pulse creates a ρ_{12} coherence in the atomic system (Mlynek, Drake, Lange and Brand [1979]). In the presence of an applied magnetic field a precession of the coherence takes place, which is detected by the polarization rotation of a probe laser beam. The apparatus used by Mlynek, Lange, Harde and Burggraf [1981] and Harde, Burggraf, Mlynek and Lange [1981] is shown in fig. 14. In those experiments a circularly polarized 10 ps pulse was used to generate hyperfine coherences in the ground and excited states of the sodium D_1 line. The sodium coherences produced a polarization rotation for a probe pulsed laser beam, linearly polarized, and delayed up to 13 ns by a variable optical line. A typical beat structure could be observed on the detected signal as function of the time delay, with Fourier components corresponding to the hyperfine splittings. A modification of the preparation phase allowed a great increase in resolution (Mlynek, Lange, Harde and Burggraf [1981]). The exciting light was composed of mode-locked pulses, and each short pulse, which was broad-band, produced an atomic coherence. If the pulse repetition frequency ω_p matched the evolution frequency ω_{21} of the atomic coherence, the coherence generation and evolution corresponded to a forced oscillation regime with a large improvement in frequency resolution. Because the ground-state atomic coherences have a long decay time, a driving of the atomic coherence could be realized even when the pulse frequency ω_p was a very high subharmonic of the ω_{21} frequency:

$$\omega_{21} = q\omega_p, \tag{3.1}$$

with $q \geqslant 1$. At first, q subharmonic orders up to 7 were realized, but Harde and Burggraf [1982, 1983, 1984] obtained q orders up to 2000. As a consequence,

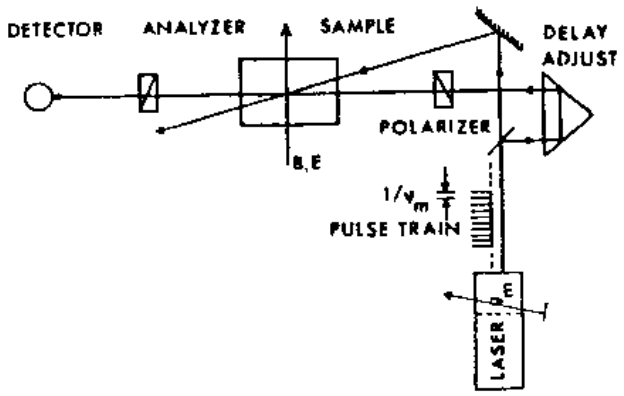

Fig. 14. Schematic of the experimental set-up for the generation and detection of three-level coherences used by Mlynek, Lange, Harde and Burggraf [1981].

the determination of sodium and rubidium ground-state hyperfine splittings and their pressure shifts were comparable in accuracy to that from standard microwave spectroscopy. In order to tune through the resonance condition, either the pulse repetition frequency ω_p was fixed and a magnetic field acting on the sodium atoms modified the energy splitting, or, more appropriately, the repetition frequency was varied.

Experiments with pulse trains were previously performed in the cascade system of fig. 1b, probing the coherence in the optical range generated between the levels $|2\rangle$ and $|1\rangle$ (Teets, Eckstein and Hänsch [1977], Eckstein, Ferguson and Hänsch [1978]). The major difference between the Λ- and cascade schemes is the different sensitivity to the optical phase: in the Λ scheme the ρ_{21} coherence depends on the optical phase difference between the two optical excitation, whereas in the cascade scheme it depends on the sum of the optical phases, as presented explicitly in eq. (2.11). Thus, for the cascade transition the requirements on the optical phase stability between successive laser pulses and the larger linewidth of the coherence resonance do not allow the Λ-scheme accuracy to be attained. The creation of the ground-state coherent population trapping in experiments with pulsed light or a train of ultrashort light pulses was investigated theoretically by Kocharovskaya and Khanin [1986] and Kocharovskaya [1990].

3.4. METROLOGY

In a search for new atomic frequency standards based on optical transitions but not affected by laser jitter and most line-broadening mechanisms, Ezekiel and his colleagues at MIT and the Rome Laboratory of Hanscom Air Force Base have

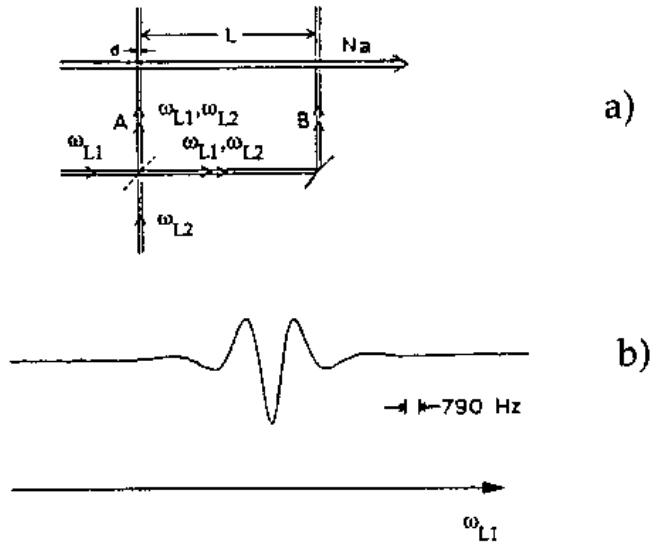

Fig. 15. (a) Schematic of the experimental set-up for obtaining Ramsey fringes in the coherent population-trapping preparation and detection; (b) Ramsey fringes for the sodium $F=1, m_F=0 \rightarrow F=2, m_F=0$ ground hyperfine transition, for a distance $L=30$ cm between preparation and interrogation zones (from Thomas, Hemmer, Ezekiel, Leiby Jr, Picard and Willis [1982]).

used the stimulated resonant Raman transitions in a three-level Λ system based on sodium ground-state hyperfine splitting (see Tench, Peuse, Hemmer, Thomas, Ezekiel, Leiby Jr, Picard and Willis [1981], Thomas, Hemmer, Ezekiel, Leiby Jr, Picard and Willis [1982]). In the resonant Raman transitions, they prepared the ground-state coherent population-trapping superposition using two resonant lasers, and monitored that preparation by light absorption. In order to reduce the transit-time broadening, they used a two-zone excitation for the Raman interaction, as illustrated by fig. 15a. That scheme is analogous to Ramsey's method of separated-microwave field excitation on an atomic beam (Ramsey [1963]). In separated-field excitations the atomic coherence created in the two interaction zones interfere and produce fringes whose widths are characteristic of the atomic transit time between the two zones. In the laser apparatus for obtaining Ramsey fringes, laser radiation at frequency ω_{L2} was obtained from laser radiation at frequency ω_{L1} through an acousto-optic shifter at the sodium hyperfine splitting with excellent frequency stability. The two circularly polarized laser beams were combined on a beam splitter so that they interacted with the sodium atomic beam in a region of 2 mm diameter at positions A and B separated up to $L=30$ cm. Fluorescence from the B region monitored the Ramsey fringes on the $F=1, m_F=0 \rightarrow F=2, m_F=0$ Raman transition. Ramsey fringes with a measured width of 650 Hz (HWHM) were obtained, as reported in fig. 15b. That

value represents the narrowest coherent population-trapping resonance measured so far. The laser power required to saturate the Raman process, 40 μW, was determined from the interaction time. Hemmer, Ontai and Ezekiel [1986] studied the Ramsey fringe detection, and Hemmer, Shahriar, Natoli and Ezekiel [1989] examined the ac Stark shift, or light shift, of the Raman resonances, occurring when the laser fields are detuned from the resonance with the upper state, as shown by eq. (2.12), for the application of the resonance as an atomic clock. A previous theoretical analysis of the light shifts was reported by de Clercq and Cérez [1983].

Hemmer, Ezekiel and Leiby Jr [1983] and Hemmer, Ontai and Ezekiel [1986] stabilized a microwave oscillator using the Ramsey fringes of coherent population trapping in sodium atoms, with a linewidth of 2.6 kHz and a fractional stability of $4\times10^{-10}\,\tau^{-1/2}$, where τ is the averaging time. Hemmer, Shahriar, Lamela-Rivera, Smith, Bernacki and Ezekiel [1993] repeated the experiment on cesium atoms, using a laser diode with microwave sidebands at the cesium ground-state hyperfine splitting. The Ramsey fringes for a 15 cm separation of the interaction zones produced a 1 kHz width, and led the authors to project a $6\times10^{-11}\,\tau^{-1/2}$ frequency stability. Thus, the Ramsey-fringe detection of the coherent trapping evolution has interesting metrological applications.

A nice extension of those Ramsey-fringe investigations was performed by Shahriar and Hemmer [1990]. For a Λ system, the coherent trapping leads to the preparation of an atomic coherence ρ_{21} that, as in eq. (2.6), evolves at angular frequency $\omega_{L1}-\omega_{L2}$, with a phase $\phi_1-\phi_2$ determined by the relative phase of two laser fields. Shahriar and Hemmer [1990] probed, or even perturbed, the evolution of the atomic coherence through the application of a microwave field at the angular frequency $\omega_{L1}-\omega_{L2}$: a microwave field may induce magnetic dipole transitions between the two hyperfine ground levels of sodium. The microwave perturbation was applied in a region intermediate between zones A and B of fig. 15a, with the atomic coherence already formed by the first interaction with the laser fields, before it was probed. When all atoms were prepared in the coherent superposition and the applied microwave field was exactly in phase with their evolution, no deformation of the coherent evolution took place and no modification was detected on the Ramsey fringes in the second zone. In contrast, if the time dependence of the microwave field was out of phase with the coherence time dependence, the atomic evolution was modified by the microwave interaction and detected in the B-zone fringes. In order to have a microwave field with the proper phase with respect to $\phi_1-\phi_2$ established by the lasers, the microwave field was generated by detecting and amplifying the beat between the two optical fields generated on a fast avalanche photodiode. This experiment

confirmed that a pure state of coherent atomic superposition was prepared by the Raman process in the first interaction region.

A three-level system, with optical and microwave radiation fields acting on all the transitions, represents a closed loop system, where the net phase of the fields has a critical effect upon population dynamics. Three-level and four-level closed loops have been examined theoretically by Buckle, Barnett, Knight, Lauder and Pegg [1986], and Kosachiov, Matisov and Rozhdestvensky [1991, 1992a,b]. Buckle, Barnett, Knight, Lauder and Pegg [1986] pointed out that those multilevel loops could be applied in more elaborate Ramsey-fringe interference investigations.

In order to improve the signal to noise ratio in the cesium-based primary frequency standard and therefore its performance, Lewis and Feldman [1981], Lewis, Feldman and Bergquist [1981], and Lewis [1984] proposed the use of two polarized laser fields tuned to hyperfine transitions of the cesium D_2 line to increase the optical pumping of cesium atoms in a specific ground state, either the $F=4$, $m_F=0$ or the $F=3$, $m_F=0$ state. Different polarizations may be used for the two lasers; however, in some cases, for instance when using two linearly polarized lasers, a three-level Λ system is formed. In such cases, the cesium preparation in a coherent population-trapping superposition produced results quite different from the intuitive ones. de Clercq, de Labachellerie, Avila, Cérez and Têtu [1984] examined theoretically cesium pumping with two linearly polarized lasers and stated that because of coherent population trapping the use of two lasers did not produce the expected increase in cesium pumping. In order to avoid coherent population trapping, these authors explored theoretically some interesting alternatives: to eliminate coherent population trapping and still produce an efficient optical pumping, the two monochromatic laser excitations must be applied alternatively, or broadband and uncorrelated laser sources must be used, so that coherence processes could not take place, leaving the optical pumping to increase the population difference.

3.5. OPTICAL BISTABILITY

A novel mechanism for optical bistability, because of the presence of the lower-level coherence, in the three-level Λ system was proposed by Walls and Zoller [1980], Walls, Zoller and Steyn-Ross [1981], and Agrawal [1981]. Walls and Zoller [1980], examining the case of a single laser inducing both optical transitions, mentioned the advantages offered by that system: a lower threshold for the bistability produced by the nonlinear response at laser intensity comparable to I_c, as well as a Doppler-free mechanism for the

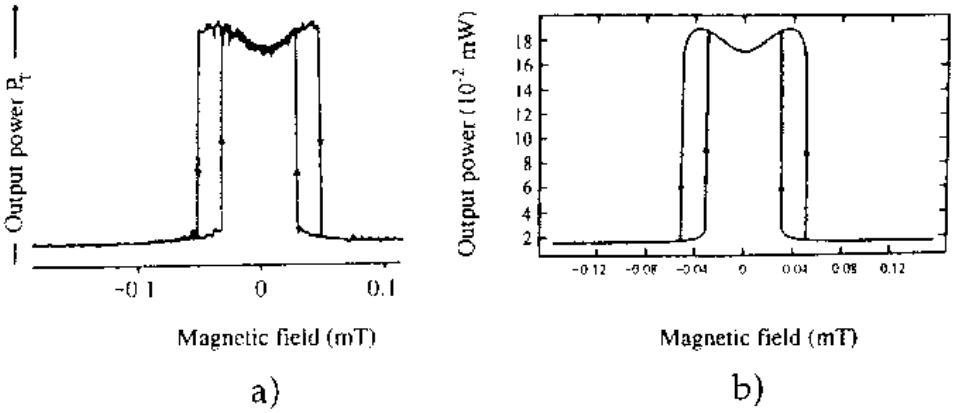

Fig. 16. (a) Measured and (b) calculated dispersive optical bistability of sodium atoms, with argon buffer gas, contained in a Fabry–Perot resonator, as detected in the output power from the cavity (from Mlynek, Mitschke, Deserno and Lange [1984]). For an accurate list of both experimental and theoretical parameters, see original reference

copropagating configuration and the relative insensitivity to the laser phase. Experimental observations of optical bistability for sodium atoms contained in an optical cavity and driven to the coherent trapping superposition, were reported by Mlynek, Mitschke, Deserno and Lange [1982, 1984]. The resonance condition for coherent population trapping was examined through the ground-state Hanle effect. This was performed on the sodium D_1 line with a cell containing a large pressure of argon buffer gas inserted into a Fabry–Perot resonator. Both absorptive and dispersive regimes of optical bistability were examined with the coherent population-trapping atomic response determining both regimes. Experimental results for the dispersive bistability, as observed on the light power transmitted from the sodium filled resonator, are shown in fig. 16a. Figure 16b shows the calculated dispersive bistability. The optical hysteresis in the resonator transmission is quite evident and is well reproduced by the analysis.

A broad triple-peaked profile, observed by Schulz, MacGillivray and Standage [1983] and MacGillivray [1983] on the intensity transmitted from a Fabry–Perot cavity containing sodium vapor, was also interpreted as optical bistability produced by coherent population trapping. A theoretical analysis by Pegg and Schulz [1985] examined the trapping process in the case of a standing wave laser field, considering that an atom, moving along the standing wave, experiences an electric strength frequency modulated because of the atomic velocity. When the frequency of that modulation becomes comparable to the splitting of the lower level in the Λ system, the coherent population-trapping preparation turns out to

depend on the laser intensity. Pegg and Schulz claimed that dispersive effects associated with that intensity-dependent resonance account for the experimental results of Schulz, MacGillivray and Standage [1983], and MacGillivray [1983].

The generation of ground state coherences, and their evolution in the presence of an applied magnetic field, is the origin of another phenomenon of nonlinear dynamics, denoted as magnetically induced polarization switching, which occurs in the same configuration of optical bistability with atoms contained in a Fabry–Perot cavity and illuminated by near resonant laser light. Polarization switching describes the particular atom–cavity response in which a significant asymmetry between the output amplitudes of σ^+ and σ^--polarized waves develops spontaneously, for a given symmetric laser input of the atom–cavity with equal amplitudes of σ^+ and σ^--polarizations, i.e., linearly polarized laser light. In polarization switching, fluctuations in the atom and cavity produce laser-output polarization configurations different from the input one. For no applied magnetic field, an input linear polarization is conserved at the output. The application of a magnetic field to the atoms, parallel to the light propagation direction, produces a circularly polarized output beam. Magnetically induced polarization switching has been studied by Parigger, Hannaford, Sandle and Ballagh [1985], Parigger, Hannaford and Sandle [1986], and Sandle, Parigger and Ballagh [1986] on samarium atoms using the transition from the lower $4f^6 6s^2\ ^7F_1$ state to the upper $4f^6 6s6p\ ^7F_0^0$ state at 570.7 nm; the $J_g = 1 \rightarrow J_e = 0$ transition allows a simple physical interpretation. In the linear basis a linearly polarized input laser light, say E_x, has a very high symmetry, so that at zero magnetic field the output laser beam from the Fabry–Perot resonator preserves that linear polarization. In the presence of a large longitudinal magnetic field B_z, the $|J_g, i\rangle$ $(i = x, y, z)$ states are no longer stationary eigenstates of the atomic Hamiltonian. In this condition the linear symmetry of the input electric field is broken and analysis of the steady state shows that under proper conditions multistability may occur with a circularly polarized laser output from the cavity containing the samarium atoms. In that multistability, an important role is played by the relaxation rate of the ground-state coherences.

3.6. FOUR-WAVE MIXING

Four-wave mixing is a nonlinear optical phase conjugation technique which allows an optical field with well defined optical characteristics to be generated from an absorbing medium. The typical geometry of optical beams applied in backward four-wave mixing is shown schematically in fig. 17a. E_1 and E_2, the pump laser waves, determine the population and coherences of the absorbing

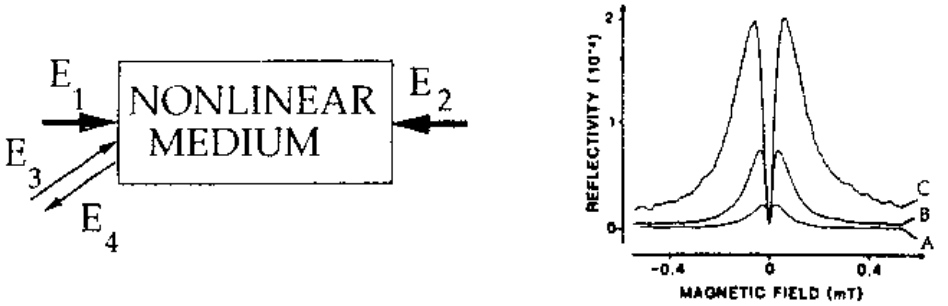

a) b)

Fig. 17. (a) Four-wave mixing geometry for investigating the coherent population-trapping nonlinearity. E_1, E_2, the pump laser waves; E_3, the probe; E_4, the conjugate generated wave. (b) Phase conjugate reflectivity E_4^2/E_3^2 versus transverse magnetic field B for different intensities of the E_1 and E_2 pump waves: (A) 0.09 W/cm^2; (B) 0.26 W/cm^2; (C) 0.94 W/cm^2, for an E_3 probe wave intensity of 0.08 W/cm^2 (Köster, Mlynek and Lange [1985]).

medium. The probe wave E_3 generates the conjugate wave E_4 through the four-wave mixing process. The pump and probe waves create a grating of population and coherences within the medium; i.e., a periodic variation in position and time of populations and coherences. The phase conjugate wave E_4 arises from the scattering of the E_3 wave off that grating. The four-wave mixing is denoted as degenerate if the four waves have the same frequency, as for the cases analyzed here.

In most cases, four-wave mixing is based on the optical nonlinearities created in a saturated two-level medium. Agrawal [1983a,b] pointed out that in a Λ three-level system driven from a single laser, the optical nonlinearities linked to the creation of a Zeeman coherence provides a new mechanism for phase conjugation. Furthermore, he noticed that the coherence saturation intensity I_c of eq. (2.26) allowed four-wave mixing in a three-level system at laser intensities lower than in a two-level system. In his analysis, based on a geometry with pump waves having opposite circular polarization, the E_4 generation efficiency, when plotted versus the lower level Zeeman splitting, presented the characteristic central dip of coherent population trapping.

These theoretical predictions were confirmed by the experimental observations of Mlynek, Mitschke, Köster and Lange [1984], Mlynek, Köster, Kolbe and Lange [1984], Köster, Mlynek and Lange [1985], and Lange, Köster and Mlynek [1986] on four-wave mixing in sodium atoms using a ground-state Hanle-effect geometry. Mlynek, Mitschke, Köster and Lange [1984] tested whether a coherent population-trapping resonance could be observed on the sodium

absorption coefficient by scanning the magnetic field around the zero value. They also measured the phase-conjugate signal on the generated E_4 wave, producing results illustrated in fig. 17b. The characteristic lineshape of coherent population-trapping resonance is evident. The pump intensities applied to the sodium atoms to realize a coherent population-trapping regime were large because the experiment operated on sodium atoms in the presence of a large buffer gas pressure (argon at 170 mbar).

While the observations by these authors were based on nearly resonant laser excitation, another set of experimental observations was performed, always on sodium atoms, using laser light detuned up to 150 GHz from the D_1 and D_2 resonance lines (Bloembergen [1985, 1987], Bloembergen and Zou [1985], Bloembergen, Zou and Rothberg [1985], Zou and Bloembergen [1986]). Because of the large detuning, the excitation to the sodium-excited states relied on the presence of collisions with a buffer gas, helium or argon, so that the phenomenon was denoted as collision-enhanced four-wave mixing. Again, narrow resonances were observed, associated with the production of ground-state coherences precessing in the magnetic field. Careful measurements of the signal intensity versus different experimental parameters such as laser power, laser detuning, and buffer gas pressure were performed.

A time-delayed four-wave mixing experiment was performed by Bouchene, Débarre, Keller, Le Gouët, Tchénio, Finkelstein and Berman [1992a,b] on an atomic vapor of strontium atoms using the $5s^2\,{}^1S_0 \rightarrow 5s5p\,{}^3P_1$ transition at 689 nm. Driven by two linear cross-polarized laser fields, this experiment behaved as the three-level V scheme of fig. 1c. The two pump laser pulses produced a coherent population trapping between the upper states whose decay time, the spontaneous emission-time of the strontium-excited state, was longer than the 10 ns pulse duration. The four-wave mixing signal was measured as a function of the delay time between the applied pump and probe pulses. A coherent population-trapping resonance was observed on the delayed time dependence of the generated four-wave mixing signal. At weak pump Rabi frequencies the trapping resonance linewidth coincided with the frequency bandwidth of the pump lasers, i.e., the inverse of their coherence time, 120 ps. At large pump Rabi frequencies the resonance linewidth was narrower than the pump laser bandwidth. The theoretical analysis by Finkelstein [1991] has shown that at large Rabi frequencies the upper-state coherence contains some transient components with long decay times generating the observed narrow linewidth.

In a recent theoretical analysis Schmidt-Iglesias [1993] has pointed out the possibility of separating within the four-wave mixing signal the contribution

of the coherent population-trapping mechanism from that of other population mechanisms.

3.7. LIGHT-INDUCED DRIFT

In light-induced drift, a transport of a laser-irradiated species inside a buffer gas takes place owing to the difference between ground and excited-state scattering cross sections with a buffer gas (Werij and Woerdman [1988], Eliel [1993]). The phenomenon depends on the number of atoms present in the excited state. Laser irradiation with two resonant laser sources may be employed to avoid hyperfine pumping or loss of atoms to another state as in other cases of spectroscopic investigations. As a consequence, in a three-level system the coherent population-trapping mechanism may be operational, with a large decrease in the excited-state population, and also a decrease in the light-induced drift.

Modification in the light-induced drift due to coherent population trapping using two-laser irradiation has been reported by de Lignie and Eliel [1989], Eliel and de Lignie [1989, 1990], and by Eliel [1993] in measurements on a sodium vapor contained in a capillary cell in the presence of xenon buffer gas. As is standard in sodium experiments, the two lasers excited the transitions from the two ground hyperfine states to either the $3^2P_{1/2}$ or $3^2P_{3/2}$ state. Experimental results for light-induced drift versus the detuning of laser 2, with laser 1 fixed in frequency, are reported in figs. 18a and 18b for the D_1 and D_2 excitation, respectively. The two single-mode lasers had orthogonal polarizations. Notice that in both experiments laser 1 was not in resonance, but detuned to the red side of the absorption transition, because light-induced drift is produced for that laser detuning. The D_1 excitation of fig. 18a, as usual, leads to a clearer evidence of a decrease in the excited-state population, and therefore in the amount of the light-induced drift. For an efficient preparation of sodium atoms in the coherent trapping superposition with D_1 excitation, the authors satisfied the condition that Rabi frequency amplitudes be small as compared to the excited-state hyperfine splitting. In effect, for Rabi frequencies comparable to the hyperfine splitting in the excited state, not all the excitation processes experience interference. For the light-induced drift with D_2 excitation, some excited-state hyperfine levels present absorption from a single hyperfine ground level, whence they do not experience the interference process, as noticed in § 2.6. Thus, a very small effect of population trapping could be observed (see fig. 18b). The linewidth of the observed coherent-trapping resonance was determined mainly by the frequency jitter of the two lasers in the MHz range. For the measurements on the D_1 data good agreement was found with a theoretical model.

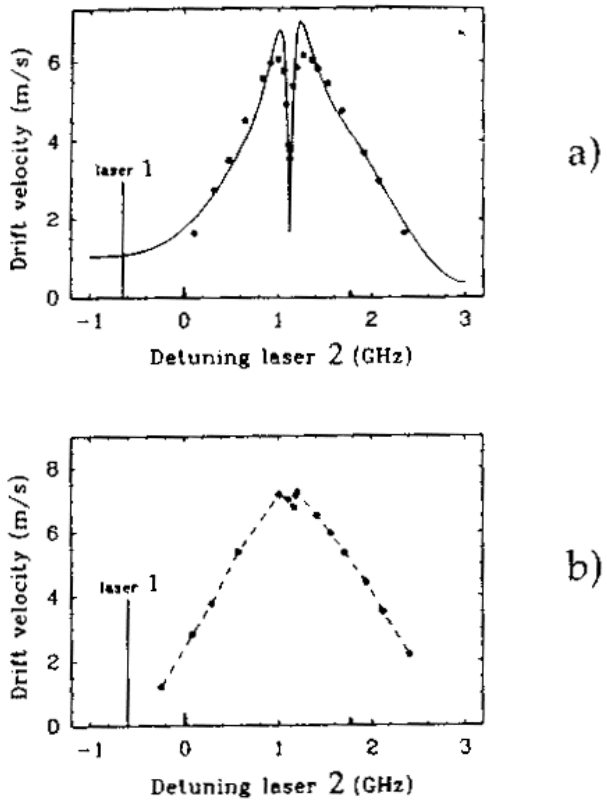

Fig. 18. Measurements of the light-induced drift velocity of sodium in 1.5 Torr Xe as a function of the detuning of laser 2 for (a) D_1 excitation and (b) D_2 excitation. The positions of the resonant frequencies for the transitions starting from the $F=1$ and $F=2$ ground hyperfine levels are marked by bars near the horizontal axes. In both cases, laser 1 was tuned around 0.6 GHz on the red side of the $F=2$ resonance, as marked. The intensities of both lasers were around 3 W/cm^2. The solid line in (a) represents the result of a model calculation (from de Lignie and Eliel [1989]).

3.8. INDEX OF REFRACTION

The large variation in the index of refraction associated with the coherent-trapping resonance, as presented in fig. 2c, has not received the same attention as the absorption coefficient. However, in the context of lasing without inversion, it has been suggested by Scully [1991] and Scully and Zhu [1992] to make use of that large increase in index of refraction in several applications to be discussed in § 7. Very recently some observations of the index of refraction around the coherent population-trapping resonance have been performed. Experimental results have been obtained by Schmidt, Hussein, Wynands and Meschede [1993, 1995] on a Λ cesium system composed of the $F=3$ and

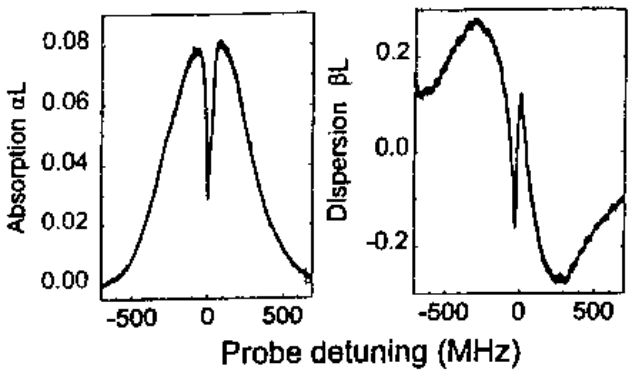

Fig. 19. Measured absorption αL (left) and dispersion nL (right), both in arbitrary units, in a rubidium cell with length $L = 7.6$ cm versus the detuning δ_{L1} of the weak probe laser on the $5^2S_{1/2}\,F = 3 \rightarrow 5^2P_{3/2}\,F = 4$ transition in the presence of a strong resonant pump laser on the $5^2P_{3/2}\,F = 4 \rightarrow 5^2D_{5/2}\,F = 5$ transition with an intensity of 250 W/cm^2 (from Xiao, Li, Jin and Gea-Banacloche [1995])

$F = 4$ ground states and the $F' = 4$ excited state: a strong laser diode excited the $F = 3 \rightarrow F' = 4$ transition, whereas a weak beam from an independent laser diode probed the $F = 4 \rightarrow F' = 4$ transition. Xiao, Li, Jin and Gea-Banacloche [1995] have reported measurements of the index of refraction, combined with measurements of the absorption coefficient, on a cascade configuration based on hyperfine levels of the $5S_{1/2}$ ground, $5P_{3/2}$ first-excited, and $5D_{5/2}$ second-excited levels of rubidium, again using independent diode lasers, similar to the lineshape measurements discussed in § 3.2. A Mach–Zender-type interferometric configuration was used in both experiments to measure the index of refraction. Experimental results are presented in fig. 19 for the measurements of the absorption coefficient and the refraction index by Xiao, Li, Jin and Gea-Banacloche [1995] for a probe laser field on the $|1\rangle \rightarrow |0\rangle$ transition and for a strong pump laser on the $|0\rangle \rightarrow |2\rangle$ transition of the cascade scheme. These results should be compared to the theoretical ones of figs. 2c and 2d. Even if the theoretical and experimental absorption coefficients and indices of refraction refer to different three-level configurations, the cascade and Λ scheme, respectively, the lineshape is a general character of the phenomenon. In the experimental results for the cascade configuration the linewidth of the one-photon transition was determined by Doppler broadening, whereas the linewidth of the coherent population-trapping resonance was determined by the Rabi frequency, as in eq. (2.25b). In the observations by Schmidt, Hussein, Wynands and Meschede [1993, 1995] on the Λ system, the final linewidth was around seventy kHz, limited partly by the transit time broadening and the residual Doppler broadening due to the angle between pump and probe laser beams.

§ 4. Coherent Population Trapping in the Continuum

The phenomena presented in the preceding section for bound states are also produced in the case of a continuum representing the upper state of the Λ system, as reviewed by Knight [1984] and Knight, Lauder and Dalton [1990]. Furthermore, coherent population-trapping features appear for a level scheme involving either a nonstructured continuum or an energy region in which the continuum is structured, as, for instance, in the presence of autoionization or predissociation resonances in a molecule. These processes involving the continuum are shown in fig. 20. Figure 20a presents the excitation by two lasers at frequencies ω_{L1} and ω_{L2} from the discrete states $|1\rangle$ and $|2\rangle$ to a continuum $|C\rangle$. Figure 20b presents an autoionizing or dissociating state $|0\rangle$, coupled to the continuum $|C\rangle$ and excited by lasers from $|1\rangle$ and $|2\rangle$ levels. The first scheme is associated with induced continuum structures, that originated through the coupling between the continuum and the dressed state corresponding to the absorption of one laser photon from either the $|1\rangle$ or $|2\rangle$ state. Whenever a discrete state and a continuum are in resonance, the mixing of those states leads to the distorted absorption lineshape known as the Fano profile (Fano [1961]). In the case of coupling between the dressed states and the continuum, a Fano lineshape is also obtained. For the continuum as the upper state, the equivalent of the excited-state occupation for discrete states is the ionization probability, i.e., the probability of being in the continuum $|C\rangle$. That probability determines the number of electrons or ions to

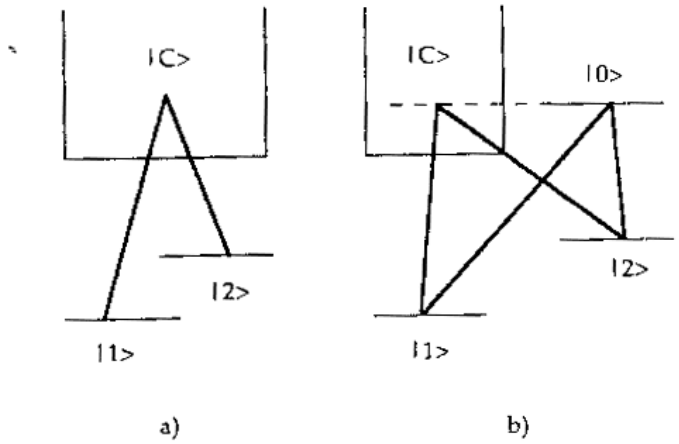

Fig. 20. Simplified three-level structures involving discrete and continuum states investigated for coherent population trapping. (a) Two transitions from discrete states are coupled to an upper continuum $|C\rangle$ by two laser radiations; (b) the upper state $|0\rangle$ of a three-level Λ scheme is coupled to the continuum $|C\rangle$ by a predissociation or autoionization mechanism.

be measured in an experiment. Thus, the ionization probability may reveal the coherent population-trapping features; in applying the laser fields in the scheme of fig. 20a, only a part of the population in the ground states is ionized because the remaining population is trapped coherently in the superposition of states $|1\rangle$ and $|2\rangle$. In the scheme of fig. 20b, two separate three-level Λ schemes are present, with Coulomb coupling between the upper level $|0\rangle$ and the continuum. Application of a single laser field, either on the $|1\rangle \dashrightarrow |0\rangle$ or $|2\rangle \dashrightarrow |0\rangle$ transition, leads to a Fano lineshape profile due to the coupling between the $|0\rangle$ state and the continuum. The simultaneous presence of two lasers produces a coherent population superposition in the lower states and generates a distortion of the Fano profile.

There have not been many experimental observations of continuum phenomena; those up to 1990 have been reviewed by Knight, Lauder and Dalton [1990]. More recently, coherent population trapping associated with a continuum structure, as in fig. 20a, has been observed in sodium ionization experiments (Shao, Charalambidis, Fotakis, Zhang and Lambropoulos [1991], Cavalieri, Pavone and Matera [1991]). Observations of the third harmonic generation through autoionization states of calcium (Faucher, Charalambidis, Fotakis, Zhang and Lambropoulos [1993]) and birefringence and dichroism in the autoionization of cesium (Cavalieri, Matera, Pavone, Zhang, Lambropoulos and Nakajima [1993]) have provided additional evidence of the phenomenon.

§ 5. Laser Cooling

In the laser manipulation of atoms, the velocity-selective coherent population trapping (VSCPT) is one method that has permitted a temperature to be reached that is lower than the landmark posed by the single-photon energy recoil (Aspect, Arimondo, Kaiser, Vansteenkiste and Cohen-Tannoudji [1988]). The other method, by Kasevich and Chu [1992], is always in a Λ system and uses sequences of stimulated Raman and optical pumping pulses with appropriate shape, the frequency spectrum of the light being tailored so that atoms with nearly zero velocity are not excited. In contrast, the basic idea of VSCPT is to pump atoms into a noncoupled state having a well-defined momentum, where atoms do not interact with the laser radiation. The final requirement for realizing a cooling scheme is to bring all atoms, or a large majority of them, in the noncoupled state with a well-defined momentum.

5.1. $J_g = 1 \rightarrow J_e = 1$ ONE-DIMENSIONAL VELOCITY-SELECTIVE COHERENT POPULATION TRAPPING

The simplest system for VSCPT is the Λ system of fig. 21a composed of the $|g_{-1}\rangle$, $|g_{+1}\rangle$, and $|e_0\rangle$ ground and excited Zeeman sublevels of the

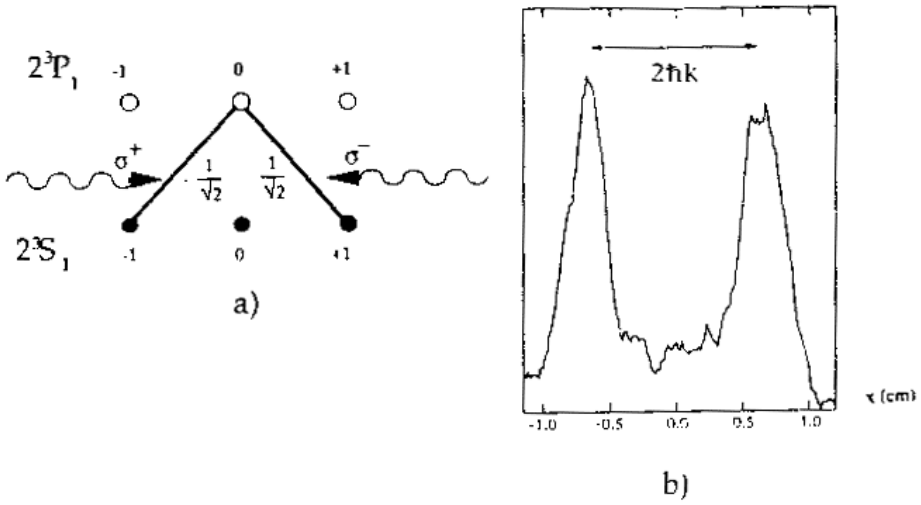

Fig. 21. VSCPT on the Λ system of the $2\,^3S_1 - 2\,^3P_1$ ^{4}He transition. (a) The ground sublevels $|J_g = 1,\ m_J = -1\rangle$ and $|J_g = 1,\ m_J = 1\rangle$ are connected to the excited state $|J_e = 1,\ m_J = 0\rangle$ by counterpropagating σ^+ and σ^- laser beams. The opposite Clebsch–Gordan coefficient on the σ^+ and σ^- transitions are shown; (b) measured position density profile of the atomic distribution at the detector, as produced by one-dimensional VSCPT in ^{4}He with $\Theta = 0.3$ ms and $\Omega_R = 0.6\,\Gamma_0$ (from Bardou, Saubamea, Lawall, Shimizu, Émile, Westbrook, Aspect and Cohen-Tannoudji [1994]). The distance between the two peaks corresponds to $2\hbar k$; from the width of each peak the temperature was estimated at $T \approx T_R/20 \approx 200$ nK.

$J_g = 1 \to J_e = 1$ transition and excited by σ^+ and σ^- circularly polarized electric fields. The atomic Hamiltonian of eq. (2.1) should be modified to include the kinetic energy for an atom moving along the z axis with momentum p_z. If the energy of the degenerate $|g_{-1}\rangle$ and $|g_{+1}\rangle$ ground states is assumed equal to zero, for an atom of mass M the Hamiltonian is:

$$\mathcal{H}_0 = \frac{p_z^2}{2M} + \hbar\omega_0 |e_0\rangle \langle e_0| . \tag{5.1}$$

The kinetic energy describing the motion along the x and y axes does not appear explicitly in the atomic evolution, but a trace over the momenta along those axes should be performed. Coherent population trapping with velocity selection is obtained when the traveling electric fields acting on the two arms of the Λ system are counterpropagating along the z axis, whereas it was noticed in § 2.7 that the configuration of copropagating laser fields generates coherent population trapping in all the velocity classes of a Doppler-broadened medium. If the counterpropagating laser fields of frequency ω_L and wavenumber k are supposed

to have the same amplitude $\mathcal{E}_L$ and phase ϕ_L, the interaction Hamiltonian of eq. (2.4) may be written:

$$V_{AL} = \frac{\Omega_R}{2}\{-\exp[-i(\omega_L t - kz + \phi_L)]\,|e_0\rangle\langle g_{-1}| + \exp[\,i(\omega_L t + kz + \phi_L)]\,|e_0\rangle\langle g_{+1}|\} + \text{h.c.}, \tag{5.2a}$$

where the Rabi frequency Ω_R is given by

$$\Omega_R = \frac{\mu_{e_0 g_{-1}}\mathcal{E}_L}{\hbar} = -\frac{\mu_{e_0 g_{+1}}\mathcal{E}_L}{\hbar}. \tag{5.2b}$$

With $\mu_{e_0 g_{-1}} = -\mu_{e_0 g_{+1}}$ because of the opposite Clebsch–Gordan coefficients on the two components of the $J_g = 1 \rightarrow J_e = 1$ transition, as shown in fig. 21a. The atom–laser interaction of the atom with each counterpropagating laser beam modifies by $\pm\hbar k$ the atomic momentum along the z axis. If the atomic momentum basis $|\alpha, p_z\rangle$ with $\alpha \in \{|e_0\rangle, |g_{-1}\rangle, |g_{+1}\rangle\}$ is used, in order to describe this change in the atomic momentum taking place along the z axis, the V_{AL} interaction may be written:

$$V_{AL} = \frac{\Omega_R}{2}\sum_{p_z}\{-|e_0, p_z + \hbar k\rangle\langle g_{-1}, p_z| + |e_0, p_z - \hbar k\rangle\langle g_{+1}, p_z|\} + \text{h.c.} \tag{5.3}$$

Equation (5.3) shows that by absorption and stimulated emission, the interaction V_{AL} couples only the following three states:

$$|g_{-1}, q - \hbar k\rangle, \qquad |e_0, q\rangle, \qquad |g_{+1}, q + \hbar k\rangle, \tag{5.4}$$

with q the atomic momentum along the z axis. As long as spontaneous emission is not taken into account, these states form a closed set to be defined as the $\mathcal{F}(q)$ family, where the q label denotes the atomic momentum in the excited state belonging to a given family. The basic role of spontaneous emission is to produce a redistribution among the different families. In effect, in a spontaneous emission process, an atom in the excited state $|e_0, q\rangle$ of the $\mathcal{F}(q)$ family emits a fluorescence photon directed arbitrarily in space, so that the atomic momentum q changes by any value between $-\hbar k$ and $\hbar k$. The main role of spontaneous emission is to produce a diffusion in the momentum space leading the atoms to the specific velocity where accumulation takes place.

A clear insight into the VSCPT mechanism is obtained by using the basis of coupled/noncoupled states. Within the $\mathcal{F}(q)$ family the following coupled/noncoupled states are formed:

$$|\mathrm{NC}(q)\rangle = \frac{1}{\sqrt{2}}\left(|g_{-1}, q - \hbar k\rangle + |g_{+1}, q + \hbar k\rangle\right),$$
$$|\mathrm{C}(q)\rangle = \frac{1}{\sqrt{2}}\left(|g_{-1}, q - \hbar k\rangle + |g_{+1}, \hbar k\rangle\right), \tag{5.5}$$

where the properties of eq. (2.17a) still apply; i.e., no transition element of the interaction Hamiltonian V_{AL} exists between $|e_0(q)\rangle$ and $|\mathrm{NC}(q)\rangle$. It may be noticed that in eq. (5.5) the noncoupled state is the symmetric linear combination of ground states, whereas in eq. (2.16) the noncoupled state is associated with the antisymmetric combination. This change arises from the opposite sign of the Rabi frequencies on the two optical transitions of fig. 21a. At this point the $p_z^2/2M$ kinetic energy term in the $\mathcal{H}_0$ Hamiltonian plays a key role. Although the $|g_{\pm 1}, q \pm \hbar k\rangle$ are eigenstates of the kinetic energy operator, $|\mathrm{NC}(q)\rangle$ and $|\mathrm{C}(q)\rangle$ are not, and the kinetic energy operator has a matrix element between them:

$$\langle \mathrm{C}(q)| \frac{p_z^2}{2M} |\mathrm{NC}(q)\rangle = \frac{\hbar k q}{M}. \tag{5.6}$$

In the schematic representation of fig. 4 for coupling and effective loss rates of the states, the kinetic energy matrix element of eq. (5.6) becomes the most important coupling between the noncoupled and coupled states if $\delta_{\mathrm{R}} = 0$ and the ground-state relaxation processes are not present. Equation (5.6) shows that the state $|\mathrm{NC}(q)\rangle$, noncoupled with respect to the absorption of laser radiation, is not stationary for the kinetic energy evolution unless the q value is equal to zero. The state $|\mathrm{NC}(0)\rangle$ is a perfect trap state because it is stable against the atom–laser interaction and also against kinetic energy coupling.

The optical Bloch equations for the density matrix of eqs. (2.5) and (2.7) have to be modified by using the Hamiltonians of eqs. (5.1) and (5.2a). Moreover, for the relaxation produced by the spontaneous emission, which at this stage is supposed to be the only relaxation process, it should be taken into account that the repopulation of the ground states occurs with a diffusion in the momentum space. As a consequence, the generalized optical Bloch equations required to describe the VSCPT process are nonlocal in the momentum space (Aspect, Arimondo, Kaiser, Vansteenkiste and Cohen-Tannoudji [1989], Castin, Wallis and Dalibard [1989]).

In the limit of $q < q_0 = \hbar k\alpha$, with the parameter α given by

$$\alpha = \frac{\Omega_R^2}{4\Gamma_0\omega_R}, \tag{5.7}$$

and the recoil frequency ω_R defined by

$$\omega_R = \frac{\hbar k^2}{2M}, \tag{5.8}$$

the $\Gamma''(q)$ loss rate for the $|NC(q)\rangle$ state results in:

$$\Gamma''(q) = \frac{8\omega_R^2}{\Omega_R^2}\Gamma_0\left(\frac{q}{\hbar k_R^2}\right)^2. \tag{5.9}$$

Because $\Gamma''(q)$ is the probability per unit time that an atom will leave the state $|NC(q)\rangle$, for an interaction time Θ, only atoms with $\Gamma''(q)\Theta < 1$ remain trapped in the noncoupled state, and that condition is satisfied by an interval δq of atomic momenta such that:

$$\left(\frac{\delta q}{\hbar k}\right)^2 < \frac{\alpha}{2\Theta\omega_R}. \tag{5.10}$$

The trap state $|NC(0)\rangle$ is filled up by the spontaneous emission diffusion in the momentum space discussed above. A significant fraction of the atoms may be trapped in the atomic momentum region defined by eq. (5.10) in a time $\Theta\omega_R \approx \alpha$, which defines the VCSPT time scale (Korsunsky, Kosachiov, Matisov, Rozhdestvensky, Windholz and Neureiter [1993], Bardou, Bouchaud, Émile, Aspect and Cohen-Tannoudji [1994]).

The trap state $|NC(0)\rangle$ superposition has the following expression:

$$|NC(0)\rangle = \frac{1}{\sqrt{2}}(|g_{-1}, -\hbar k\rangle + |g_{+1}, \hbar k\rangle), \tag{5.11}$$

and its spatial dependence is given by

$$\langle z|NC(0)\rangle = \exp(+ikz)\,|g_{-1}\rangle + \exp(-ikz)\,|g_{+1}\rangle. \tag{5.12}$$

A measurement of the atomic momentum on the $|NC(0)\rangle$ states gives $p_z = \pm\hbar k$. The momentum distribution of the atoms cooled by VSCPT presents two peaks at $\pm\hbar k$ with a width given by eq. (5.10), as in the experiments. VSCPT experiments have been performed on ^{4}He metastable atoms using the transition $2^3S_1 \rightarrow 2^3P_1$,

where the recoil temperature T_R, defined as $k_B T_R/2 = \hbar\omega_R$, is 4 μK (Aspect, Arimondo, Kaiser, Vansteenkiste and Cohen-Tannoudji [1988], Bardou, Saubamea, Lawall, Shimizu, Émile, Westbrook, Aspect and Cohen-Tannoudji [1994], Doery, Widmer, Bellanca, Buell, Bergeman, Metcalf and Vredenbregt [1995]). Figure 21b illustrates the atomic distribution measured by Bardou, Saubamea, Lawall, Shimizu, Émile, Westbrook, Aspect and Cohen-Tannoudji [1994] in an experiment on helium atoms precooled by sub-Doppler laser-cooling techniques, in order to realize a very long interaction time Θ with the laser radiation and a very narrow final distribution of the atomic momenta. Converting the final momentum distribution into an effective temperature by $k_B T/2 = (\delta q)^2/2M$, the authors associated an effective temperature of 200 nK with the data of fig. 21b. The atomic momentum distributions of the $J_g = 1 \to J_e = 1$ VSCPT cooling are well described theoretically through the solution of the generalized optical Bloch equations (Aspect, Arimondo, Kaiser, Vansteenkiste and Cohen-Tannoudji [1989], Arimondo [1992]). Doery, Widmer, Bellanca, Buell, Bergeman, Metcalf and Vredenbregt [1995] have analyzed the atomic momentum distribution through the quantum-mechanical eigenstates of the total ground-state Hamiltonian, using both analytical expressions and numerical calculations.

At very long interaction times Θ the two peaks of fig. 21b become more narrow, as indicated by eq. (5.10), but a question arises whether the number of cooled atoms keeps increasing or starts to decrease. Bardou, Bouchaud, Émile, Aspect and Cohen-Tannoudji [1994] pointed out the very peculiar nonstationary behavior, with a break of the ergodicity, presented by the VSCPT at interaction times longer than α/ω_R. In fact, only atoms in the $|\mathrm{NC}(q = 0)\rangle$ state, a set of zero measure, are perfectly trapped. In contrast, at any interaction time, however long, the atoms in $|\mathrm{NC}(q \approx 0)\rangle$ states have a finite probability to escape from the noncoupled state and to start a diffusion in the momentum space. Because the atomic evolution is dominated by a random sequence of those rare events, the VSCPT is described through a regime, denoted as the Levy flight regime, different from the Brownian motion distribution of other cooling schemes. The authors have examined the VSCPT efficiency through the Levy flight statistical analysis. An alternative approach for the VSCPT at long interaction times is based on quantum Monte Carlo simulations, as introduced by Cohen-Tannoudji, Bardou and Aspect [1992]. Figure 22 shows results from a Monte Carlo simulation for the fraction of trapped atoms (defined as those atoms in the noncoupled states with $|\Delta q| \leqslant \hbar k/8$) versus the interaction time Θ, for parameters similar to those of fig. 21b. It may be observed that at interaction times much longer than $\Theta\omega_R = \alpha$, the fraction of trapped atoms decreases.

The above analysis can be transferred in toto to another laser configuration

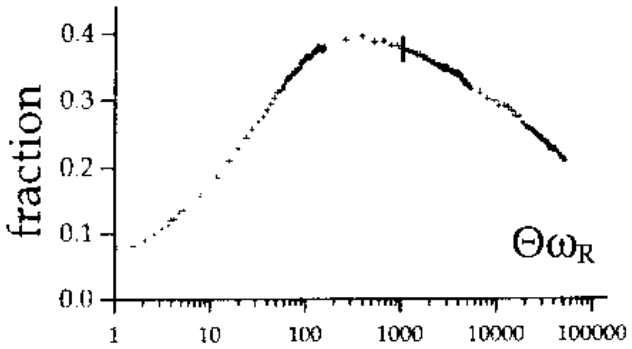

Fig. 22. Fraction of the trapped atoms, defined as $|\delta q| < 0.25\,\hbar k$, versus the interaction time $\Theta\omega_R$ calculated from a quantum Monte Carlo analysis for one-dimensional VSCPT ^{4}He with $\Omega_R = 0.333\,\Gamma_0$, and $\alpha = 1$. The vertical bar represents the uncertainties originating in the quantum Monte Carlo analysis.

with a relevant role in laser cooling, the so-called lin $\perp$ lin configuration. This is composed of two counterpropagating traveling laser fields, linearly polarized along orthogonal axes, the x and y axes. In fact, the analysis of the $J_g = 1 \rightarrow J_e = 1$ transition on the linear atomic basis of fig. 7b has shown that the $\{|g_x\rangle, |e_z\rangle, |g_y\rangle\}$ states give rise to a three-level Λ system that can be excited by two laser fields linearly polarized along the y and x axes, respectively. VSCPT can then be realized with excitation by counterpropagating lin $\perp$ lin laser fields, as reported in the ^{4}He experiment by Aspect, Arimondo, Kaiser, Vansteenkiste and Cohen-Tannoudji [1988] and discussed by Kaiser [1990].

Alekseev and Krylova [1992a,b, 1993] developed an original approach to solving analytically the density matrix equations for the VSCPT with traveling counterpropagating waves. Through a Fourier transformation for the momentum dependence and a Laplace transformation for the time dependence of the density matrix elements, a high-order local differential equation was derived and solved. They obtained a Lorentzian form for the momentum atomic distribution that well interpreted the results of the numerical calculations by Aspect, Arimondo, Kaiser, Vansteenkiste and Cohen-Tannoudji [1989] and Arimondo [1992] for times $\Theta \leqslant \alpha/\omega_R$. Thus, that analytical form could not reproduce the long-term Levy flight regime. Alekseev and Krylova [1992b,1993], Mauri [1990], and Arimondo [1992] have derived, through a simple model with atomic momentum diffusion and a trap state, a rate equation that could analyze the VSCPT at intermediate interaction times.

The $J_g = 1 \rightarrow J_e = 1$ VSCPT in one dimension has been theoretically extended to the laser configuration with two circularly polarized standing-wave electromagnetic fields acting on the two transitions of the Λ system (Hemmer,

Prentiss, Shahriar and Bigelow [1992], Shahriar, Hemmer, Prentiss, Chu, Katz and Bigelow [1993], Shahriar, Hemmer, Prentiss, Marte, Mervis, Katz, Bigelow and Cai [1993], Marte, Dum, Taïeb, Zoller, Shahriar and Prentiss [1994], Weidemüller, Esslinger, Ol'shanii, Hemmerich and Hänsch [1994]). The standing-wave electric fields are written as $\mathcal{E}_L \cos(kz + \phi_{21}/2)\sigma^+[\exp(i\omega_{L1}t) + \text{c.c.}]/2$ and $\mathcal{E}_L \cos(kz - \phi_{21}/2)\sigma^-[\exp(i\omega_{L1}t) + \text{c.c.}]/2$, where σ^+ and σ^- represent the unit vectors for the circular polarizations. For simplicity the amplitudes of the two waves have been assumed equal. An important role in this laser configuration is played by the relative phase difference ϕ_{21}. For instance, at $\phi_{21} = \pi/4$ the standing-wave configuration is equivalent to the laser configuration of lin $\perp$ lin counterpropagating waves, where VSCPT produces a noncoupled state similar to that of eq. (5.12) but a combination of $|g_x\rangle$ and $|g_y\rangle$ states. For the standing-wave configuration the V_{AL} interaction may be written:

$$V_{AL} = \frac{\Omega_R}{2} \sum_{p_z} \Big[-\exp(i\phi_{21}/2)\left(|e_0, p_z - \hbar k\rangle + |e_0, p_z + \hbar k\rangle\right)\langle g_{-1}, p_z| + \exp(-i\phi_{21}/2)\left(|e_0, p_z + \hbar k\rangle + |e_0, p_z - \hbar k\rangle\right)\langle g_{+1}, p_z| \Big] + \text{h.c.} \tag{5.13}$$

For this atom–laser interaction, the following noncoupled state exists:

$$|\text{NC}(q)\rangle = \tfrac{1}{2}\left[\exp(-i\phi_{21}/2)\left(|g_{-1}, q - \hbar k\rangle + |g_{-1}, q + \hbar k\rangle\right) + \exp(i\phi_{21}/2)\left(|g_{+1}, q + \hbar k\rangle + |g_{+1}, q - \hbar k\rangle\right)\right], \tag{5.14}$$

as can be verified by applying the V_{AL} of eq. (5.13) to this state. For the $|\text{NC}(q)\rangle$ state the evolution under the kinetic energy Hamiltonian leads to a stationary state only for $q = 0$. Thus, the standing-wave laser configuration leads to a noncoupled state with atomic momentum components at $\pm\hbar k$, similar to those of the counterpropagating traveling-wave configuration. However, in the coordinate space the $|\text{NC}(0)\rangle$ trap state of the standing-wave configuration results:

$$\langle z|\text{NC}(0)\rangle = \cos\left(kz - \frac{\phi_{21}}{2}\right)|g_{-1}\rangle + \cos\left(kz + \frac{\phi_{21}}{2}\right)|g_{-1}\rangle, \tag{5.15}$$

with a spatial dependence different from eq. (5.12). The analysis of the fraction of trapped atoms for the standing-wave configuration is more difficult than for the traveling-wave configuration, because, due to the form of the atom-laser interaction of eq. (5.13), each of the ground states is connected to two excited states. Therefore, it is not possible to find closed families of states. For the

values $\phi_{21} = 0$ and $\phi_{21} = \pi$ of the relative phase of the two standing waves, the VSCPT mechanism does not act any more; for those phases the two laser fields produce a standing-wave field linearly polarized along the y and x axes, respectively. The linear atomic basis of fig. 7b shows that a linearly polarized laser, acting on the $J_g = 1 \rightarrow J_e = 1$ transition, produces a depopulation pumping into a dark state without any velocity selection.

The real advantage of the standing-wave configuration is the presence of a force produced by the laser cooling polarization gradient mechanism (Shahriar, Hemmer, Prentiss, Marte, Mervis, Katz, Bigelow and Cai [1993], Marte, Dum, Taïeb, Zoller, Shahriar and Prentiss [1994]). The role of the polarization gradient is twofold: to produce a precooling of the initial atomic momentum distribution at short atom–laser interaction times, and to provide a confinement of the atomic velocities in the long interaction time limit. In effect, the traveling-wave VSCPT suffers the drawbacks of relying on the spontaneous emission atomic diffusion only for reaching the trap state and on the occurrence of the Levy flight regime at interaction times longer than α/ω_R with a decrease in the fraction of trapped atoms. It is expected that for the standing-wave configuration at those long interaction times, the fraction of trapped atoms does not give the decrease shown in fig. 22. Marte, Dum, Taïeb, Zoller, Shahriar and Prentiss [1994] have pointed out that it is not possible to satisfy simultaneously the requirements on laser detuning and Rabi frequency for efficient use of the polarization gradient force and for trapping the atoms in a narrow momentum distribution. Thus, they proposed alternating the laser configuration between standing-wave and traveling-wave in order to take good advantage of both schemes. Numerical calculations confirmed the advantages obtained through this alternate operation, but in an experiment the preservation of the ground-state phase coherence in the operations could be difficult to realize. The use of a Doppler-cooling force to increase the laser cooling efficiency on Λ schemes with $k_1 \neq k_2$ or $\Gamma_{0\rightarrow 1} \neq \Gamma_{0\rightarrow 2}$ has been discussed by Korsunsky, Kosachiov, Matisov, Rozhdestvensky, Windholz and Neureiter [1993].

Much theoretical work has concentrated on the use of a semiclassical theory, based on the Fokker–Planck equation, to describe the atomic velocity distribution function in the VSCPT (Minogin and Rozhdestvensky [1985], Minogin, Ol'shanii and Shulga [1989], Gornyi and Matisov [1989], Minogin, Ol'shanii, Rozhdestvensky and Yakobson [1990], Korsunsky, Kosachiov, Matisov, Rozhdestvensky, Windholz and Neureiter [1993], Korsunsky, Snegiriov, Gordienko, Matisov and Windholz [1994]). The Fokker–Planck equation is a powerful approach widely used for describing laser cooling (Minogin and Letokhov [1986]), but it is based on the hypothesis that the atomic velocity

distribution is wider that the photon momentum, a hypothesis not satisfied in the subrecoil regime reached by VSCPT. Thus, the Fokker–Planck equation can be used to describe the three-level Λ system laser-cooling only in the regime above the recoil limit. However, as pointed out by Korsunsky, Kosachiov, Matisov, Rozhdestvensky, Windholz and Neureiter [1993], some general conclusions about the dynamics of laser cooling based on coherent population trapping, which can be drawn from the semiclassical theory, ought to be valid in all the regimes of laser cooling, including the subrecoil VSCPT.

The Fokker–Planck equation, in Rozhdestvensky and Yakobson [1991], Kosachiov, Matisov and Rozhdestvensky [1992d], Korsunsky, Kosachiov, Matisov, Rozhdestvensky, Windholz and Neureiter [1993], Korsunsky, Snegiriov, Gordienko, Matisov and Windholz [1994], and the Fourier–Laplace transformation of the density matrix equations in Matisov, Korsunsky, Gordienko and Windholz [1994], have been used to investigate the modification in the coherent population-trapping laser cooling produced by the presence of a relaxation mechanism for the ground-state coherence not included in the evolution of the coupled/noncoupled states reported above. As in § 2.3 for the decrease in coherent population trapping produced by the relaxation of the ground-state coherence, the VSCPT efficiency also decreases because of that relaxation. The VSCPT limit associated with the presence of the Γ_{12} relaxation rate has been derived in Arimondo [1994]. The loss rate of the $|\mathrm{NC}(q_{\mathrm{trap}})\rangle$ state with the maximum q_{trap} momentum should be equal to Γ_{12}:

$$\Gamma''(q_{\mathrm{trap}}) = \Gamma_{12}, \tag{5.16a}$$

and using eq. (5.9) the minimum VSCPT temperature T_{min} produced in the presence of coherence relaxation is

$$k_{\mathrm{B}} T_{\mathrm{min}} = \frac{q_{\mathrm{trap}}^2}{M} = 4\hbar \frac{\Omega_{\mathrm{R}}^2 \Gamma_{12}}{\Gamma_0 \omega_{\mathrm{R}}}. \tag{5.16b}$$

With the typical values of coherence relaxation rate Γ_{12}, this limit temperature is smaller than that reached in Doppler or polarization-gradient cooling.

Kosachiov, Matisov and Rozhdestvensky [1992c, 1993] examined the laser cooling associated with coherent population trapping in the configuration known as the double-Λ scheme, where both ground states $|1\rangle$ and $|2\rangle$ are connected by dipole transitions to two different excited states, a configuration extensively introduced within the context of lasing without inversion. They found that the efficiency of the laser-cooling process is strongly affected by the relative phase of the ground-state coherences formed by the two separate Λ schemes. Matisov,

Gordienko, Korsunsky and Windholz [1995] have investigated through different approaches the noncoupled states formed in the atomic configuration of three levels in cascade, obtaining some results that appear promising for extending VSCPT to highly excited states. Gornyi, Matisov and Rozhdestvensky [1989b], Korsunsky, Matisov and Rozhdestvensky [1992], and Kosachiov, Matisov and Rozhdestvensky [1992c] considered laser cooling associated with coherent population trapping for Λ- or cascade schemes where one transition is in the optical region and the other one in the radiofrequency or microwave region, so that the photon momenta for the two transitions are largely different. Thus, VSCPT can be applied to a wider class of atomic systems.

Goldstein, Pax, Schernthanner, Taylor and Meystre [1995] considered the influence of the dipole–dipole interaction between ground and excited atoms on the $J=1 \rightarrow J=1$ VSCPT in one dimension. The main result is that, although the noncoupled state survives the inclusion of the dipole–dipole interactions, the presence of this interaction significantly slows down the cooling process, without affecting the final temperature.

5.2. HIGH-J ONE-DIMENSIONAL VELOCITY-SELECTIVE COHERENT POPULATION TRAPPING

A one-dimensional generalization to atomic transitions of the type $J \rightarrow J$ and $J \rightarrow J-1$ has been reported by Mauri, Papoff and Arimondo [1991] and Papoff, Mauri and Arimondo [1992]. Under irradiation with σ^+,σ^- counterpropagating traveling waves, a superposition of ground states can be formed which experiences interference in all the transitions to excited states. For instance, for the $J_g=2 \rightarrow J_e=2$ transition between hyperfine states of the ^{87}Rb resonance line, the M structure of Zeeman sublevels presented in fig. 7c can be extracted, where for each Λ scheme a destructive interference inhibits the absorption to an excited state. For that case, with equal amplitudes of the two traveling wave lasers, the following noncoupled superposition exists:

$$|\mathrm{NC}(q)\rangle = \sqrt{\frac{36}{17}}\left[\frac{1}{\sqrt{2}}|g_{-2}, q-2\hbar k\rangle - \frac{1}{\sqrt{3}}|g_0, q\rangle + \frac{1}{\sqrt{2}}|g_{+2}, q+2\hbar k\rangle\right], \tag{5.17}$$

where the coefficients of the ground state wavefunctions are determined by the Clebsch–Gordan coefficients for the adjacent σ^+,σ^- transitions. However, this noncoupled state, at variance with that of eq. (5.11) for the $J=1 \rightarrow J=1$ transition, does not present the nice feature of being an eigenstate of the kinetic-energy operator for some q value. Even for $q=0$, the three wavefunctions of

eq. (5.17) present different kinetic energy values. That kinetic energy difference, $4\hbar\omega_R$ for a heavy mass atom, is a very small quantity, so that the $|NC(0)\rangle$ state is a transient or leaky VSCPT state, i.e., not stable but with a long lifetime. This leaky VSCPT is not a very efficient way to realize VSCPT sub-recoil cooling. Ol'shanii [1991] has suggested, through application of the Stark effect, a way to transform the noncoupled leaky states into nonleaky ones. If the atomic Hamiltonian part is modified so that the atomic energy difference between the $|g_0\rangle$ and $|g_{\pm 2}\rangle$ states is exactly equal to $4\hbar\omega_R$, the three wavefunctions of the $|NC(0)\rangle$ superposition of eq. (5.17) will have again the same energy by summing up the atomic and kinetic energies. As a consequence the $|NC(0)\rangle$ state becomes an eigenstate of the total energy and a nonleaky VSCPT regime can be realized. Whereas the original suggestion was based on the atomic energy shift of $\mathcal{H}_0$, through the Stark effect of an applied dc electric field, more recently Ol'shanii [1994] and Foot, Wu, Arimondo and Morigi [1994] have shown that the same result could be obtained more simply by making use of the dynamic Stark shift produced by a separate nonresonant laser field. Figure 23 shows the theoretical prediction for the measured atomic momentum distribution $P(p_z)$ in the case of VSCPT with σ^+,σ^- laser fields interacting with the resonant $F=2 \rightarrow F=2$ transition of ^{87}Rb for an interaction time of 4 ms. The peaks at $p_z = 0, \pm 2\hbar k$ are produced by a momentum measurement on the $|NC(0)\rangle$ state of eq. (5.17). It may be noticed that when the ac Stark effect is present in order to produce nonleaky noncoupled states, the efficiency in the VSCPT preparation is greatly enhanced.

Doery, Gupta, Bergeman, Metcalf and Vredenbregt [1995] have proposed another approach for the preparation of a nonleaky VSCPT trap state, using a configuration similar to that of fig. 7c, but having asymmetrical arms in each Λ transition. Furthermore, detunings of the two lasers from the Raman resonance condition are essential. For realizing the asymmetric Λ scheme, the ground-state Zeeman levels $m=0$ and $m=\pm 2$ should belong to two different hyperfine states, $F=1$ and $F=2$, respectively, and the laser beams should not have the same frequency. For the ^{87}Rb hyperfine states, supposing equal Rabi frequencies for the two circularly polarized counterpropagating beams, the following noncoupled combination should be considered:

$$|NC(q,t)\rangle = \frac{1}{\sqrt{3}}\left[\,|F=2, m_F=-2; q-2\hbar k\rangle - e^{-i(\delta_{L2}-\delta_{L1})t}\,|F=1, m_F=0; q\rangle + |F=2, m_F=2; q+2\hbar k\rangle\right], \tag{5.18}$$

in analogy to eq. (2.28b). The realization of a nonleaky state is based on the fact that, as indicated in fig. 4, the effective loss rate of the noncoupled state

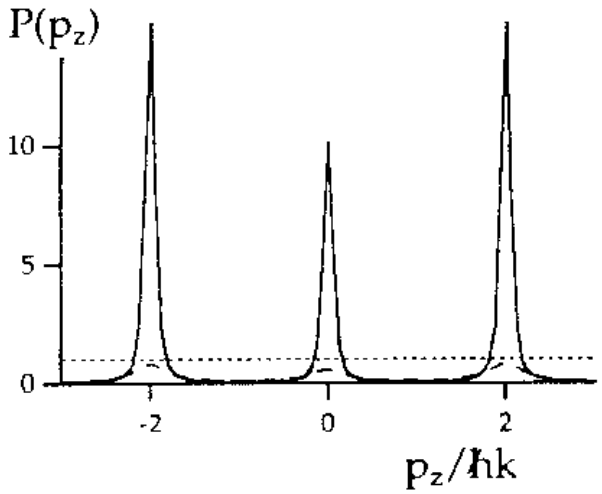

Fig. 23. Theoretical evolution of the atomic momentum distribution $P(p_z)$ for onedimensional VSCPT on the $5^2S_{1/2}\,F=2 \rightarrow 5^2P_{3/2}\,F=2$ ^{87}Rb transition with a nonleaky noncoupled state (continuous line), and with a leaky one (dashed line). Parameters $\Omega_{R1}=\Omega_{R2}=0.2\,\Gamma_0$ at $\Theta\omega_R=100$, i.e., $\Theta\approx 4$ ms. The dotted line represents the initial atomic momentum distribution.

depends on both the kinetic energy and the Raman detuning. For suitable laser frequencies, the Raman detuning may compensate exactly the kinetic energy leakiness, so that a nonleaky state is produced. All these schemes have yet to be tested experimentally.

5.3. TWO- AND THREE-DIMENSIONAL VELOCITY-SELECTIVE COHERENT POPULATION TRAPPING

The generalization from 1D to higher dimensions was started by Aspect, Arimondo, Kaiser, Vansteenkiste and Cohen-Tannoudji [1989] with a laser configuration which gave rise to a trapping state but had poor efficiency in the pumping process. Mauri, Papoff and Arimondo [1991], Mauri and Arimondo [1991, 1992], and Arimondo [1992] have discussed configurations for VSCPT in two dimensions for the $J_g=1 \rightarrow J_e=1$ and $J_g=1 \rightarrow J_e=0$ transitions with an efficient filling of the trap states provided by the presence of Doppler- and polarization-gradient forces acting on the atoms, also calculating the VSCPT efficiency.

Ol'shanii and Minogin [1991a,b, 1992], Taichenachev, Tumaikin, Ol'shanii and Yudin [1991] and Taichenachev, Tumaikin, Yudin and Ol'shanii [1992a,b] pointed out other schemes for generalizing VSCPT states in 2D and 3D on the basis of elegant formal relations. Their approach is based on a few

formal statements: for a $J=1$ state, as for a spin one particle, the spatial wavefunction is described by a vector state $\psi(r)$; the transition amplitude induced by the V_{AL} interaction with an electric field of amplitude $\mathcal{E}_L(r)$, for the $J_g=1 \rightarrow J_e=1$ case with vector states $\psi_g(r)$ and $\psi_e(r)$, in analogy to eq. (2.32a), is proportional to the following integral:

$$\langle e, J=1|\, V_{AL}\, |g, J=1\rangle \propto \int \mathrm{d}r \psi_e^*(r) \cdot \left[\mathcal{E}_L(r) \times \psi_g(r)\right], \tag{5.19}$$

with a vector product between $\mathcal{E}_L(r)$ and $\psi_g(r)$, and a scalar product with $\psi_e(r)$. If the following spatial dependence is imposed on the ground-state wavefunction:

$$\psi_g^{NC}(r) = \alpha \mathcal{E}_L(r), \tag{5.20}$$

with α being c-number, then $\psi_g^{NC}(r)$ has a zero transition amplitude for the laser excitation and, thus, describes a noncoupled state. Moreover, the wave equation satisfied by the electric field amplitude $\mathcal{E}_L(r)$ has the same formal structure as the Schrödinger equation with kinetic energy satisfied by the wavefunction $\psi_g^{NC}(r)$, with eigenvalue $\hbar\omega_R$. Thus, the laser spatial configuration determines the spatial and momentum characteristics of the noncoupled state. For the $J_g=1 \rightarrow J_e=0$ case, the transition amplitude induced by the V_{AL} interaction is proportional to the following integral, in analogy to eq. (2.32b):

$$\langle e, J_e=0|\, V_{AL}\, |g, J_g=1\rangle \propto \int \mathrm{d}r \psi_e^*(r) \left[\mathcal{E}_L(r) \cdot \psi_g(r)\right]. \tag{5.21}$$

so that the spatial vector of the noncoupled state is given by a vector product operation

$$\psi_g^{NC}(r) = e \times \mathcal{E}_L(r) \tag{5.22}$$

with e the electric field polarization. Also for this case $\psi_g^{NC}(r)$ is an eigenstate of the kinetic energy with eigenvalue $\hbar\omega_R$. Because from eqs. (5.20) and (5.22) the spatial distribution $|\psi_g^{NC}(r)|^2$ of the VSCPT atomic wavefunction depends on $|\mathcal{E}_L(r)|^2$, nonuniform polarization and nonuniform intensity produce a localization of the trapped atoms at the maxima of the electric field.

Laser configurations with σ^+,σ^- counterpropagating plane waves along two or three axes were examined in detail by Ol'shanii and Minogin [1991a,b, 1992]: the momentum representation of the noncoupled state contained momentum components at the positions $\pm\hbar k$ along two or three axes. For the

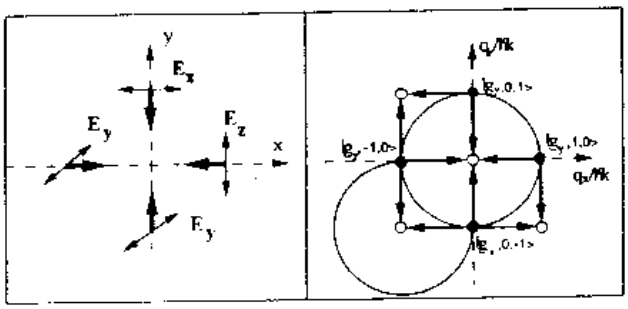

a) b)

c)

Fig. 24. (a) Schematic diagram of the laser configuration for two-dimensional VSCPT, with counterpropagating lin ⊥ lin laser beams along two directions; (b) solid circles represent the four atomic momentum components, at $\pm\hbar k$ along the two axes, contributing to the noncoupled state, with interfering transitions to excited states (open circles). Circles represent families of states; the wavefunctions of the noncoupled state belong to several families; (c) image of the detected atomic position distribution for VSCPT in two dimensions in ^{4}He, with experimental parameters: $\Omega_R = 0.8\,\Gamma_0$; $\delta_L = 0.5\,\Gamma_0$; interaction time $\Theta = 0.5$ ms. The momentum distribution consists of four peaks as in (b); the peak widths are evidence of a subrecoil two-dimensional VSCPT (from Lawall, Bardou, Saubamea, Shimizu, Leduc, Aspect and Cohen-Tannoudji [1994]).

$J_g = 1 \rightarrow J_e = 1$ case, the lin ⊥ lin configuration of counterpropagating lasers in two dimensions, examined by Arimondo [1992], is represented in fig. 24a. Using the selection rules for the linear polarization basis of fig. 7b, the corresponding noncoupled state is obtained as the superposition of $|g_i, q_x, q_y\rangle$ $(i = x, y, z)$ wavefunctions. This is represented schematically in fig. 24b, together with the interference channels in the excitation to upper states. For both σ^+,σ^- and lin ⊥ lin configurations, the wavefunctions composing the noncoupled state do not belong to closed families, so that the efficiency in the preparation of the noncoupled state has not yet been calculated. The configuration of counterpropagating σ^+,σ^- laser fields for VSCPT in two dimensions has been realized by Lawall, Bardou, Saubamea, Shimizu, Leduc, Aspect and Cohen-

Tannoudji [1994] for ^{4}He atoms precooled in a magneto-optical trap using the same $J_g = 1 \rightarrow J_e = 1$ transition of VSCPT in one dimension. After precooling, the helium atoms interacted for 0.5 ms with the four counterpropagating laser beams and were prepared in an noncoupled state similar to that represented in fig. 24b. After the VSCPT cooling, the atoms were falling, due to gravity, onto a CCD camera that recorded an image of the atomic position distribution. Figure 24c shows an image from this camera, with the four spots produced by the detection of the wavefunctions composing the two-dimensional noncoupled state. From the measured width of the individual peaks, as on the vertical profile on the peak at the right of fig. 24c, a temperature around sixteen times smaller than the helium recoil limit was estimated. Examining VSCPT as a function of the laser parameters, the authors deduced the presence of nonspecified laser cooling forces that contribute to the efficiency in the filling of the noncoupled state.

Combinations of linearly and circularly polarized laser fields were examined by Taichenachev, Tumaikin, Yudin and Ol'shanii [1992a,b] for VSCPT on the $J_g = 3/2 \rightarrow J_e = 1/2$ and $J_g = 2 \rightarrow J_e = 1$ transitions.

The idea of atomic states decoupled from the laser field because of quantum interferences was extended by Dum, Marte, Pellizzari and Zoller [1994] to cases in which the electric field amplitudes have a spatial dependence limited in space similar to that of a laser trap, so that the spatial atomic wavefunction also would present a confinement.

§ 6. Adiabatic Transfer

The aim of adiabatic transfer is to transfer an atom or molecule from one lower level of the Λ scheme to the other one by using properly tailored laser pulses, with as large an efficiency as possible. The adiabatic transfer in three- and multilevel systems was investigated theoretically by Oreg, Hioe and Eberly [1984], and Carroll and Hioe [1988]. They demonstrated that by using conditions for the time dependence of the Rabi frequencies $\Omega_{R1}(t)$ and $\Omega_{R2}(t)$ defined as anti-intuitive, a complete transfer of population from level $|1\rangle$ to level $|2\rangle$ is realized. Adiabatic transfer is a consequence of one of the $|NC\rangle$ properties already discussed. From eq. (2.18), $|NC\rangle$ is an eigenstate of the $\mathcal{H}_0 + V_{AL}$ Hamiltonian with zero eigenvalue. If the Hamiltonian is modified adiabatically, so that the system remains in this state, the occupation of the $|NC\rangle$ remains constant. Let us consider a sequence of laser pulses applied to the $|1\rangle \rightarrow |0\rangle$ and $|2\rangle \rightarrow |0\rangle$ transitions, with the time evolution of the electric field amplitudes

described by functions $\Omega_{R1}(t)$ and $\Omega_{R2}(t)$, so that $|NC(t)\rangle$ assumes the following form:

$$|NC(t)\rangle = \frac{\Omega_{R2}(t)}{G}|1\rangle - \frac{\Omega_{R1}(t)}{G}|2\rangle, \tag{6.1}$$

with G given by eq. (2.16b). Adiabatic transfer is realized for a sequence of Rabi frequency time dependencies such as those shown in fig. 25a. If the laser acting on the $|2\rangle \rightarrow |0\rangle$ transition is applied initially, the $|NC\rangle$ state coincides with state $|1\rangle$ where the entire atomic or molecular system is supposed to be concentrated. If the laser acting on the $|2\rangle \rightarrow |0\rangle$ transition is progressively switched off while the laser pulse acting on the $|1\rangle \rightarrow |0\rangle$ transition is switched on (see fig. 25a), eq. (6.1) shows that at the end $|NC(t)\rangle$ coincides with $|2\rangle$, so that in the adiabatic regime the system occupies state $|2\rangle$. The counterintuitive pulse sequence is based on a laser being applied to the second transition at the beginning, and a laser to the first transition at the end. The requirements on the validity of the adiabaticity condition are (Oreg, Hioe and Eberly [1984], Kuklinski, Gaubatz, Hioe and Bergmann [1989], Carroll and Hioe [1990], Band and Julienne [1991a], Shore, Bergmann, Oreg and Rosenwaks [1991], Marte, Zoller and Hall [1991], Shore, Bergmann and Oreg [1992]):

$$\Omega_{R1}, \Omega_{R2} \gg \Gamma_0, \qquad \Omega_{R1}, \Omega_{R2} \gg \frac{1}{T}, \tag{6.2}$$

where T represents the time duration of the two laser pulses. If broad-band lasers are used for the excitation, the spontaneous emission damping rate in the first relation of eq. (6.2) should be replaced by the laser bandwidth, which is equivalent to a damping rate of the optical coherences, as in § 2.8 (He, Kuhn, Schiemann and Bergmann [1990], Kuhn, Coulston, He, Schiemann and Bergmann [1992]).

The first experimental results of adiabatic transfer were obtained on a Na_2 beam with a transfer from the electronic ground and vibrationally excited level $X^1\Sigma_g^+$ ($v = 0$, $J = 5$) to another vibrational one $X^1\Sigma_g^+$ ($v = 5$, $J = 5$) using a three-level Λ system with upper electronic excited level $A^1\Sigma_u^+$ ($v = 7$, $J = 6$) (Gaubatz, Rudecki, Becker, Schiemann, Külz and Bergmann [1988], Kuklinski, Gaubatz, Hioe and Bergmann [1989], Gaubatz, Rudecki, Schiemann and Bergmann [1990]). The counterintuitive time-dependent pulse sequence was created using the time-dependent interaction of sodium molecules crossing c.w. laser beams with separate excitations by the two lasers at different positions along the beam axis. That separated excitation modified drastically the amount of the population transferred to the final state, such as for the realization of

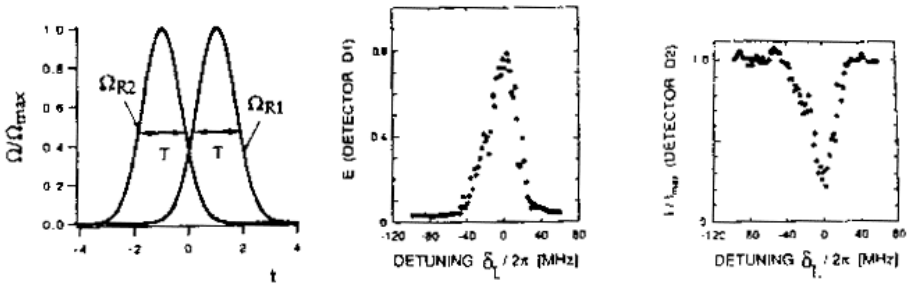

a) b) c)

Fig. 25. (a) Schematic representation of the time dependence for the Rabi frequencies required for adiabatic transfer from level |1⟩ to level |2⟩; (b) experimental results for the adiabatic transfer efficiency between the $X^1\Sigma_g^+$ ($v=0$, $J=5$) and $X^1\Sigma_g^+$ ($v=5$, $J=5$) levels of Na_2 molecules versus the laser 2 frequency, with laser 1 in resonance, and the temporal pulse sequence which maximizes the transfer; (c) experimental results for the fluorescence from excited state $A^1\Sigma_u^+$ ($v=7$, $J=6$) involved in the adiabatic transfer showing the resonant decrease associated with coherent population trapping (from Gaubatz, Rudecki, Schiemann and Bergmann [1990]).

the proper pulsed laser sequence. Figure 25b shows experimental results from Gaubatz, Rudecki, Schiemann and Bergmann [1990] for the transfer efficiency at laser fixed positions scanning the frequency of laser 2, with laser in resonance, with a maximum efficiency around 0.8. Figure 25c shows experimental results for the fluorescence from the upper excited state versus the laser 2 frequency. Corresponding to the maximum of the adiabatic transfer, a minimum was obtained in the excited-state population versus laser frequency, as evidence of coherent population trapping. A similar setup for adiabatic transfer was used by Liedenbaum, Stolte and Reuss [1989], and Dam, Oudejans and Reuss [1990] in a molecular beam of ethylene, C_2H_4, in a three-level cascade configuration. A CO_2 laser induced the transition $gs(4,1,3) \rightarrow \nu_7(5,0,5)$, and from there a color center laser induced the transition to $\nu_7 + \nu_9(5,1,4)$. Schiemann, Kuhn, Steuerwald and Bergmann [1993] demonstrated a highly efficient and selective population transfer in NO_2 molecules in the electronic ground $X_2H_{1/2}$ state from vibrational level $v=0$ to level $v=6$, using pulsed lasers properly delayed to realize the counterintuitive sequence of fig. 25a. Sussman, Neuhauser and Neusser [1994] have realized the adiabatic transfer on a Λ system of the C_6H_6 molecule, with pulsed lasers in the counterintuitive time sequence, for preparation in a specific rotational state of a vibronic state of that polyatomic molecule. That transfer was detected through the decrease in the population of the excited state in the Λ system, which represents the coherent population-trapping characteristics.

The adiabatic transfer with a continuum as the upper level of the Λ scheme has been examined theoretically by Carroll and Hioe [1992]. Coulston and Bergmann [1992] have examined the modifications in the process produced by the presence of additional levels close to $|0\rangle$ and $|2\rangle$, such as for the vibra-rotational manifolds of molecular states. Band and Julienne [1991b] have considered the adiabatic transfer in a four-level system and demonstrated that a significant population transfer can be achieved, even if a four-level system does not support coherent population-trapping states.

The concept of adiabatic transfer has been extended by Marte, Zoller and Hall [1991] to the case of noncoupled entangled states involving atomic momentum, such as those involved in the VSCPT processes [see eqs. (5.5) and (5.17)]. For a three-level $J_g = 1 \rightarrow J_e = 1$ atom interacting with two counterpropagating σ^+/σ^- laser beams, such that the linear superposition of eq. (5.5) describes the noncoupled state, the counterintuitive application of a σ^+,σ^- sequence will transfer an atom from the initial $|g_{-1}, p - \hbar k\rangle$ state to the final $|g_{+1}, p + \hbar k\rangle$ state with a modification of the atomic momentum by two times $\hbar k$. For a higher J transition, such as $J_g = 2 \rightarrow J_e = 2$ with the noncoupled state given by eq. (5.17), the adiabatic transfer produces a larger coherent and selective modification of the atomic momentum by $4\hbar k$. The adiabaticity conditions for the photon momentum transfer are those of eq. (6.2), and are quite easily satisfied. Theoretical analyses for alkali atoms have been performed by Weitz, Young and Chu [1994a], and Foot, Wu, Arimondo and Morigi [1994]. The adiabatic transfer between the entangled states of internal and momentum variables has been realized experimentally by different groups. Pillet, Valentin, Yuan and Yu [1993], Goldner, Gerz, Spreeuw, Rolston, Westbrook, Phillips, Marte and Zoller [1994a,b], and Valentin, Yu and Pillet [1994] have demonstrated, using the D_2 excitation of cesium atoms precooled by sub-Doppler techniques, a momentum transfer up to $8\hbar k$ between the extreme Zeeman sublevels of the $F = 4$ hyperfine level, with an efficiency up to 0.5. The off-resonant transitions to other excited states of the $3^2P_{3/2}$ manifold limited the efficiency, which should be larger using the D_1 excitation to the $6^2P_{1/2}$ manifold where the hyperfine separation is larger. Lawall and Prentiss [1994] realized the adiabatic transfer on ^{4}He metastable atoms in a beam using the $2^3S_1 \rightarrow 2^3P_0$ transition, with an efficiency of transfer up to 0.9 for a change of atomic momentum by $2\hbar k$. Using multiple interaction of the lasers with the atomic beam, Lawall and Prentiss [1994] obtained momentum changes up to $6\hbar k$. An immediate application is in atomic interferometry with the adiabatic transfers used as atomic beam splitters. In fact, an atomic interferometer based on adiabatic transfer between the cesium $6^2S_{1/2}$ hyperfine states $|F = 3, m_F = 0\rangle$ and $|F = 4, m_F = 0\rangle$ using a

σ^+,σ^- polarization configuration has been demonstrated by Weitz, Young and Chu [1994b]. Using the D_1 excitation, a coherent transfer of 140 photon momenta to cesium atoms with an efficiency of 0.95 per exchanged photon was reported.

§ 7. "Lasing Without Inversion"

The idea of lasing without inversion was developed independently by two groups in Russia and the United States, Kocharovskaya and Khanin [1988] and Scully, Zhu and Gavrielides [1989], respectively. The aim is to produce a laser system where the population in the excited atomic, or molecular, state is smaller that the population in the lower state. The states without inversion are defined according to the atomic, or molecular, basis, in the absence of applied radiation fields. Much attention has been given to the subject, both theoretically and experimentally, due to the attractive possibility of converting a coherent low-frequency input into a coherent high-frequency output, without any requirement on population inversion between the high-frequency emitting levels. At the present stage, several mechanisms giving rise to the phenomenon of "lasing without inversion" have been identified, as seen in the reviews by Kocharovskaya [1992] and Scully [1992]. One of those mechanisms has been based on coherent population trapping, and up to now the large majority of the experimental verifications of amplification without inversion is based on this phenomenon. In effect, this mechanism of "lasing without inversion" should be classified as an inversion in the hidden basis of the coupled/noncoupled states. This mechanism of "lasing without inversion" (or more precisely, amplification without inversion (AWI), because a cavity is required to convert an amplifier into a laser), can be easily analyzed when the transformation from the atomic basis $\{|1\rangle, |2\rangle, |0\rangle\}$ to the coherent-trapping basis $\{|\mathrm{NC}\rangle, |\mathrm{C}\rangle, |0\rangle\}$ is applied, as in fig. 26 (Kocharovskaya, Mauri and Arimondo [1991], Kocharovskaya, Mauri, Zambon and Arimondo [1992]). For the coupled/noncoupled basis, the interaction of the atoms with the externally applied electric field acts only on the $|\mathrm{C}\rangle$ and $|0\rangle$ states. In a system at thermal equilibrium, the states $|1\rangle$ and $|2\rangle$ are equally populated, as represented schematically in fig. 26a, and the excited state $|0\rangle$ contains a small population. The population of the $|\mathrm{C}\rangle$ state may be transferred to the $|\mathrm{NC}\rangle$ state through one of the appropriate mechanisms for creating coherent population trapping already described in this review, or one of those to be discussed later in this section. Perfect coherent population trapping is realized with $\rho_{\mathrm{C,C}} \simeq 0$, and an efficient trapping corresponds to $\rho_{\mathrm{NC,NC}} \gg \rho_{\mathrm{C,C}}$, as shown

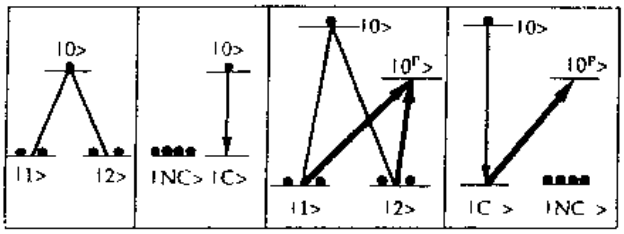

Fig. 26 (a) and (b) Energy levels for amplification without inversion for the Λ scheme, and (c) and (d) for the double-Λ scheme. In (a) and (c) the bare atomic basis is used, and in (b) and (d) the coupled/noncoupled basis is used. The depopulation pumping between coupled and noncoupled levels is schematically represented by the transfer of the black dots.

in fig. 26b. In these conditions, if a population inversion is realized between the levels $|0\rangle$ and $|C\rangle$; i.e.,

$$\rho_{0,0} \gg \rho_{C,C}, \tag{7.1}$$

an amplification of the radiation on the $|0\rangle \rightarrow |C\rangle$ transition could be obtained. This amplification is produced by an inversion between states $|0\rangle$ and $|C\rangle$ in the atomic basis of coupled/noncoupled states, but in the atomic basis of bare states $\{|1\rangle, |2\rangle, |0\rangle\}$ no population inversion exists, because $\rho_{1,1} + \rho_{2,2} = \rho_{C,C} + \rho_{NC,NC} \gg \rho_{0,0}$! This simple presentation exemplifies the concept of amplification in a hidden basis, the basis of the coupled/noncoupled states.

The possibility of obtaining gain in a Λ system on the condition of coherent population trapping is also understood by examining the plot of $\mathrm{Im}(\rho_{01})$, proportional to the absorption coefficient, as shown in fig. 2c, with the very narrow peak at the center which has been defined as electromagnetic-induced transparency (Kocharovskaya [1992], Scully [1992]). By pumping a small amount of the population into the excited state $|0\rangle$, a contribution with opposite sign is added to the absorption coefficient, which could bring that peak above the horizontal axis and create a condition of amplification.

If the condition $\rho_{0,0} \gg \rho_{C,C}$ corresponds to AWI, the operation of a laser requires three levels inside a cavity with the gain larger than the cavity losses. It should be noted that the amplification on the coupled/noncoupled basis corresponds to an amplification of a bichromatic field, i.e., two electromagnetic field waves with frequencies $\omega_{L,1}$ and $\omega_{L,2}$, equal to the two transitions $|0\rangle \rightarrow |1\rangle$ and $|0\rangle \rightarrow |2\rangle$ in the bare atomic basis. If the two frequencies have the same cavity loss κ, and the two optical transitions of the three-level system have

the same absorption coefficient α, the condition for lasing is a straightforward application of the condition for lasing based on a two-level system:

$$\rho_{00} - \rho_{C,C} \geqslant \frac{2\kappa}{\alpha L}, \tag{7.2}$$

where L is the length of the cavity, supposed to be filled uniformly with the three-level medium, presenting amplification without inversion.

The condition of amplification, or more precisely of no absorption, is valid only with respect to the $|NC\rangle$, $|C\rangle$ states of eqs. (2.16), as determined by the process that has prepared those states. In order to realize amplification of a bichromatic electromagnetic field, composed of two different components $\mathcal{E}_{L1}\exp[-i(\omega_{L1}t+\phi_{L1})]$ and $\mathcal{E}_{L2}\exp[-i(\omega_{L2}t+\phi_{L2})]$, the $|NC\rangle$ state should really be noncoupled for that amplified field. As a consequence, the atomic amplitudes and the amplitudes of the electric field components to be amplified by the noninverted medium, should satisfy a matching condition. If the $|1\rangle$ and $|2\rangle$ levels are degenerate in energy, the amplified field has only one frequency component, and the separation between the two modes of the electric field originates from polarization selection rules. On the contrary, if $|1\rangle$ and $|2\rangle$ are separated in energy, the amplified bichromatic field has components at two different frequencies ω_{L1} and ω_{L2}. In this scheme, defined by Fill, Scully and Zhu [1990] as a quantum beat laser, the beat frequency $\omega_{L1} - \omega_{L2}$ should match the evolution frequency of the ground state coherence. Amplification of a bichromatic field also imposes a phase matching condition: in a laser cavity, neglecting cavity losses and frequency pulling with respect to the interaction with the three-level system, the laser field relative phase should be opposite to that of the ground-state coherence. Fill, Scully and Zhu [1990] have derived, for different schemes of creation of the coherent population trapping, the phase-matching equation to be satisfied by the relative phase $\phi_{L1} - \phi_{L2}$ of the two lasers.

The relation (2.20) between the density matrix elements in the coupled/noncoupled basis and in the bare atomic basis shows, that in order to have a small value of $\rho_{C,C}$, the occupation of the noncoupled state, the atomic coherence $|\rho_{12}|$ should be large. The different applications of coherent population trapping for lasing without inversion, both theoretically and experimentally, are really connected to the differences in the preparation of a large atomic coherence ρ_{12} with a small occupation of the $|C\rangle$ state and a large occupation of the $|NC\rangle$ state. An efficient process for the realization of amplification without inversion is based on the double-Λ scheme, as shown in fig. 26c, with the two lower levels, $|1\rangle$ and $|2\rangle$ connected by dipole transitions to the upper levels $|0\rangle$ and $|0^P\rangle$ (Fill, Scully and Zhu [1990], Kocharovskaya, Li and

Mandel [1990], Kocharovskaya and Mandel [1990], Khanin and Kocharovskaya [1990], Kocharovskaya, Mauri and Arimondo [1991], Kocharovskaya, Mauri, Zambon and Arimondo [1992]). A pump bichromatic laser field, with amplitudes $\mathcal{E}_{L1}^{P}\exp[-i\phi_{L1}^{P}]$ and $\mathcal{E}_{L2}^{P}\exp[-i\phi_{L2}^{P}]$ resonant with the $|1\rangle \rightarrow |0^{P}\rangle$ and $|2\rangle \rightarrow |0^{P}\rangle$ transitions to the pumping level $|0^{P}\rangle$, prepares the coherent trapping superposition in the ground state, so that an amplification of a bichromatic field from state $|0\rangle$, with amplitudes $\mathcal{E}_{L1}\exp(-i\phi_{L1})$ and $\mathcal{E}_{L2}\exp(-i\phi_{L2})$, takes place. The preparation of the $|C^{P}\rangle$ and $|NC^{P}\rangle$ states, shown in fig. 26d, takes place through the depopulation pumping process, as discussed in § 2.3, with coupled and noncoupled states given by:

$$|NC^{P}\rangle = \frac{1}{\sqrt{|\mu_{0^{P}1}\mathcal{E}_{L1}^{P}|^{2} + |\mu_{0^{P}2}\mathcal{E}_{L2}^{P}|^{2}}}\left(\mu_{0^{P}2}\mathcal{E}_{L2}^{P}e^{-i\phi_{L2}^{P}}|1\rangle - \mu_{0^{P}1}\mathcal{E}_{L1}^{P}e^{-i\phi_{L1}^{P}}|2\rangle\right),$$

$$|C^{P}\rangle = \frac{1}{\sqrt{|\mu_{0^{P}1}\mathcal{E}_{L1}^{P}|^{2} + |\mu_{0^{P}2}\mathcal{E}_{L2}^{P}|^{2}}}\left(\mu_{0^{P}1}\mathcal{E}_{L1}^{P}e^{-i\phi_{L1}^{P}}|1\rangle + \mu_{0^{P}1}\mathcal{E}_{L2}^{P}e^{-i\phi_{L2}^{P}}|2\rangle\right). \tag{7.3}$$

However, these coupled and noncoupled states should coincide with those on the transitions to the $|0\rangle$ state, so that the following self-consistent condition between the amplitudes of all the fields applied to the double-Λ system should be satisfied:

$$\frac{\mu_{01}\mathcal{E}_{L1}\exp(-i\phi_{L1})}{\mu_{02}\mathcal{E}_{L2}\exp(-i\phi_{L2})} = \frac{\mu_{0^{P}1}\mathcal{E}_{L1}^{P}\exp(-i\phi_{L1}^{P})}{\mu_{0^{P}2}\mathcal{E}_{L2}^{P}\exp(-i\phi_{L2}^{P})}. \tag{7.4}$$

Kocharovskaya and Mandel [1990] have derived the conditions for the realization of steady-state AWI in the double-Λ scheme taking into account the simultaneous interaction of the four-level system with the two pairs of bichromatic fields. The important condition to be satisfied for the realization of this AWI was that the population of the lasing level $|0\rangle$ should be larger than that of the pumping level $|0^{P}\rangle$. More precisely, the following condition results:

$$\rho_{0,0} - \rho_{0^{P},0^{P}} > \frac{\Gamma_{21}}{\Gamma_{0^{P}}}. \tag{7.5}$$

This relation states than in order to obtain AWI, a population inversion should be realized between the two upper levels, but of course no population inversion is required between these levels and the ground ones. The relation derives from the competition in the creation of coherent population trapping between the two separate Λ schemes of the double Λ. In fact, the population in the

$|0^P\rangle$ state contributes through spontaneous emission or one-photon processes to the pumping of the population in the coupled state $|C\rangle$, whose presence decreases the amplification and increases the threshold of amplification without inversion. In the case of generation of short-wavelength radiation by pumping with a longer wavelength laser, level $|0\rangle$ is higher in energy than level $|0^P\rangle$, and in thermodynamic equilibrium the population of the $|0\rangle$ top level is smaller than that of the $|0^P\rangle$ intermediate level. Thus, the above threshold condition (7.5) cannot be satisfied without external pumping.

The above discussion points out the close equivalence between the double-Λ scheme and a four-level laser. In fact, optical pumping in a four-level system represents an alternative way to realize amplification on the same double-Λ scheme without creation of coherences. For instance, on the same level structure of fig. 26c, pumping from the $|2\rangle$ state to the $|0^P\rangle$ state followed by spontaneous emission down to the $|1\rangle$ level could produce an inversion between $|0\rangle$ and $|2\rangle$. The threshold condition required for amplification on this optical pumping scheme is exactly equivalent to those for AWI in the double Λ (Kocharovskaya, Mauri, Zambon and Arimondo [1992], Fleischhauer and Scully [1994]). These last authors also pointed out that schemes combining optical pumping with the creation of coherences could produce a further reduction of the threshold.

An alternative way to create a lower-state coherence is through the application of a microwave field resonant with the lower-state splitting, as shown schematically in fig. 27a (Scully, Zhu and Gavrielides [1989], Fill, Scully and Zhu [1990], Khanin and Kocharovskaya [1990]). The generated lower-state coherence can be expressed through coupled/noncoupled states. Again, for a population of the $|0\rangle$ level larger than that of the coupled state, amplification takes place, with inversion in the basis of the coupled/noncoupled states. The main difference between the double-Λ scheme and the microwave field is that in the double-Λ scheme the depopulation pumping of the coupled state leads to the preparation of a pure density matrix state, i.e., with all the atoms prepared in the noncoupled state. For microwave-generated coherence, starting from the nonpure state of the thermal occupation of ground states, the application of a microwave-coherent field cannot produce a pure state. As a consequence, the gain in the microwave case is always smaller than in the double-Λ scheme. The thermal nonpure occupation of the ground states leads to the following condition for AWI: $\rho_{00} \geqslant \min(\rho_{11}, \rho_{22})$ (Mandel and Kocharovskaya [1993]).

Another scheme for the realization of amplification without inversion, actually the first one proposed by Kocharovskaya and Khanin [1988] and examined later by Fleischhauer, Keitel, Scully and Su [1992], is based on the application to the

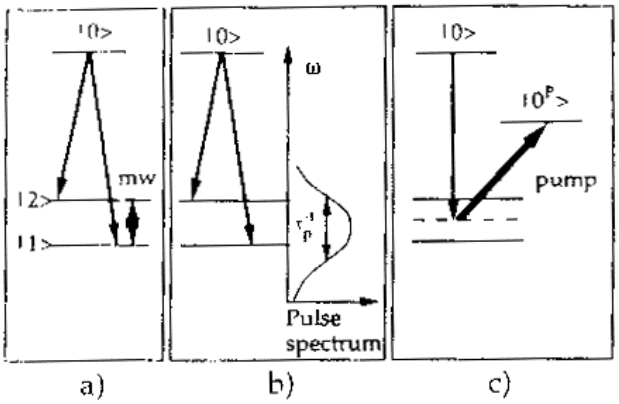

Fig. 27. Additional schemes for amplification without inversion based on coherent population trapping: (a) preparation of the coherent trapping superposition through a microwave field and amplification of the bichromatic field; (b) coherent trapping superposition formed by an ultrashort laser pulse with duration τ_p; (c) four-level scheme with pump laser to the level $|0^P\rangle$ tuned halfway between the ground levels with amplified laser also tuned halfway between ground levels.

three-level system of a short laser pulse, as in fig. 27b and as for the experiments described in § 3.3. In order for the short pulse with temporal duration τ_p to interact with both the ω_{01} and ω_{02} optical transitions and to probe the low-frequency coherence ρ_{21}, the relation $1/\tau_p \gg \omega_{21}$ must be satisfied. As usual, the gain is based on the preparation of a small population in the upper $|0\rangle$ level, with population in the lower states lying in the $|NC\rangle$ state. The $|NC\rangle$ occupation should have been realized before the pulse arrival, by applying a microwave field, using the double-Λ scheme, or by applying a train of pulses as described in § 3.3.

The last scheme involving coherent population trapping, proposed by Narducci, Doss, Ru, Scully, Zhu and Keitel [1991], is based on the combination of the double-Λ scheme and the dressed-state approach of § 2.4 and fig. 5a: a coherent population-trapping preparation is performed on one Λ system and amplification is achieved on the second Λ system, as shown in fig. 27c. Only one laser is required for the preparation stage, and only one laser is used for the amplification process, both lasers being tuned at the center frequency between the two groundstate levels.

The scheme of fig. 27c was tested in the first experiment of inversionless amplification performed on sodium atoms by Gao, Guo, Guo, Jin, Wang, Zhao, Zhang, Jiang, Wang and Jiang [1992], with lower levels being the hyperfine states of $3^2S_{1/2}$ ground level, $3^2P_{3/2}$ as the $|0\rangle$ amplification state, and $3^2P_{1/2}$ as the $|0^P\rangle$ preparation state. In the experiment a discharge through the helium/argon buffer gas prepared the required small occupation in the excited sodium states, and a strong pulsed laser on the $\{|1\rangle, |2\rangle\} \rightarrow |0^P\rangle$ transitions produced the

coherent trapping superposition. The amplification of a c.w. dye laser on the $|0\rangle \rightarrow \{|1\rangle, |2\rangle\}$ transitions was monitored, through a boxcar detector, during the application of the pulsed laser. These authors have reported AWI, and Gao, Zhang, Cui, Guo, Jiang, Wang, Jin and Li [1994] have measured the excited-state population through the absorption of a second c.w. dye laser from the excited state in order to verify that no population inversion in the bare states was created by the strong preparation pulse. The positive result of that experiment has generated some discussion in the lasing-without-inversion community: the possibility of a real population inversion between the excited state and ground states produced by the pulsed laser was ruled out in their direct absorption measurements. Because the experiment was performed in a transient regime, a theoretical analysis of the transient AWI was performed by Doss, Narducci, Scully and Gao [1993], proving that amplification is also reached in the transient regime. A later analysis by Meyer, Rathe, Graf, Zhu, Fry, Scully, Herling and Narducci [1994] showed that no coherence between the ground state hyperfine levels could have been created in that sodium experiment.

Clearer evidence of AWI, based on the scheme of fig. 27c, was obtained by Kleinfeld and Streater [1994] in potassium atoms, using the ground $4^2S_{1/2}$ hyperfine levels, $4^2P_{3/2}$ as the preparation state, and $4^2P_{1/2}$ as the amplifying state. Continuous lasers were used for both preparation and amplification, tuned at the center between the two ground hyperfine states separated by 462 MHz. The upper-state population in the amplifying state was produced making use of the transfer from $4^2P_{3/2}$ to $4^2P_{1/2}$ in collisions between potassium and helium buffer gas. The experimental results were very similar to those predicted in the theoretical analysis by Narducci, Doss, Ru, Scully, Zhu and Keitel [1991], with some unexplained features of additional absorption dips just outside the gain peaks.

In the experiments by Nottelman, Peters and Lange [1993] and by Lange, Nottelman and Peters [1994], a coherent population trapping in the ground state of a Λ scheme was created through a train of picosecond pulses, as shown in fig. 27b and as analyzed in § 3.3. A second picosecond pulse probed, at different delay times, the amplification without inversion. Samarium atoms on the $J_g = 1 \rightarrow J_e = 0$ transition (as in the experiment by Parigger, Hannaford and Sandle [1986] discussed in § 3.5), in the presence of an applied magnetic field along the z axis, were irradiated by a train of 30 ps laser pulses, with electric field polarization along the y axis, a ground-state Hanle-effect configuration. When the matching condition of eq. (3.1) was satisfied, the picosecond pulse-train pumped atoms out of the $|J_g, C\rangle = |J_g = 1, y\rangle$ state and created the $|J_g, NC\rangle \equiv |J_g = 1, x\rangle$ coherent superposition of states, as from the selection

rules of eq. (2.32b). However, in the presence of a magnetic field B, that superposition is not an eigenstate and the atomic wavefunction experiences a time evolution. Because of the energy separation $\omega_{21} = 2g\mu_B B/\hbar$ between the $|J_g, m_J = 1\rangle$ and $|J_g, m_J = -1\rangle$ eigenstates of the atomic Hamiltonian, starting from a perfect atomic preparation at time $t = 0$ in the noncoupled state, the atomic wavefunction $|\psi_g(t)\rangle$ at time t is:

$$|\psi_g(t)\rangle = \cos\frac{\omega_{21}t}{2}\,|\mathrm{NC}\rangle - \sin\frac{\omega_{21}t}{2}\,|\mathrm{C}\rangle\,. \tag{7.6}$$

From eq. (7.6) it can be seen that the absorption from the $|\mathrm{C}\rangle$ part of $|\psi_g(t)\rangle$ varies with the delay time of the probe pulse. At $t_d = \pi/2\omega_{21}$, the occupation of the coupled state is equal to one half the initial value; at $t_d = \pi/\omega_{21}$ the occupation of the coupled state is equal to 1, and it is 0 at $t_d = 2\pi/\omega_{21}$. In order to realize AWI, a third pulse, linearly polarized along the z axis, pumped a few atoms from the ground $|J_g = 1, z\rangle$ state to the $|J_e = 0\rangle$ state, and the amplification between the excited $|J_e = 0\rangle$ state and the $|\mathrm{C}\rangle \equiv |J_g = 1, y\rangle$ state was probed by the delayed pulse. Depending on the delay time, the coupled-state occupation produced different contributions, so that at a proper delay time an inversion between $|J_e = 0\rangle$ and $|J_g = 1, \mathrm{C}\rangle$ could be realized with no population inversion in the Zeeman atomic basis. Actually, the experiment was operated slightly differently from that presented: at a fixed delay time of the probe, the tuning of the occupation of the coupled state was realized by varying the splitting ω_{21} through an applied magnetic field B. Moreover, the maximum value of the generated ground-state coherence was only 0.14, so that the full occupation of the coupled or noncoupled states could not be realized. Finally, while the relatively long decay time of the ground-state coherence (~15 ns) was beneficial for the experiment, the comparable decay time of the optical coherence (≈ 9 ns) implied that the atomic dispersion affected the pulse propagation, and the length of the samarium cell could not be increased. Thus, as stated by the authors, the measured amplification of 7% did not seem exciting, but was obtained with an optically thin sample.

Another experiment by Fry, Li, Nikonov, Padmabandu, Scully, Smith, Tittel, Wang, Wilkinson and Zhu [1993] was based on the sodium D_1 resonance line. A detailed analysis and presentation of the experimental results has been published in a series of four papers: Meyer, Rathe, Graf, Zhu, Fry, Scully, Herling and Narducci [1994], Nikonov, Rathe, Scully, Zhu, Fry, Li, Padmabandu and Fleischhauer [1994], Padmabandu, Li, Su, Fry, Nikonov, Zhu, Meyer and Scully [1994], and Graf, Arimondo, Fry, Nikonov, Padmabandu, Scully and Zhu [1995]. The level configuration involved in this experiment was based on two

σ^+ circularly polarized lasers exciting hyperfine components of the D_1 line and has already been presented in fig. 7f. The two laser beams, with linewidth ≈ 30 MHz and frequency difference matching the 1.77 GHz ground hyperfine splitting, were generated through an acousto-optic frequency shifter. The first step in the experiment was to test the production of the coherent population-trapping superposition by the bichromatic σ^+ radiation: one of the pumping lasers was switched off through a fast Q-switch and the transient absorption of the sodium atoms on the remaining pumping beam, as a consequence the destruction of the coherent trapping was monitored. The time evolution of the transmitted light was in good agreement with theoretical predictions. AWI was realized by pumping atoms to the excited $F = 2$ state from the ground $F = 2$, $m_F = 2$ level not involved in the coherent trapping superposition, through application of a weak excitation σ^- polarized light. As soon as the population inversion was established, an amplification of the bichromatic σ^+ radiation was observed. The amount of coherence established between the ground levels was not specified; however, in a theoretical analysis, which well reproduced the experimental results, a ground-state coherence around 0.10–0.12 was reported. The observed dependence of the coherent trapping superposition on the helium buffer gas has been discussed in § 2.8.

The last experiment in the coherent population-trapping application by van der Veer, van Dienst, Dönszelmann and van Linden van den Heuvell [1993], operated on a cascade scheme based on the ^{112}Cd $5s^2\,{}^1S_0 \rightarrow 5s5p\,{}^3P_1 \rightarrow 5s6s\,{}^3S_1$ levels, with transitions at wavelengths 326 nm and 308 nm. A longitudinal magnetic field B_z in the mT range produced an energy splitting of the excited $^3P_1$ state. Nanosecond-pulsed dye lasers, with frequency bandwidths in the GHz range to match the Doppler-broadening of the absorption lines, counterpropagated through a cadmium cell. The two lasers were linearly polarized, and the preparation, as well as the amplification processes are well understood in the level scheme based on the linearly polarized atomic basis of fig. 28a. Laser 1, linearly polarized along the x axis, excited the cadmium atoms from the $|{}^1S, J_g = 0\rangle$ state to the $|{}^3P_1, x\rangle$ state. Laser 2, linearly polarized along the y axis, transferred atoms to the $|{}^3S_1, z\rangle$ state. From there, amplification could be produced with emission towards the $|{}^3P_1, y\rangle$ state. This interpretation of AWI comes out very naturally in the hidden basis, whereas in the Zeeman atomic basis the interpretation of amplification without inversion requires a careful analysis of the atomic coherences created in the intermediate $^3P_1$ state. The presence of amplification was tested by monitoring the gain of a seed laser transmitted through the cadmium cell, and a gain of 4.3 was measured. The amplification was monitored in two different regimes. In the first one, laser 2

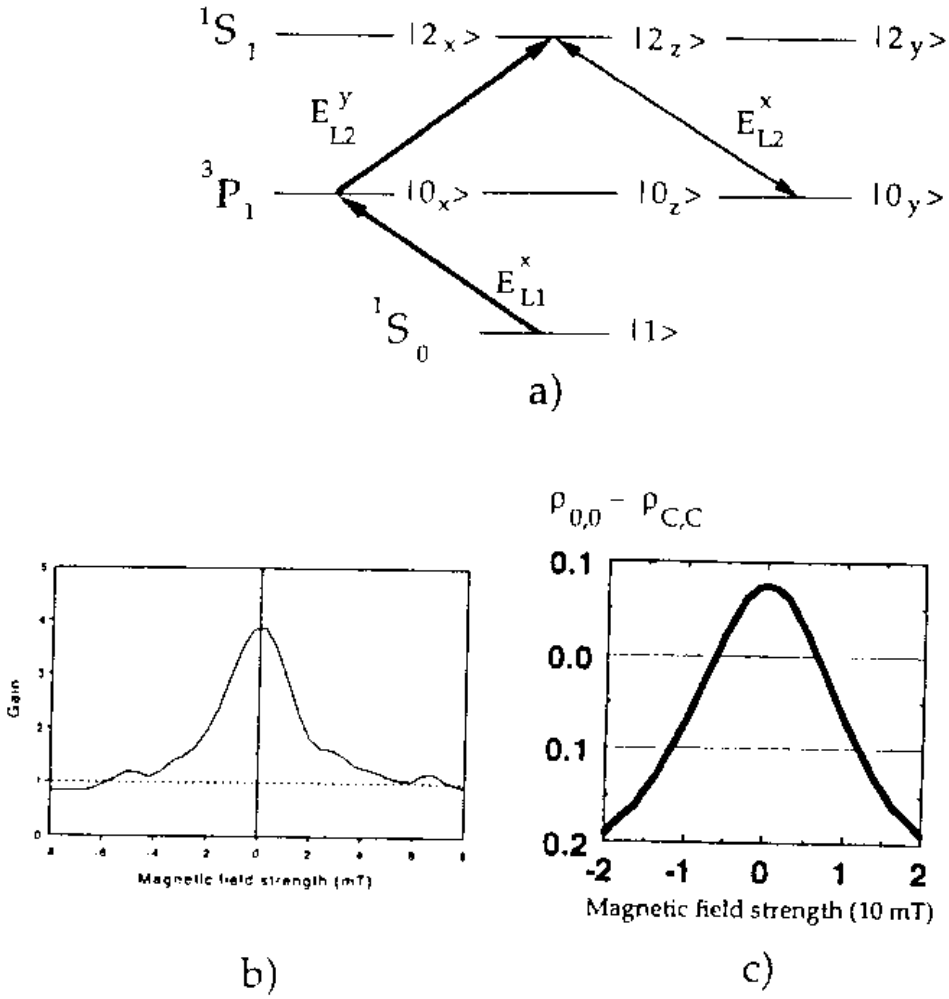

Fig. 28. (a) Level scheme, in the linear atomic basis (see § 2.6), for the ^{112}Cd AWI experiment, and (b) measured AWI gain versus applied magnetic field, with a loss of gain at the larger magnetic field due to the absence of population inversion (from van der Veer, van Dienst, Dönszelmann and van Linden van den Heuvell [1993]); (c) hidden basis population inversion in a ^{87}Rb double-Λ scheme versus an applied magnetic field; spontaneous emission rate $\Gamma_0 = 0.24\,\Gamma_0^P$, pumping rate $0.05\,\Gamma_0^P$ to excited state $|0\rangle$, Rabi frequencies $\Omega^P_{R1} = \Omega^P_{R2} = 0.12\,\Gamma_0^P$, and interaction time for preparation of the coupled/noncoupled state $\Theta = 83\,\Gamma_0^P$ (adapted from Kocharovskaya, Mauri and Arimondo [1991]).

was delayed by 30 ns with respect to laser 1, and when the amplification was measured versus the applied magnetic field, the periodic evolution between the coupled and noncoupled states could be monitored. In the second regime the two lasers produced simultaneous excitation to the top level of the cascade scheme, and the amplification was observed as a function of the magnetic field with

experimental results reported in fig. 28b. Figure 28c reports the results of a theoretical analysis for the population inversion in the hidden basis, proportional to the gain, as a function of the applied magnetic field, derived for the double-Λ scheme of ^{87}Rb atoms in Kocharovskaya, Mauri and Arimondo [1991]. The strong similarity between the two figures evidences the common features of evolution between coupled/noncoupled or $|x\rangle/|y\rangle$ states.

The use of the index of refraction has been considered in the context of amplification without inversion (Scully [1991, 1992], Fleischhauer, Keitel, Scully and Su [1992], Fleischhauer, Keitel, Scully, Su, Ulrich and Zhu [1992], Friedmann and Wilson-Gordon [1993]). It has already been noted (see fig. 2d and § 3.8) that a large index of refraction can be generated in the conditions of coherent population trapping. The use of that large index of refraction could be inhibited by the absorption coefficient of the material, which is large outside of the Raman resonance (see fig. 2c). However, by preparing the three-level system with a small population in the upper $|0\rangle$ state, a contribution to the absorption with opposite sign could be created, which is really an amplification, so that a regime may be realized with the large index of refraction occurring at a laser frequency where the absorption coefficient is effectively equal to zero. Applications of the enhancement of the index of refraction, considered by Scully [1991], are to the realization of phase-matching in the laser acceleration of electrons, to the increase of the resolving power in a microscope, and to the development of a new class of magnetometers. The experiments by Schmidt, Hussein, Wynands and Meschede [1993, 1995] and Xiao, Li, Jin and Gea-Banacloche [1995] on the index of refraction, as discussed in § 3.8, have been performed with the aim of modifying the group velocity for propagation inside a medium pumped so that it gives rise to coherent population trapping. A group velocity $v_g = c/1280$ has been reported by the first group of authors.

Attention here has been concentrated on schemes where no population inversion exists in the basis of the bare atomic states, but a population inversion is found in the basis of coupled/noncoupled states, or equivalently in the basis of dressed states. Other schemes of amplification without inversion have been identified where population inversion does not appear to occur in any basis (Kocharovskaya [1992]). However, the transformation from the bare-atomic basis to the dressed-state basis transforms population differences into coherences, so that the gain can be associated with the creation of coherences (Agarwal [1991a], Bhanu Prasad and Agarwal [1991]). Even if the amplification cannot be described simply through a population inversion in an appropriate basis, the role of coherence population trapping cannot be excluded. For instance, in an asymmetrical Λ scheme with level $|2\rangle$ metastable and the Rabi frequency Ω_{R2}

quite large, AWI can be realized on the $|0\rangle \rightarrow |1\rangle$ transition (Imamoglu, Field and Harris [1991]). For that process, Cohen-Tannoudji, Zambon and Arimondo [1993] pointed out the important role played by coherent population trapping. For $\Omega_{R1} \ll \Omega_{R2}$, the ground state $|1\rangle$ coincides with the noncoupled state, so that even a small population in the $|0\rangle$ state may be able to produce amplification.

Dowling and Bowden [1993] have considered AWI in a dense medium, where the near dipole–dipole interactions modify the local microscopic electric field through volume polarization, as in the Lorenz–Lorentz local field correction. This dipole–dipole interaction also would affect the phenomenon of coherent population trapping in a dense medium, with a frequency shift and a distortion of the resonance lineshapes.

§ 8. Coherences Created by Spontaneous Emission

The possibility of creating ground-state coherences in a Λ or V system was first considered by Agarwal [1974], but has received more attention recently in the context of lasing without inversion (Imamoglu [1989], Javanainen [1992], Fleischhauer, Keitel, Narducci, Scully, Zhu and Zubairy [1992]). In general the role of spontaneous emission is to erase the coherences through destructive interferences from the vacuum modes contributing to the excited state decay. However, in some particular cases those interferences do not cancel completely and a coherence may even be created by the spontaneous emission process. The most relevant case is for the Λ system when the two optical transitions $|0\rangle \rightarrow |1\rangle$ and $|0\rangle \rightarrow |2\rangle$ are completely equivalent from the point of view of the electric dipole emission, which requires two transitions at the same frequency but also with the same angular momentum quantum numbers. Javanainen [1992] considered the decay from a $|J_e = 1, m_J = 0\rangle$ level to two degenerate $|1\rangle$ and $|2\rangle$ ground levels, both of them with $J_g = 0$ quantum numbers. It is quite unlikely that such a configuration will be found in atoms, but it should not be completely excluded for molecular levels. In the case of these degenerate levels being found, the spontaneous emission terms in eq. (2.8) should be modified because of constructive interference in the upper level decay to both ground states. A new term should appear in the evolution of the ground state coherence:

$$\left.\frac{\mathrm{d}\tilde{\rho}_{12}}{\mathrm{d}t}\right|_{\text{sp.em.}} = \frac{\Gamma_0}{4}\rho_{00}. \tag{8.1}$$

Thus, ground-state coherence would be created in the spontaneous emission decay from the $|0\rangle$ state. Javanainen [1992] has pointed out that the superposition

principle requires the creation of that coherence. If the linear symmetric and antisymmetric combinations of ground states are considered, i.e., the coupled and noncoupled states, the upper state is dipole-connected to the coupled state only, and by spontaneous emission it will decay only to that coupled state. An atomic preparation of the coupled state through spontaneous emission implies that a coherence between the $|1\rangle$ and $|2\rangle$ ground states is formed. It is quite obvious that any experiment dealing with coherent population trapping will be affected dramatically by the presence of that coherence.

§ 9. Pulse-Matching and Photon Statistics

The research on lasing without inversion has shown that the preparation of a coherent population-trapping superposition modifies the interaction with radiation. As a consequence, properly tailored atomic superpositions may produce particular properties of the electromagnetic fields interacting with those superpositions. This section presents the application of coherent population trapping for modifying radiation field properties.

In the proposal of matched pulses by Harris [1993], a three-level system, supposed to be prepared in the $|NC\rangle$ state, was probed by a bichromatic electromagnetic field, $\mathcal{E}_{L1}(z,t)\,\boldsymbol{u}_1 \cos(\omega_{L1}t+\phi_1)$ and $\mathcal{E}_{L2}(z,t)\,\boldsymbol{u}_2 \cos(\omega_{L2}t+\phi_2)$, with time-varying envelope, applied to the two arms of a Λ system. Interacting with the $|NC\rangle$ state, the Fourier components of the input electromagnetic field, which are matched in their frequency difference, amplitude, and phase so as to preserve the atomic preparation in the noncoupled state, do not experience any absorption. On the contrary, the nonmatched Fourier components experience an absorption and are attenuated in the propagation. As a consequence, after a characteristic propagation distance, the transmitted field contains only Fourier components matched in amplitude and phase to the noncoupled state, and those components do not experience any further absorption. This concept of matched pulses has a strict connection with the observation by Dalton and Knight [1982a,b], reported in § 2.8, that critical cross-correlated fields acting on the two arms of the Λ system may preserve the coherent population-trapping preparation.

The idea of pulse matching has been formalized by the introduction of the normal modes by Harris [1994] and dressed field modes by Eberly, Pons and Haq [1994]. In effect, as the atomic time evolution is greatly simplified by using the $|NC\rangle$ state, for which eq. (2.18) expresses a time-independent evolution, a similar relation may be written for a combination of the electric field $\mathcal{E}_{L1}(z,t)$ and $\mathcal{E}_{L2}(z,t)$ components propagating through the three-level medium. The matched-

or dressed field combinations are linear combinations of the slowly varying envelopes $\mathcal{E}_{L1}(z, t)$ and $\mathcal{E}_{L2}(z, t)$, and can be derived from the Maxwell equations for propagation through the three-level system. The dressed fields represent a more general concept. If the atomic wavefunction $|\psi_g\rangle$ is written through the amplitudes a_1 and a_2 for the ground states of the Λ system:

$$|\psi_g\rangle = \frac{1}{\sqrt{|a_1|^2 + |a_2|^2}} (a_1 |1\rangle + a_2 |2\rangle), \tag{9.1}$$

the dressed-field states are defined through their Rabi frequencies Ω_C and Ω_{NC}

$$\begin{pmatrix} \Omega_C \\ \Omega_{NC} \end{pmatrix} = \begin{pmatrix} a_1 & a_2 \\ -a_2 & a_1 \end{pmatrix} \begin{pmatrix} \Omega_{R1} \\ \Omega_{R2} \end{pmatrix}, \tag{9.2}$$

where Ω_{R1} and Ω_{R2} are the Rabi frequencies for the fields acting on the $|1\rangle \rightarrow |0\rangle$ and $|2\rangle \rightarrow |0\rangle$ transitions. This linear transformation produces a coupled/noncoupled combination of the electric fields such that the Ω_C coupled field component is heavily absorbed during the propagation whereas the Ω_{NC} noncoupled field component propagates without attenuation. Under conditions of fast evolution of the excited-state population and optical coherences and of slow evolution of the ground-state coherences (fast and slow as compared to the pulse duration) the atomic amplitudes a_1 and a_2 of eq. (9.1) are determined by the initial conditions of the electric field amplitude. As a consequence, the input electric field determines the occupation amplitudes of the atomic wavefunction and fixes the linear combination Ω_{NC} of the nonattenuated electric field: the normal modes of Harris [1993] are defined by those atomic amplitudes and the Ω_C, Ω_{NC} Rabi frequencies. Normal modes may be realized in the propagation of a bichromatic pulse pair where the occupation of the coupled state is fixed through an initial interaction with the pulse pair. The pulse-pair propagation causes a distortion of the initial pulse edge and an unperturbed propagation of the remaining part of the pulse. Other methods for the preparation of the coherent trapping superposition may be also devised. Cerboneschi and Arimondo [1995] pointed out that the double-Λ scheme of fig. 26c is convenient for realizing pulse matching with great flexibility, because a pulse pair on one Λ system prepares the noncoupled superposition, whereas the pulse pair on the second Λ experiences pulse matching without any distortion of the initial edge. Notice that the definition of the dressed-field pulses by Eberly, Pons and Haq [1994] treats on the same footing the atomic superposition states and those classified as dark states in § 2.6.

Agarwal [1993] has generalized the idea of coherent population trapping by considering a quantized electromagnetic field in an approach similar to that used in the case of dressed states, but considering electromagnetic states with a very low photon number. Starting from the quantized field Hamiltonian of eq. (2.29) describing two field modes interacting with a Λ system, Agarwal searched for a wavefunction corresponding to a generalized atom–field noncoupled state, in the form of an entangled state of the atomic and field variables:

$$|\mathrm{NC_{AF}}\rangle = \mathbb{N}\,(g_{R2}c_1\,|1\rangle - g_{R1}c_2\,|2\rangle) \otimes |\psi_{\mathrm{field}}\rangle\,, \tag{9.3}$$

with the c_1 and c_2 coefficients and the $\mathbb{N}$ normalization constant to be determined. For the state $|\mathrm{NC_{AF}}\rangle$ to be an eigenvalue of the quantized Hamiltonian with zero eigenvalue, the radiation field $|\psi_{\mathrm{field}}\rangle$ wavefunction should satisfy the following equation:

$$(c_1 a_{R1} - c_2 a_{R2})\,|\psi_{\mathrm{field}}\rangle = 0, \tag{9.4}$$

with a_{R1} and a_{R2} the annihilation operators of the two field modes. The general solution of eq. (9.4) is obtained in terms of coherent states $|z_{R1}, z_{R2}\rangle$ associated with the two modes of the field:

$$|\psi_{\mathrm{field}}\rangle = \int q(z_{R1}) \left| z_{R1}, \frac{c_2}{c_1} z_{R1} \right\rangle \mathrm{d}z_{R1}, \tag{9.5}$$

with the c_1, c_2 coefficients and the function $q(z_{R1})$ fixed from the initial conditions of the system. The important point of this equation is that it describes two fields matched in their mode mean value:

$$\frac{\langle a_{R1}\rangle}{\langle a_{R2}\rangle} = \frac{c_1}{c_2}, \tag{9.6}$$

but also in their photon statistics, because from eq. (9.5) it results that the coherent states of the two modes are replicas of each other, only scaled by the c_1/c_2 factor.

The coherent population-trapping mechanism has determined the correlations of the two field modes. Jain [1994] has shown how the correlation in the phase noise of the two modes can be utilized for measurements limited only by the coherent-state shot noise. Agarwal, Scully and Walther [1994] have described how the ground-state coherence leads to a noise-free transfer of energy between a pump laser and a probe laser acting on the two arms of the Λ scheme. Fleischhauer [1994], investigating the correlations in the phase

fluctuations of the laser beams propagating through a three-level Λ system, pointed out the importance of the adiabatic response of the atomic coherence with respect to the phase or amplitude fluctuations of the field. In the adiabatic limit the atomic system responds promptly, and any modification in the field drives the atom into a new coherent superposition, again decoupled from the fields. In contrast, in the regime of nonadiabatic response, the atom remains in the initial noncoupled state on the time scale of the phase/amplitude field fluctuations, and those fluctuations will be damped out. In closely related papers involving the application of coherences and preparation of atoms in ground-state superpositions, the possibility of reduction of the intensity or phase noise in the three-level system has been discussed by several authors (Agarwal [1991b], Gheri and Walls [1992], Fleischhauer, Rathe and Scully [1992]). A discussion of those results will not be reported here because a clear definition of the role of coherent population trapping has not been established.

A linear superposition of ground states noncoupled to laser radiation has been considered by Cirac, Parkins, Blatt and Zoller [1993] for the motion of an ion in a trap. The ground states were associated with different vibrational states of the ionic motion. The noncoupled state formed by that superposition should present properties of squeezing in the atomic motion. Parkins, Marte, Zoller and Kimble [1993], and Parkins, Marte, Zoller, Carnal and Kimble [1995] have proposed a scheme for the preparation of general coherent superpositions of photon-number states. Three-level atoms initially in state $|1\rangle$ should experience an adiabatic transfer process, through proper time dependencies of Rabi frequencies, crossing a cavity where a laser field resonant with the transition $|1\rangle \rightarrow |0\rangle$ is present, whereas a vacuum field acts on the $|0\rangle \rightarrow |2\rangle$ transition. As a consequence of the atomic adiabatic transfer process to state $|2\rangle$, a cavity mode with one photon at frequency ω_{12} is created. The atomic adiabatic transfer allows the generation of photons in the cavity mode starting from the laser field acting on the $|1\rangle \rightarrow |0\rangle$ transition. Sequences of atoms passing through the cavity can be used to generate Fock states of higher photon number. The adiabatic transfer from properly tailored noncoupled atomic superpositions in high-J angular momentum states allows the generation of arbitrary superpositions of Fock states.

§ 10. Conclusions

Quantum-mechanical interference effects involving the existence of two different paths for the final process are well known in laser spectroscopy investigations, and they have been fully exploited in order to improve the spectroscopy

resolution. Coherent population trapping is an interesting example of that quantum interference, based on the preparation of a quantum-mechanical superposition state and an interference in the interaction with two modes of the electromagnetic field. As described above, the phenomenon has been observed and exploited in a large variety of experimental configurations. Furthermore, references in this review point out that the number of suggested new applications presented in the last few years is quite large. The most exciting and most promising applications for further development are those connected with the manipulations of atoms and molecules and electromagnetic fields. Adiabatic transfer and velocity-selective coherent population trapping allow preparation in a given state of internal and/or external variables, for which elegant theoretical schemes and experimental results have been reported. The manipulation of electromagnetic fields through coherent trapping superposition states represents its counterpart; the coherence created in the quantum-mechanical superposition state should allow the production of electromagnetic fields with specific and interesting correlation properties, with the initial information to be transferred to the optical field stored inside the three-level atomic coherence. Up to now, only several theoretical ideas and few experimental realizations have been reported, if we include within this class of manipulation the experiments on amplification without inversion. In any case, it is interesting to point out that, because coherently prepared systems have so many particular properties, the researchers in this field have been inspired to classify them as a new state of matter called "phaseonium", short for "phase coherent atomic ensemble" (Scully [1992]). Devices based on phaseonium, referred to also as "phasers", are not yet available, but the interest into the subject is growing among quantum optics researchers.

Furthermore, the proposals for extensions and applications of coherent population trapping are expanding. Not all of them have been reported here because of space limitations, but it is noteworthy that Tumaikin and Yudin [1991] have proposed to transfer to superconductivity the concept of coherent population trapping, looking for a quantum superposition of electron states decoupled from the electron–photon interaction. Applications to time-domain optical data storage have been presented by Hemmer, Cheng, Kierstead, Shahriar and Kim [1994]. Also, it has been pointed out by Zaretsky and Sazonov [1994] that in an experiment of nuclear decay, the creation of a coherent population-trapping superposition of atomic states with different hyprfine couplings could modify the angular distribution of the emitted γ rays. Moreover, the coherent superposition of states has been extended theoretically by Lindberg and Binder [1995] to a three-level Λ system in a GaAs quantum well, the lower state being associated to the heavy-hole and light-hole excitons. In this system the absorption

of a bichromatic laser pulse should show up through the characteristic coherent population-trapping decrease.

Some features of coherent population trapping have become more or less understood, but they are not yet fully exploited. For instance, the laser cooling application of coherent population trapping is based on the atomic preparation in a quantum-mechanical superposition of two states with different space dependence. That quantum-mechanical superposition may produce an atomic interference, either over a limited region of time and space or in consistent way over all of time and space. This interference has been considered by the researchers active in velocity-selective coherent population trapping, and its implications for atomic interferometry are quite important (Aspect, Arimondo, Kaiser, Vansteenkiste and Cohen-Tannoudji [1989], Lawall, Bardou, Saubamea, Shimizu, Leduc, Aspect and Cohen-Tannoudji [1994]). However, those experiments certainly pose a high technical challenge in atomic manipulation.

Coherent population trapping represents only an example of the richness of phenomena taking place in the interaction of radiation fields with multilevel atomic or molecular systems. More complicated interference schemes involving a larger number of levels and of radiation fields, as in the closed-loop multilevel structures, may provide new possibilities not yet explored. Similar to adiabatic transfer whose exploitation has taken a considerable amount of time after its original proposition, other interesting phenomena may be buried inside the theoretical analyses of multilevel systems. Coherent population trapping is connected to a conservation law, valid for a three-level system. Some other interesting possibilities may remain to be exploited within the conservation laws related to different observables in experiments involving a multilevel system interacting with several radiation fields. Several of those conservation laws involve excited states, and thus superpositions that are not stable against spontaneous emission, which may lead to applications in processes involving short pulse sequences. In any case, this field of research is very active and its extensions are too widely spread to be accurately forecast.

Acknowledgments

This work largely originated from the shared interest in the subject and collaboration throughout the years with G. Alzetta, C. Cohen-Tannoudji, O.A. Kocharovskaya, and M.O. Scully. I am grateful to G. Agarwal for having suggested the preparation of this review, to all those authors who permitted the use of their figures, to J. Cooper and J. Hall for a careful reading of the manuscript, and to C. Menotti for checking the proofs.

References

Adachi, S., H. Niki, Y. Izawa, S. Nakai and C. Yamanaka, 1991, Opt. Commun. **81**, 364.

Agap'ev, B.D., M.B. Gornyi and B.G. Matisov, 1993, Physics-Uspekhi **36**, 763.

Agarwal, G.S., 1974, Quantum Statistical Theories of Spontaneous Emissions and Their Relation to Other Approaches, Springer Tracts in Modern Physics, Vol. 70 (Springer, Berlin) p. 1.

Agarwal, G.S., 1991a, Phys. Rev. A **44**, R28.

Agarwal, G.S., 1991b, Phys. Rev. Lett. **67**, 980.

Agarwal, G.S., 1993, Phys. Rev. Lett. **71**, 1351.

Agarwal, G.S., M.O. Scully and H. Walther, 1994, Opt. Commun. **106**, 237.

Agrawal, G.P., 1981, Phys. Rev. A **24**, 1399.

Agrawal, G.P., 1983a, Phys. Rev. A **28**, 2286.

Agrawal, G.P., 1983b, J. Phys. Colloq. **44**, C2-125.

Akul'shin, A.M., A.A. Celikov and V.L. Velichansky, 1991, Opt. Commun. **84**, 139.

Akul'shin, A.M., and M. Ohtsu, 1994, Quantum Electron. **24**, 561.

Alekseev, V.Z., and D.D. Krylova, 1992a, JETP Lett. **55**, 321.

Alekseev, V.Z., and D.D. Krylova, 1992b, Laser Phys. **2**, 781.

Alekseev, V.Z., and D.D. Krylova, 1993, Opt. Commun. **95**, 319.

Alzetta, G., 1978, in: Coherence in Spectroscopy and Modern Physics, eds F.T. Arecchi, R. Bonifacio and M.O. Scully (Plenum, New York) p. 219.

Alzetta, G., A. Gozzini, L. Moi and G. Orriols, 1976, Nuovo Cimento B **36**, 5.

Alzetta, G., L. Moi and G. Orriols, 1979, Nuovo Cimento B **52**, 209.

Arimondo, E., 1987, in: Interaction of Radiation with Matter, a Volume in Honor of Adriano Gozzini, eds G. Alzetta, E. Arimondo, F. Bassani and L. Radicati (Scuola Normale Superiore, Pisa) p. 343.

Arimondo, E., 1992, in: Laser Manipulation of Atoms and Ions, Proc. Enrico Fermi Summer School, eds E. Arimondo, W.D. Phillips and F. Strumia (North-Holland, Amsterdam) p. 191.

Arimondo, E., 1994, in: Fundamentals of Quantum Optics III, Lecture Notes in Physics, Vol. 420, ed. F. Ehlotzky (Springer, Berlin) p. 170.

Arimondo, E., and G. Orriols, 1976, Lett. Nuovo Cimento **17**, 333.

Aspect, A., E. Arimondo, R. Kaiser, N. Vansteenkiste and C. Cohen-Tannoudji, 1988, Phys. Rev. Lett. **61**, 826.

Aspect, A., E. Arimondo, R. Kaiser, N. Vansteenkiste and C. Cohen-Tannoudji, 1989, J. Opt. Soc. Am. B **6**, 2112.

Aspect, A., and R. Kaiser, 1990, Foundations of Physics **20**, 1413.

Ballagh, R.J., and C. Parigger, 1986, in: Optical Bistability III, eds H.M. Gibbs, N. Peyghambarian, P. Mandel and S.D. Smith (Springer, Berlin) p. 227.

Band, Y.B., and P.S. Julienne, 1991a, J. Chem. Phys. **94**, 5291.

Band, Y.B., and P.S. Julienne, 1991b, J. Chem. Phys. **95**, 5681.

Bardou, F., J.P. Bouchaud, O. Émile, A. Aspect and C. Cohen-Tannoudji, 1994, Phys. Rev. Lett. **72**, 203.

Bardou, F., B. Saubamea, J. Lawall, K. Shimizu, O. Émile, C. Westbrook, A. Aspect and C. Cohen-Tannoudji, 1994, C.R. Acad. Sci. Paris, Série II **318**, 877.

Bell, W.E., and H.L. Bloom, 1961, Phys. Rev. Lett. **6**, 280, 623.

Beterov, I.M., and V.P. Chebotayev, 1969, JETP Lett. **9**, 127.

Bhanu Prasad, G., and G.S. Agarwal, 1991, Opt. Commun. **86**, 409.

Bloembergen, N., 1985, Ann. Phys. (France) **10**, 681.

Bloembergen, N., 1987, in: Interaction of Radiation with Matter, a Volume in Honor of Adriano Gozzini, eds G. Alzetta, E. Arimondo, F. Bassani and L. Radicati (Scuola Normale Superiore, Pisa) p. 145.

Bloembergen, N., and Y.H. Zou, 1985, in: Laser Spectroscopy VII, eds T.W. Hänsch and Y.R. Shen (Springer, Berlin) p. 186.
Bloembergen, N., Y.H. Zou and L.J. Rothberg, 1985, Phys. Rev. Lett. **54**, 186.
Bouchene, M.A., A. Débarre, J.-C. Keller, J.L. Le Gouët, P. Tchénio, V. Finkelstein and P.R. Berman, 1992a, Europhys. Lett. **18**, 409.
Bouchene, M.A., A. Débarre, J.-C. Keller, J.L. Le Gouët, P. Tchénio, V. Finkelstein and P.R. Berman, 1992b, J. Phys. II (France) **2**, 621.
Buckle, S.J., S.M. Barnett, P.L. Knight, M.A. Lauder and D.T. Pegg, 1986, Opt. Acta **33**, 1129.
Carroll, C.E., and F.T. Hioe, 1988, J. Opt. Soc. Am. B **5**, 1335.
Carroll, C.E., and F.T. Hioe, 1990, Phys. Rev. A **42**, 1522.
Carroll, C.E., and F.T. Hioe, 1992, Phys. Rev. Lett. **68**, 3523.
Castin, Y., H. Wallis and J. Dalibard, 1989, J. Opt. Soc. Am. B **6**, 2046.
Cavalieri, S., M. Matera, F.S. Pavone, J. Zhang, P. Lambropoulos and T. Nakajima, 1993, Phys. Rev. A **47**, 4219.
Cavalieri, S., F.S. Pavone and M. Matera, 1991, Phys. Rev. Lett. **67**, 3673.
Cerboneschi, E., and E. Arimondo, 1995, Phys. Rev. A **52**, R1823.
Cirac, J.I., A.S. Parkins, R. Blatt and P. Zoller, 1993, Phys. Rev. Lett. **70**, 556.
Cohen-Tannoudji, C., F. Bardou and A. Aspect, 1992, in: Laser Spectroscopy X, eds M. Ducloy, E. Giacobino and G. Camy (World Scientific, Singapore) p. 3.
Cohen-Tannoudji, C., J. Dupont-Roc and G. Grynberg, 1992, Atoms-Photons Interactions (Wiley, New York)
Cohen-Tannoudji, C., and A. Kastler, 1966, in: Progress in Optics, Vol. V, ed. E. Wolf (North-Holland, Amsterdam) p. 1.
Cohen-Tannoudji, C., and S. Reynaud, 1977, J. Phys. B **10**, 2311.
Cohen-Tannoudji, C., B. Zambon and E. Arimondo, 1993, J. Opt. Soc. Am. B **10**, 2107.
Corney, A., 1977, Atomic and Laser Spectroscopy (Clarendon Press, Oxford).
Coulston, G.W., and K. Bergmann, 1992, J. Chem. Phys. **96**, 3467.
Dalibard, J., S. Reynaud and C. Cohen-Tannoudji, 1987, in: Interaction of Radiation with Matter, a Volume in Honor of Adriano Gozzini, eds G. Alzetta, E. Arimondo, F. Bassani and L. Radicati (Scuola Normale Superiore, Pisa) p. 29.
Dalton, B.J., and P.L. Knight, 1982a, J. Phys. B **15**, 3997.
Dalton, B.J., and P.L. Knight, 1982b, Opt. Commun. **42**, 411.
Dalton, B.J., and P.L. Knight, 1983, in: Laser Physics, Lecture Notes in Physics, Vol. 182, eds J.D. Harvey and D.F. Walls (Springer, Berlin) p. 213.
Dalton, B.J., R. McDuff and P.L. Knight, 1985, Opt. Acta **32**, 61.
Dam, N., L. Oudejans and J. Reuss, 1990, Chem. Phys. **140**, 217.
de Clercq, E., and P. Cérez, 1983, Opt. Commun. **45**, 91.
de Clercq, E., M. de Labachelleríe, G. Avila, P. Cérez and M. Têtu, 1984, J. Phys. (France) **45**, 239.
de Lignie, M.C., and E.R. Eliel, 1989, Opt. Commun. **72**, 205.
Decomps, B., M. Dumont and M. Ducloy, 1976, in: Laser Spectroscopy of Atoms and Molecules, ed. H. Walther (Springer, Berlin) p. 283.
Doery, M.R., R. Gupta, T.H. Bergeman, H. Metcalf and E.J.D. Vredenbregt, 1995, Phys. Rev. A **51**, 2334.
Doery, M.R., M.T. Widmer, M.J. Bellanca, W.F. Buell, T.H. Bergeman, H. Metcalf and E.J.D. Vredenbregt, 1995, Phys. Rev. A **52**, 2295.
Doss, H.M., L.M. Narducci, M.O. Scully and J.Y. Gao, 1993, Opt. Commun. **95**, 57.
Dowling, J.P., and C.M. Bowden, 1993, Phys. Rev. Lett. **70**, 1421.
Dum, R., P. Marte, T. Pellizzari and P. Zoller, 1994, Phys. Rev. Lett. **73**, 2829

Eberly, J.H., M.L. Pons and H.R. Haq, 1994, Phys. Rev. Lett. **72**, 56.
Eckstein, J.N., A.I. Ferguson and T.W. Hänsch, 1978, Phys. Rev. Lett. **40**, 847.
Eliel, E.R., 1993, in: Advances in Atomic, Molecular and Optical Physics, Vol. 30, eds D. Bates and B. Bederson (Academic Press, New York) p. 199.
Eliel, E.R., and M.C. de Lignie, 1989, in: Laser Spectroscopy IX, eds M.S. Feld, J.E. Thomas and A. Mooradian (Academic Press, New York) p. 23.
Eliel, E.R., and M.C. de Lignie, 1990, in: Coherence and Quantum Optics VI, eds J.H. Eberly, L. Mandel and E. Wolf (Plenum Press, New York) p. 269.
Fano, U., 1961, Phys. Rev. **124**, 1866.
Faucher, O., D. Charalambidis, C. Fotakis, J. Zhang and P. Lambropoulos, 1993, Phys. Rev. Lett. **70**, 3004.
Feld, M.S., M.M. Burns, T.U. Kühl, P.G. Pappas and D.E. Murnick, 1980, Opt. Lett. **5**, 79.
Feld, M.S., and A. Javan, 1969, Phys. Rev. **177**, 540.
Feld, M.S., A. Sanchez, A. Javan and B.J. Feldman, 1974, in: Spectroscopie sans Largeur Doppler de Systèmes Moléculaires Simples, Colloques Internationaux no. 217 (CNRS, Paris) p. 87.
Feldman, B.J., and M.S. Feld, 1972, Phys. Rev. A **5**, 899.
Fill, E.E., M.O. Scully and S.Y. Zhu, 1990, Opt. Commun. **77**, 36.
Finkelstein, V., 1991, Phys. Rev. A **43**, 4901.
Fleischhauer, M., 1994, Phys. Rev. Lett. **72**, 989.
Fleischhauer, M., C.H. Keitel, L.M. Narducci, M.O. Scully, S.Y. Zhu and M.S. Zubairy, 1992, Opt. Commun. **94**, 599.
Fleischhauer, M., C.H. Keitel, M.O. Scully and C. Su, 1992, Opt. Commun. **87**, 109.
Fleischhauer, M., C.H. Keitel, M.O. Scully, C. Su, B.T. Ulrich and S.Y. Zhu, 1992, Phys. Rev. A **46**, 1468.
Fleischhauer, M., U. Rathe and M.O. Scully, 1992, Phys. Rev. A **46**, 1992.
Fleischhauer, M., and M.O. Scully, 1994, Opt. Commun. **105**, 79.
Foot, C.J., H. Wu, E. Arimondo and G. Morigi, 1994, J. Phys. II (France) **4**, 1913.
Friedmann, H., and A.D. Wilson-Gordon, 1993, Opt. Commun. **98**, 303.
Fry, E.S., X. Li, D.E. Nikonov, G.G. Padmabandu, M.O. Scully, A.V. Smith, F.K. Tittel, C. Wang, S.R. Wilkinson and S.Y. Zhu, 1993, Phys. Rev. Lett. **70**, 3235.
Gao, J.Y., C. Guo, X.Z. Guo, G.X. Jin, P. Wang, J. Zhao, H.Z. Zhang, Y. Jiang, D.H. Wang and D. Jiang, 1992, Opt. Commun. **93**, 323.
Gao, J.Y., H.Z. Zhang, H.F. Cui, X.Z. Guo, Y. Jiang, Q.W. Wang, G.X. Jin and J.S. Li, 1994, Opt. Commun. **110**, 590.
Gaubatz, U., P. Rudecki, M. Becker, S. Schiemann, M. Külz and K. Bergmann, 1988, Chem. Phys. Lett. **149**, 463.
Gaubatz, U., P. Rudecki, S. Schiemann and K. Bergmann, 1990, J. Chem. Phys. **92**, 5363.
Gea-Banacloche, J., Y. Li, S. Jin and M. Xiao, 1995, Phys. Rev. **51**, 576.
Gheri, K.M., and D.F. Walls, 1992, Phys. Rev. Lett. **68**, 3428.
Gieler, M., F. Aumayr and L. Windholz, 1992, Phys. Rev. Lett. **69**, 3452.
Glushko, B., and B. Kryzhanovsky, 1992, Phys. Rev. A **46**, 2823.
Goldner, L.S., C. Gerz, R.J.C. Spreeuw, S.L. Rolston, C.I. Westbrook, W.D. Phillips, P. Marte and P. Zoller, 1994a, Phys. Rev. Lett. **72**, 997.
Goldner, L.S., C. Gerz, R.J.C. Spreeuw, S.L. Rolston, C.I. Westbrook, W.D. Phillips, P. Marte and P. Zoller, 1994b, Quantum Opt. **6**, 387.
Goldstein, E., P. Pax, K.J. Schernthanner, B. Taylor and P. Meystre, 1995, Appl. Phys. B **60**, 161.
Gorlicki, M., and M. Dumont, 1974, Opt. Commun. **11**, 166.
Gornyi, M.B., and B.G. Matisov, 1989, Opt. Spectrosc. **66**, 567.
Gornyi, M.B., B.G. Matisov and Yu.V. Rozhdestvensky, 1989a, Sov. Phys.-JETP **68**, 728.

Gornyi, M.B., B.G. Matisov and Yu.V. Rozhdestvensky, 1989b, Sov. Tech. Phys. Lett. **15**, 981.
Gozzini, A., F. Mango, J.H. Xu, G. Alzetta, F. Maccarrone and R.A. Bernheim, 1993, Nuovo Cimento D **15**, 709.
Graf, M., E. Arimondo, E.S. Fry, D.E. Nikonov, G.G. Padmabandu, M.O. Scully and S.Y. Zhu, 1995, Phys. Rev. A **51**, 4030.
Gray, H.R., R.M. Whitley and C.R. Stroud Jr, 1978, Opt. Lett. **3**, 218.
Hanle, W., 1923, Naturwissenschaften **11**, 690.
Hänsch, T., R. Keil, A. Schabert and P. Toschek, 1969, Z. Phys. **266**, 293.
Hänsch, T., and P. Toschek, 1970, Z. Phys. **236**, 213
Happer, W., 1972, Rev. Mod Phys. **44**, 169.
Harde, H., and H. Burggraf, 1982, Opt. Commun. **40**, 441.
Harde, H., and H. Burggraf, 1983, in: Laser Spectroscopy VI, eds H.P. Weber and W. Lüthy (Springer, Berlin) p. 117
Harde, H., and H. Burggraf, 1984, in: Coherence and Quantum Optics V, eds. L. Mandel and E. Wolf (Plenum Press, New York) p. 993.
Harde, H., H. Burggraf, J. Mlynek and W. Lange, 1981, Opt. Lett. **6**, 290.
Harris, S.E., 1993, Phys. Rev. Lett. **70**, 552.
Harris, S.E., 1994, Phys. Rev. Lett. **72**, 52.
He, G.Z., A. Kuhn, S. Schiemann and K. Bergmann, 1990, J. Opt. Soc. Am. B **7**, 1960.
Hemmer, P.R., K.Z. Cheng, J. Kierstead, M.S. Shahriar and M.K. Kim, 1994, Opt. Lett. **19**, 296.
Hemmer, P.R., S. Ezekiel and C.C. Leiby Jr, 1983, Opt. Lett. **8**, 440.
Hemmer, P.R., G. Ontai and S. Ezekiel, 1986, J. Opt. Soc. Am. B **3**, 219.
Hemmer, P.R., M.G. Prentiss, M.S. Shahriar and N.P. Bigelow, 1992, Opt. Commun. **89**, 335.
Hemmer, P.R., M.S. Shahriar, H. Lamela-Rivera, S.P. Smith, B.E. Bernacki and S. Ezekiel, 1993, J. Opt. Soc. Am. B **10**, 1326.
Hemmer, P.R., M.S. Shahriar, V.D. Natoli and S. Ezekiel, 1989, J. Opt. Soc. Am. B **6**, 1519.
Hioe, F.T., 1983, Phys. Rev. A **28**, 879.
Hioe, F.T., 1984a, Phys. Rev. A **29**, 3434.
Hioe, F.T., 1984b, Phys. Rev. A **30**, 3097.
Hioe, F.T., and C.E. Carroll, 1988, Phys. Rev. A **37**, 3000.
Hioe, F.T., and J.H. Eberly, 1981, Phys. Rev. Lett. **47**, 838.
Imamoglu, A., 1989, Phys. Rev. A **40**, 2835.
Imamoglu, A., J.E. Field and S.E. Harris, 1991, Phys. Rev. Lett. **66**, 1154.
Jain, M., 1994, Phys. Rev. A **50**, 1899.
Janik, G., W. Nagourney and H. Dehmelt, 1985, J. Opt. Soc. Am. B **2**, 1251.
Javanainen, J., 1992, Europhys. Lett. **17**, 407.
Kaiser, R., 1990, Thèse de Doctorat (École Normale Supérieure, Paris) unpublished.
Kaivola, M., N. Bjerre, O. Poulsen and J. Javanainen, 1984, Opt. Commun. **49**, 418.
Kaivola, M., P. Thorsen and O. Poulsen, 1985, Phys. Rev. A **32**, 1985.
Kasevich, M., and S. Chu, 1992, Phys. Rev. Lett. **69**, 1741.
Kelley, P.L., P.J. Harshman, O. Blum and T.K. Gustafson, 1994, J. Opt. Soc. Am. B **11**, 2298.
Kennedy, T.A.B., and S. Swain, 1984, J. Phys. B **17**, L389.
Khanin, Y.I., and O.A. Kocharovskaya, 1990, J. Opt. Soc. Am. B **7**, 2016.
Kleinfeld, J.A., and A.D. Streater, 1994, Phys. Rev. A **49**, R4301.
Knight, P.L., 1982, Nature **297**, 16.
Knight, P.L., 1984, Comm. At. Mol. Phys. **15**, 193.
Knight, P.L., M.A. Lauder and B.J. Dalton, 1990, Phys. Rep. **190**, 1.
Kocharovskaya, O.A., 1990, Sov. J. Quantum Electron. **20**, 14.
Kocharovskaya, O.A., 1992, Phys. Rep. **219**, 175.

Kocharovskaya, O.A., and Y.I. Khanin, 1986, Sov. Phys.-JETP 63, 945.
Kocharovskaya, O.A., and Y.I. Khanin, 1988, JETP Lett. **48**, 630.
Kocharovskaya, O.A., R.D. Li and P. Mandel, 1990, Opt. Commun. 77, 215.
Kocharovskaya, O.A., and P. Mandel, 1990, Phys. Rev. A **42**, 523.
Kocharovskaya, O.A., F. Mauri and E. Arimondo, 1991, Opt. Commun. **84**, 393.
Kocharovskaya, O.A., F. Mauri, B. Zambon and E. Arimondo, 1992, in: Laser Spectroscopy X, eds M. Ducloy, E. Giacobino and G. Camy (World Scientific, Singapore) p. 307.
Korsunsky, E.A., D.V. Kosachiov, B.G. Matisov, Yu.V. Rozhdestvensky, L. Windholz and C. Neureiter, 1993, Phys. Rev. A **48**, 1419.
Korsunsky, E.A., B.G. Matisov and Yu.V. Rozhdestvensky, 1992, Sov. Phys.-JETP **75**, 595
Korsunsky, E.A., A. Snegiriov, V. Gordienko, B.G. Matisov and L. Windholz, 1994, Z. Phys. D. **30**, 23.
Kosachiov, D.V., B.G. Matisov and Yu.V. Rozhdestvensky, 1991, Opt. Commun. **85**, 209
Kosachiov, D.V., B.G. Matisov and Yu.V. Rozhdestvensky, 1992a, Sov. Phys. Tech. Phys **37**, 26.
Kosachiov, D.V., B.G. Matisov and Yu.V. Rozhdestvensky, 1992b, J. Phys. B **25**, 2473.
Kosachiov, D.V., B.G. Matisov and Yu.V. Rozhdestvensky, 1992c, Sov. Phys.-JETP **75**, 4.
Kosachiov, D.V., B.G. Matisov and Yu.V. Rozhdestvensky, 1992d, Sov. J. Quantum Electron. **22**, 663.
Kosachiov, D.V., B.G. Matisov and Yu.V. Rozhdestvensky, 1993, Europhys. Lett. **22**, 11.
Köster, E., J. Mlynek and W. Lange, 1985, Opt. Commun. **53**, 53.
Kuhn, A., G.W. Coulston, G.Z. He, S. Schiemann and K. Bergmann, 1992, J. Chem. Phys. **96**, 4215.
Kuklinski, J.R., U. Gaubatz, F.T. Hioe and K. Bergmann, 1989, Phys. Rev. A **40**, 6741.
Lange, W., E. Köster and J. Mlynek, 1986, in: Optical Bistability III, eds H.M. Gibbs, N. Peyghambarian, P. Mandel and S.D. Smith (Springer, Berlin) p. 252.
Lange, W., A. Nottelman and C. Peters, 1994, Quantum Opt. **6**, 273.
Lawall, J., F. Bardou, B. Saubamea, K. Shimizu, M. Leduc, A. Aspect and C. Cohen-Tannoudji, 1994, Phys. Rev. Lett. **73**, 1915.
Lawall, J., and M. Prentiss, 1994, Phys. Rev. Lett. **72**, 993.
Letokhov, V.S., and V.P. Chebotayev, 1977, in: Nonlinear Laser Spectroscopy, Vol. 4, ed. D.L. McAdam (Springer, Berlin).
Lewis, L., 1984, Progr. Quantum Electr. **8**, 153.
Lewis, L.L., and M. Feldman, 1981, in: Proc. 35th Annual Frequency Control Symp. (Electronic Industries Association, Washington, DC) p. 612.
Lewis, L.L., M. Feldman and J.C. Bergquist, 1981, J. Phys. Colloq. **42**, C8-271.
Li, Y., and M. Xiao, 1995, Phys. Rev. A **51**, R2703.
Liedenbaum, C., S. Stolte and J. Reuss, 1989, Phys. Rep. **178**, 1.
Lindberg, M., and R. Binder, 1995, Phys. Rev. Lett **75**, 1403.
Lounis, B., and C. Cohen-Tannoudji, 1992, J. Phys. II (France) **2**, 579.
MacGillivray, W.R., 1983, in: Laser Physics, Lecture Notes in Physics, Vol. 182, eds J.D. Harvey and D.F. Walls (Springer, Berlin) p. 41.
Mandel, P., and O.A. Kocharovskaya, 1993, Phys. Rev. A **47**, 5003.
Manka, A.S., H.M. Doss, L.M. Narducci, P. Ru and G.-L. Oppo, 1991, Phys. Rev. A **43**, 3748.
Marte, P., R. Dum, R. Taïeb, P. Zoller, M.S. Shahriar and M.G. Prentiss, 1994, Phys. Rev. A **49**, 4826.
Marte, P., P. Zoller and J.L. Hall, 1991, Phys. Rev. A **44**, R4418.
Matisov, B.G., V. Gordienko, E.A. Korsunsky and L. Windholz, 1995, Sov. Phys.-JETP **80**, 386.
Matisov, B.G., E.A. Korsunsky, V. Gordienko and L. Windholz, 1994, Laser Phys. **4**, 835.
Mauri, F., 1990, Tesi di Laurea in Fisica (Università di Pisa) unpublished

Mauri, F., and E. Arimondo, 1991, Europhys. Lett. **8**, 717–722.
Mauri, F., and E. Arimondo, 1992, Appl. Phys. B **54**, 420.
Mauri, F., F. Papoff and E. Arimondo, 1991, in: Proc. LIKE Workshop, eds L. Moi et al. (ETS Editrice, Pisa) p. 89.
Mazets, I.E., and B.G. Matisov, 1992, Sov. Phys.-JETP **74**, 13.
McLean, R.J., R.J. Ballagh and D.M. Warrington, 1985, J. Phys. B **18**, 2371.
Meyer, G.M., U.W. Rathe, M. Graf, S.Y. Zhu, E.S. Fry, M.O. Scully, G.H. Herling and L.M. Narducci, 1994, Quantum Opt. **6**, 231.
Minogin, V.G., and V.S. Letokhov, 1986, Laser Light Pressure on Atoms (Gordon and Breach, New York).
Minogin, V.G., M.A. Ol'shanii, Yu.V. Rozhdestvensky and N.N. Yakobson, 1990, Opt. Spectrosc. **68**, 29.
Minogin, V.G., M.A. Ol'shanii and S.U. Shulga, 1989, J. Opt. Soc. Am. B **6**, 2108.
Minogin, V.G., and Yu.V. Rozhdestvensky, 1985, Sov. Phys.-JETP **61**, 1156.
Mishina, T., Y. Fukuda and T. Hashi, 1988, Opt. Commun. **66**, 25.
Mlynek, J., K.H. Drake, G. Kersten, D. Frölich and W. Lange, 1981, Opt. Lett. **6**, 87.
Mlynek, J., K.H. Drake, W. Lange and H. Brand, 1979, in: Laser Spectroscopy IV, eds H. Walther and K.W. Rothe (Springer, Berlin) p. 616.
Mlynek, J., E. Köster, J. Kolbe and W. Lange, 1984, J. Opt. Soc. Am. B **1**, 532
Mlynek, J., W. Lange, H. Harde and H. Burggraf, 1981, Phys. Rev. A **24**, 1099
Mlynek, J., F. Mitschke, R. Deserno and W. Lange, 1982, Appl. Phys. B **28**, 135.
Mlynek, J., F. Mitschke, R. Deserno and W. Lange, 1984, Phys. Rev. A **29**, 1297.
Mlynek, J., F. Mitschke, E. Köster and W. Lange, 1984, in: Coherence and Quantum Optics V, eds L. Mandel and E. Wolf (Plenum Press, New York) p. 1179.
Murnick, D.E., M.S. Feld, M.M. Burns, T.U. Kühl and P.G. Pappas, 1979, in: Laser Spectroscopy IV, eds H. Walther and K.W. Rothe (Springer, Berlin) p. 195.
Narducci, L.M., H.M. Doss, P. Ru, M.O. Scully, S.Y. Zhu and C.H. Keitel, 1991, Opt. Commun. **81**, 379.
Narducci, L.M., M.O. Scully, G.-L. Oppo, P. Ru and J.R. Tredicce, 1990, Phys. Rev. A **42**, 1630.
Nicolini, C., 1980, Tesi di Laurea in Fisica (Università di Pisa) unpublished.
Nikonov, D.E., U.W. Rathe, M.O. Scully, S.Y. Zhu, E.S. Fry, X. Li, G.G. Padmabandu and M. Fleischhauer, 1994, Quantum Opt. **6**, 245.
Notkin, G.E., S.G. Rautian and A.A. Feoktistov, 1967, Sov. Phys.-JETP **25**, 1112.
Nottelman, A., C. Peters and W. Lange, 1993, Phys. Rev. Lett. **70**, 1783
Ol'shanii, M.A., 1991, J. Phys. B **24**, L583.
Ol'shanii, M.A., 1994, Opt. & Spectrosc. **76**, 174.
Ol'shanii, M.A., and V.G. Minogin, 1991a, in: Proc. LIKE Workshop, eds L. Moi et al. (ETS Editrice, Pisa) p. 99
Ol'shanii, M.A., and V.G. Minogin, 1991b, Quantum Opt. **3**, 317.
Ol'shanii, M.A., and V.G. Minogin, 1992, Opt. Commun. **89**, 393.
Omont, A., 1977, J. Prog. Quantum Electron. **5**, 69.
Oreg, J., F.T. Hioe and J.H. Eberly, 1984, Phys. Rev. A **29**, 690
Ornols, G., 1979, Nuovo Cimento B **53**, 1.
Padmabandu, G.G., X. Li, C. Su, E.S. Fry, D.E. Nikonov, S.Y. Zhu, G.M. Meyer and M.O. Scully, 1994, Quantum Opt. **6**, 261
Papoff, F., F. Mauri and E. Arimondo, 1992, J. Opt. Soc. Am. B **9**, 321.
Parigger, C., P. Hannaford and W.J. Sandle, 1986, Phys. Rev. A **34**, 2058.
Parigger, C., P. Hannaford, W.J. Sandle and R.J. Ballagh, 1985, Phys. Rev. A **31**, 4043.
Parkins, A.S., P. Marte, P. Zoller, O. Carnal and H.J. Kimble, 1995, Phys. Rev. A **51**, 1578.

Parkins, A.S., P. Marte, P. Zoller and H.J. Kimble, 1993, Phys. Rev. Lett. **71**, 3095
Pegg, D.T., 1986, Opt. Commun. **57**, 185.
Pegg, D.T., and W.E. Schulz, 1985, Opt. Commun. **53**, 274.
Pillet, P., C. Valentin, R.-L. Yuan and J. Yu, 1993, Phys. Rev. A **48**, 845.
Radmore, P.M., and P.L. Knight, 1982, J. Phys. B **15**, 561.
Ramsey, N., 1963, Molecular Beams (Oxford University Press, London).
Rozhdestvensky, Yu.V., and N.N. Yakobson, 1991, Sov. Phys.-JETP **72**, 936.
Sandle, W.J., C. Parigger and R.J. Ballagh, 1986, in: Optical Chaos, SPIE Proc. **667**, 62
Sargent III, M., M.O. Scully and W.E. Lamb Jr, 1974, Laser Physics (Addison-Wesley, Reading, MA).
Schiemann, S., A. Kuhn, S. Steuerwald and K. Bergmann, 1993, Phys. Rev. Lett. **71**, 3637.
Schlossberg, H.R., and A. Javan, 1966, Phys. Rev. **150**, 267.
Schmidt, O., Z. Hussein, R. Wynands and D. Meschede, 1993, in: Technical Digest EQEC '93, Firenze 1993, eds P. de Natale, R. Meucci and S. Pelli, p. 215.
Schmidt, O., Z. Hussein, R. Wynands and D. Meschede, 1995, in: Technical Digest QELS '95 (Optical Society of America, Washington, DC) p. QThD5.
Schmidt-Iglesias, C., 1993, Opt. Commun. **97**, 88.
Schubert, M., I. Siemers and R. Blatt, 1989, Phys. Rev. A **39**, 5098.
Schulz, W.E., W.R. MacGillivray and M.C. Standage, 1983, Opt. Commun. **45**, 67.
Scully, M.O., 1991, Phys. Rev. Lett. **67**, 1855
Scully, M.O., 1992, Phys. Rep. **219**, 191.
Scully, M.O., 1994, Quantum Opt. **6**, 203.
Scully, M.O., and S.Y. Zhu, 1992, Opt. Commun. **87**, 134.
Scully, M.O., S.Y. Zhu and A. Gavrielides, 1989, Phys. Rev. Lett. **62**, 2813
Series, G.W., 1978, Phys. Rep. **43**, 1.
Shahriar, M.S., and P.R. Hemmer, 1990, Phys. Rev. Lett. **65**, 1865.
Shahriar, M.S., P.R. Hemmer, M.G. Prentiss, A. Chu, D.P. Katz and N.P. Bigelow, 1993, Opt. Commun. **103**, 453.
Shahriar, M.S., P.R. Hemmer, M.G. Prentiss, P. Marte, J. Mervis, D.P. Katz, N.P. Bigelow and T. Cai, 1993, Phys. Rev. A **48**, R4035
Shao, Y.L., D. Charalambidis, C. Fotakis, J. Zhang and P. Lambropoulos, 1991, Phys. Rev. Lett. **67**, 3669.
Shore, B.W., 1990, The Theory of Coherent Atomic Excitation, Vol. 2 (Wiley, New York)
Shore, B.W., K. Bergmann and J. Oreg, 1992, Z. Phys. D **23**, 33
Shore, B.W., K. Bergmann, J. Oreg and S. Rosenwaks, 1991, Phys. Rev. A **44**, 7442
Siemers, I., M. Schubert, R. Blatt, W. Neuhauser and P.E. Toschek, 1992, Europhys. Lett. **18**, 139.
Smirnov, V.S., A.M. Tumaikin and V.I. Yudin, 1989, Sov. Phys.-JETP **69**, 913.
Stettler, J.D., C.M. Bowden, N.M. Witriol and J.H. Eberly, 1979, Phys. Lett. **73A**, 171.
Sussman, R., R. Neuhauser and H.J. Neusser, 1994, J. Chem. Phys. **100**, 4784.
Swain, S., 1982, J. Phys. B **15**, 3405.
Taichenachev, A.V., A.M. Tumaikin, M.A. Ol'shanii and V.I. Yudin, 1991, JETP Lett. **53**, 351.
Taichenachev, A.V., A.M. Tumaikin and V.I. Yudin, 1994, Laser Phys. **4**, 124
Taichenachev, A.V., A.M. Tumaikin, V.I. Yudin and M.A. Ol'shanii, 1992a, Laser Phys. **2**, 32.
Taichenachev, A.V., A.M. Tumaikin, V.I. Yudin and M.A. Ol'shanii, 1992b, Sov. Phys.-JETP **74**, 952.
Takagi, K., R.F. Curl and R.T.M. Su, 1975, Appl. Phys. **7**, 181.
Teets, R., J.N. Eckstein and T.W. Hänsch, 1977, Phys. Rev. Lett. **38**, 760
Tench, R.E., B.W. Peuse, P.R. Hemmer, J.E. Thomas, S. Ezekiel, C.C. Leiby Jr, R.H. Picard and C.R. Willis, 1981, J. Phys. Colloq. **42**, C8-45.
Théobald, G., N. Dimarcq, V. Giordano and P. Cérez, 1989, Opt. Commun. **71**, 256.

Thomas, J.E., P.R. Hemmer, S. Ezekiel, C.C. Leiby Jr, R.H. Picard and C.R. Willis, 1982, Phys. Rev. Lett. **48**, 867.
Toschek, P.E., and W. Neuhauser, 1981, in: Atomic Physics 7, eds D. Kleppner and F.M. Pipkin (Plenum, New York) p. 529.
Tumaikin, A.M., and V.I. Yudin, 1990, Sov. Phys.-JETP **71**, 43.
Tumaikin, A.M., and V.I. Yudin, 1991, Physica B **175**, 161.
Valentin, C., J. Yu and P. Pillet, 1994, J. Phys. II (France) **4**, 1925.
van der Veer, W.E., R.J.J. van Dienst, A. Donszelmann and H.B. van Linden van den Heuvell, 1993, Phys. Rev. Lett. **70**, 3243.
Walls, D.F., and P. Zoller, 1980, Opt. Commun. **34**, 260.
Walls, D.F., P. Zoller and M.L. Steyn-Ross, 1981, IEEE J. Quantum Electron. **QE-17**, 380.
Weidemüller, M., T. Esslinger, M.A. Ol'shanii, A. Hemmerich and T.W. Hänsch, 1994, Europhys. Lett. **27**, 109.
Weitz, M., B.C. Young and S. Chu, 1994a, Phys. Rev. A **50**, 2438.
Weitz, M., B.C. Young and S. Chu, 1994b, Phys. Rev. Lett. **73**, 2563.
Werij, H.G.C., and J.P. Woerdman, 1988, Phys. Rep. **169**, 145.
Whitley, R.M., and C.R. Stroud Jr, 1976, Phys. Rev. A **14**, 1498.
Wilcox, L.R., and W.E. Lamb Jr, 1960, Phys. Rev. **119**, 1915.
Xiao, M., Y.Y. Li, S. Jin and J. Gea-Banacloche, 1995, Phys. Rev. Lett. **74**, 666.
Xu, J.H., 1994, Ph.D. thesis (Scuola Normale Superiore, Pisa) unpublished.
Yoo, H.I., and J.H. Eberly, 1985, Phys. Rep. **118**, 239.
Young, L., T. Dinneen and N.B. Mansour, 1988, Phys. Rev. A **38**, 3812.
Zaretsky, D.F., and S.B. Sazonov, 1994, JETP Lett. **60**, 699.
Zou, Y.H., and N. Bloembergen, 1986, Phys. Rev. A **33**, 1730.